SLAC-R-930
September-14-2009

# FACET

Facility for Advanced Accelerator
Experimental Tests at SLAC

## Conceptual Design Report

Published September 2009

Prepared for the Department of Energy under contract number DE-AC03-76SF00515 by SLAC National Accelerator Laboratory, Operated by Stanford University for the U. S. Department of Energy. Printed in the United States of America.

# List of Authors and Contributors

## FACET Project Group

J. Amann, K. Bane, L. Bentson, D. Blankenship, E. Carrone, J. Chan, R. Chestnut, S. DeBarger, F.-J. Decker, A. DeLira, R. Erickson, C. Hast, M.J. Hogan, B. Ilinets, R. Iverson, J. Keller, J. Kenny, J. Krebs, N. Li, J.J Lipari, D.B. MacFarlane, S. Mao, P. Miller, Y. Nosochkov, T.O. Raubenheimer, P. Rodriguez, M. Santana, J.T. Seeman, A. Seryi, H. Shin, R. Singh, C. Spencer, P. Tenenbaum, J. Vollaire, D. Walz, W. Wittmer, M. Woodley and G. Yocky

*SLAC National Accelerator Laboratory*

## Contributors to the PWFA Development Discussion and Scientific Case

I. Blumenfeld[1], C.E. Clayton[2], F.-J. Decker[1], M.J. Hogan[1], C. Huang[2], R. Ischebeck[1], R.H. Iverson[1], C. Joshi[2], T. Katsouleas[7], N. Kirby[1], W. Lu[2], K.A. Marsh[2], W.B. Mori[2], P. Muggli[8], E. Oz[8], S. Pei[1], T.O Raubenheimer[1], A. Seryi[1], R.H. Siemann[1], P. Tenenbaum[1], D. Walz[1], X. Wang[8], and M. Zhou[2]

## Contributors to the Discussion of Additional Scientific Opportunities

*Advanced Accelerator Research*

H. Badakov[2], I. Blumenfeld[1], C.E. Clayton[2], A. Cook[2], F.-J. Decker[1], M.J. Hogan[1], C. Huang[2], R. Ischebeck[1], R.H. Iverson[1], C. Joshi[2], A. Kanareykin[3], T. Katsouleas[7], N. Kirby[1], W. Lu[2], K. A. Marsh[2], W.B. Mori[2], P. Muggli[8], E. Oz[8], J.B. Rosenzweig[2], A. Seryi[1], R.H. Siemann[1], M.C. Thompson[4], R. Tikhoplav[2], G. Travish[2], D. Walz[1], X. Wang[8], and M. Zhou[2]

*Accelerator Instrumentation Development*

C. Hast[1], D.B. MacFarlane[1], T. Markiewicz[1], T.O Raubenheimer[1], and M. Woods[1]

*THz Radiation and Basic Energy Sciences*

Y. Acremann[5], A. Dobin[6], S.J. Gamble[9], A.M. Lindenberg[5,10], A.Nilsson[11], H. Ogasawara[1], H.C. Siegmann[5], and J. Stohr[1]

[1] SLAC National Accelerator Laboratory, Stanford University
[2] University of California at Los Angeles
[3] Euclid TechLabs, LLC
[4] Lawrence Livermore National Laboratory
[5] Photon Ultrafast Laser Science and Engineering Center (PULSE), Stanford University
[6] Seagate Technologies
[7] Pratt School of Engineering, Duke University
[8] University of Southern California
[9] Department of Applied Physics, Stanford University
[10] Department of Materials Science, Stanford University
[11] X-ray Laboratory for Advanced Materials (XLAM), Stanford University

# Preface

This Conceptual Design Report (CDR) describes the design of FACET. It will be updated to stay current with the developing design of the facility. This CDR begins as the baseline conceptual design and will evolve into an "as-built" manual for the completed facility.

The Executive Summary, **Chapter 1**, gives an introduction to the FACET project and describes the salient features of its design.

**Chapter 2** gives an overview of **FACET**. It describes the general parameters of the machine and the basic approaches to implementation.

The **FACET** project does not include the implementation of specific scientific experiments either for plasma wake-field acceleration for other applications. Nonetheless, enough work has been done to define potential experiments to assure that the facility can meet the requirements of the experimental community. **Chapter 3**, Scientific Case, describes the planned plasma wakefield and other experiments.

**Chapter 4**, Technical Description of FACET, describes the parameters and design of all technical systems of FACET. FACET uses the first two thirds of the existing SLAC linac to accelerate the beam to about 20GeV, and compress it with the aid of two chicanes, located in Sector 10 and Sector 20. The Sector 20 area will include a focusing system, the generic experimental area and the beam dump.

**Chapter 5**, Management of Scientific Program, describes the management of the scientific program at FACET.

**Chapter 6**, Environment, Safety and Health and Quality Assurance, describes the existing programs at SLAC and their application to the FACET project. It includes a preliminary analysis of safety hazards and the planned mitigation.

**Chapter 7**, Work Breakdown Structure, describes the structure used for developing the cost estimates, which will also be used to manage the project. The chapter defines the scope of work of each element down to level 3.

# Table of Contents

# 1 Executive Summary

## 1.1 Introduction

Advanced accelerator research is of central importance to the long-term health of national and international high energy physics. Experiments on future acceleration techniques require high-quality, forefront facilities. Plasma wakefield acceleration, with its potential for a 1000-fold or more increase in acceleration gradient, is one of the most promising approaches to advancing the energy frontier. FACET will be an experimental facility that provides short, intense pulses of electrons and positrons to excite plasma wakefields and study a variety of critical issues associated with plasma acceleration.

## 1.2 Project Highlights

The facility will use the first two thirds of the linac and will contain the following new elements:

1. New beamlines in Sector 20 of the linac, consisting of a final focus and a chicane. The beamline will be able to operate with either electrons or positrons. The chicane will be upgradeable to a dual "sailboat" configuration, for simultaneous operation with electrons and positrons;
2. Addition of a second arm to the existing chicane in Sector 10 to allow operation with positrons;
3. An experimental area at the Sector 20 focal point configured to allow a variety of scientific experiments.

## 1.3 Performance Characteristics

FACET will deliver high quality beams for plasma wakefield accelerator research and for other scientific applications. The main beam parameters are summarized in Table 1-1. (The Key Performance Parameters for CD-4, Project Completion, are defined in the FACET Project Execution Plan).

**Table 1-1.** Main Performance Characteristics of FACET

| | |
|---|---|
| Energy | 20 to 23 GeV |
| Particles | Electrons and positrons |
| Charge per pulse | > 2 x $10^{10}$ (3.2 nC) $e^-$ or $e^+$ per pulse |
| Pulse length at IP ($\sigma_z$) | < 100 μm |
| Spot size at IP ($\sigma_{x,y}$) | < 100 μm |
| Typical pulse rep. rate | 30 Hz |

SLAC is the only place in the world with such high peak current, high energy electron and positron beams. With FACET, SLAC will support a unique program for plasma wakefield acceleration and for other scientific applications.

## 1.4 Cost and Schedule

The Total Estimated Cost of FACET is in the range $14.0M-$15.4M. The Total Project Cost is in the range $14.5M-$16.0M. A two year construction schedule is proposed.

## 1.5 Acquisition Strategy

The contractor for acquisition of FACET is SLAC National Accelerator Laboratory, operated by Stanford University for the U.S. Department of Energy.

# 2 FACET Overview

## 2.1 Introduction

The mission of the DOE Office of Science (SC) is "To advance basic research and the instruments of science that are the foundations for DOE's applied missions, a base for U.S. technology innovation, and a source for remarkable insights into our physical and biological world and the nature of matter and energy." Within SC, the High Energy Physics (HEP) mission includes "understanding how our universe works at its most fundamental level. This is done by discovering the most elementary constituents of matter and energy, exploring the basic nature of space and time itself, and probing the interactions between them. These fundamental ideas are at the heart of physics and hence all of the physical sciences. To enable these discoveries, HEP supports theoretical and experimental research in both elementary particle physics and fundamental accelerator science and technology".

Advanced accelerator research is of central importance to the long-term health of national and international high energy physics. Experiments on future acceleration techniques require high-quality, forefront facilities. Plasma wakefield acceleration, with its potential for a 1000-fold or more increase in acceleration gradient, is one of the most promising approaches for dramatic reduction in the size and cost of future accelerators, particularly high-energy electron-positron colliders. The Mission Need Statement for an Advanced Plasma Accelerator Facility was signed by Dr. Raymond Orbach, Under Secretary for Science, on January 28, 2008 and Critical Decision 0 (CD-0) was approved on February 27, 2008. The Facility for Advanced Accelerator Experimental Tests (FACET) will be an experimental facility that provides short, intense pulses of electrons and positrons to excite plasma wakefields and study a variety of critical issues associated with plasma acceleration.

SLAC is the only place in the world with the high peak current, high energy electron and positron beams required to continue the development of beam driven plasma wakefield acceleration. With FACET, SLAC will support a unique program of research on plasma wakefield acceleration, particularly for application to high energy physics. This includes accelerating both electron and positron beams to high energies with a small emittance and narrow energy spread, and demonstrating efficient energy extraction from the plasma wake. This research will be carried out by strong collaborations between university and laboratory groups and will attract some of the brightest students in the field of beam physics.

## 2.2 Goals and Mission

The goal of the FACET Project is to create a facility to support research on plasma wakefield acceleration using both electrons and positrons. The FACET facility will use the first 2 kilometers of the SLAC linac along with a new experimental area at Sector 20 in the existing linac tunnel, upstream of the LCLS injector. At the Sector 20 location along the linac, the beam has an energy in excess of 20 GeV, and the emittance is very small. By installing a new focusing system at Sector 20, the beam can be focused and compressed in length to sizes appropriate for plasma wakefield acceleration research. An additional bunch compressor in Sector 10 is required to provide short positron bunches. The overall site layout for the accelerator complex at SLAC is shown schematically in Figure 2-1 with the modified areas highlighted in red.

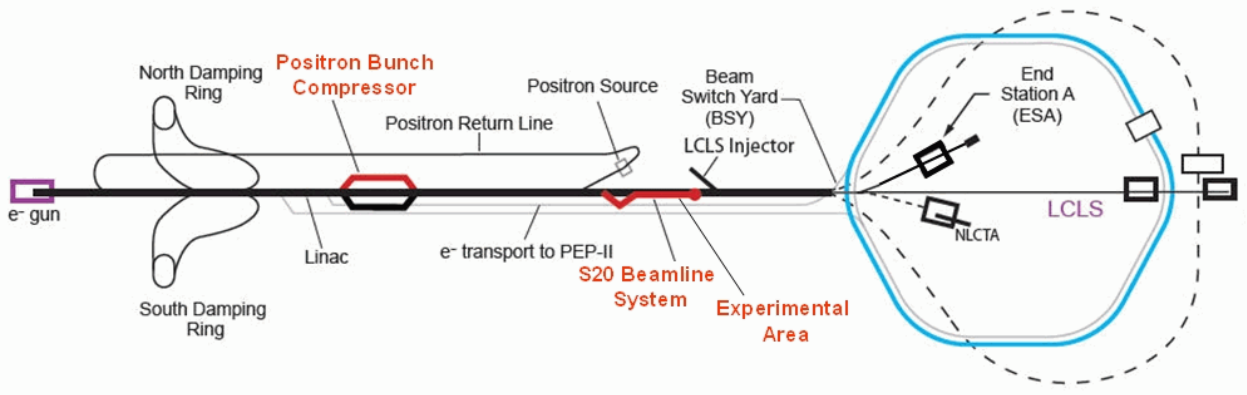


**Figure 2-1.** Schematic of the SLAC site with proposed FACET modifications to the linac systems marked in red.

## 2.3 Analysis of Alternatives

The FACET project will create a facility for advanced plasma acceleration studies, using a drive beam to create the plasma. This is one of two promising approaches to plasma acceleration, and the other laser-driven approach is being pursued elsewhere. SLAC is the only place in the world with the high peak current, high energy electron and positron beams required to conduct particle-beam-driven plasma wakefield acceleration studies. There are no other technically comparable existing facilities in the U.S. that could be used or upgraded for this purpose. The existing SLAC linac provides several tens of GeV acceleration at tremendous cost savings for FACET. Creating a new facility elsewhere would cost at least a billion dollars. Therefore, no alternative locations for FACET were considered, since creating the facility at SLAC was the only reasonable alternative.

Once it was known that the FFTB would no longer be available for high energy accelerator physics experiments, several possible replacement facilities were investigated. These included creating a facility in the South Arc [1], in the SLAC linac B Line target room [2] (in Figure 2-1 the South Arc is shown by a dashed line going down from the end of the linac and the B Line is a dashed line pointing in the direction of NLCTA). A configuration where beam would be brought to End Station A (ESA in Figure 2-1) was also considered but ruled out since the needed beam properties could not be achieved without a major rebuild due to the large bend angle. Either of the South Arc or B Line configurations would require creating a new kilometer-long bypass beamline from the 2/3-point of the linac to the end. In summary, all of these alternatives had inferior performance to FACET in terms of providing the required beam quality, minimizing the extent of new beamlines, optimizing cost and schedule efficiency, and providing operational flexibility.

## 2.4 Project Schedule

Table 2-1 shows the preliminary schedule for the Critical Decisions for the FACET project. Following the methodology outlined by DOE Order 413.3A, a tailored and phased approach has been applied to the FACET schedule. The FACET project is a straightforward modification of the existing linac at Sectors 10 and 20 and is well within the technical capabilities of SLAC. Because the FACET design is well advanced, critical decisions CD-2 and CD-3 will be

combined. The fabrication, installation and validation and verification schedule for Sector 20 and Sector 10 beamlines is staggered in time, and therefore, CD-4 critical decision is split into two phases. CD-4A will be achieved after validation and verification of Sector 20 beamlines with electron beam, and CD-4B after the Sector 10 positron chicane is completed and validation and verification of the whole beamline with positron beam is finished. The foreseen upgrade of LCLS, which will use the first two thirds of the linac, determines the window of opportunity for FACET scientific program to be five years after the project completion (CD-4B).

| Critical decision | Description | Date |
|---|---|---|
| CD-0 | Mission Need Approval | Feb 2008 (Actual) |
| CD-1 | Preliminary Baseline Range Approval | Aug 2009 |
| CD2/3 | Performance Baseline and Start of Construction Approval | Dec 2009 |
| CD-4A | Electron Beamlines Completed | Jan 2011 |
| CD-4B | Project Completion | Sep 2011 |

**Table 2-1.** Preliminary Schedule

## 2.5 Cost Estimate

The FACET project is a Major Item of Equipment (MIE). The preliminary Total Estimated Cost (TEC) range for the FACET project is 14.0 – 15.4 million in as spent dollars. The preliminary Other Project Cost (OPC) is $0.5 – 0.6 M. The preliminary Total Project Cost (TPC) range is 14.5 – 16.0 million in as spent dollars. The cost range is due to variation of design maturity and definition of the scope of work for the sub-systems. The TPC, broken down to level 2 WBS elements as shown in Table 2-2 below, includes design, hardware procurement, project management, safety and health, quality assurance, installation, acceptance testing, initial system validation and verification and contingency. The baseline cost will be approved at CD-2.

| WBS | Description | Estimated Minimum Cost | Estimated Maximum Cost |
|---|---|---|---|
| 1.1 | Project Management | 1.2 | 1.3 |
| 1.2 | Sector 20 Beamline Systems | 2.8 | 3.0 |
| 1.3 | Experimental Area | 0.4 | 0.5 |
| 1.4 | Sector 10 Bunch Compressor System | 1.6 | 1.7 |
| 1.5 | Common Systems | 4.3 | 4.8 |
| | Contingency | 3.7 | 4.1 |
| 2.0 | Other Project Costs | 0.5 | 0.6 |
| **FACET Total Project Costs** | | 14.5 | 16.0 |

**Table 2-2.** Preliminary Cost Range

Most of the hardware components installed for FACET will allow about two decades of lifetime,

however the foreseen upgrade of LCLS, which will use the first two thirds of the linac, determines the window of opportunity for FACET scientific program to be five years after the project completion (CD-4B). Some components in the existing beamlines may also require additional upgrades if their lifetime would be extended beyond five years. FACET will cost roughly $6 million annually to operate and maintain. Decontamination and decommissioning costs are anticipated to be modest (less than $1 million) and will take into account reuse of FACET hardware for other SLAC projects, salvage wherever needed and proper disposal of contaminated components as waste. Conservatively assuming a FACET TPC of $16 million (i.e., top of the current range) and five years of operational service, the total life cycle cost for FACET would amount to approximately $47 million.

## 2.6 Funding Requirements

About two years construction schedule is proposed for FACET project. In order to meet this schedule, the funds will be made available as shown in Table 2-3. The table presents the funding profile at the low end of the cost range with 36% contingency.

| FACET Projected Funding Profile (M$) | FY09 | FY10 | Total |
|---|---|---|---|
| Project Costs (WBS 1.0) | 3.5 | 10.5 | 14.0 |
| Other Project Costs (WBS 2.0) | 0.5 | 0.0 | 0.5 |
| **Total Project Costs (TPC)** | 4.0 | 10.5 | 14.5 |

**Table 2-3.** Projected Funding Profile

## 2.7 Risk Assessment and Mitigation Strategies

Risk management is based on a graded approach in which levels of risk are assessed for project activities and elements. This assessment is based upon the potential consequences of an activity or an element failure, as well as the probability of occurrence. Risk minimization is implemented by planning the advanced procurements and by preparing alternative technical solutions.

Risk assessments are conducted throughout the project lifecycle. Risks identified include technical, cost and schedule risks. The project Risk Management Plan details the process for identifying, evaluating, mitigating, and managing risks in compliance with DOE Order 413.3a. The project Risk Registry is reviewed and updated monthly.

### 2.7.1 Technical Risks

The components required for the FACET project are similar to others recently built at SLAC, for which there are numerous technical and cost benchmarks. Much of the hardware will be reused or refurbished equipment already existing at SLAC. Only a small part of the technical equipment will be ordered from commercial vendors. There are a few components for which moderate technical challenges may affect cost and schedule; however, potential negative effects will be mitigated via advanced procurement and/or development of back-up technical solutions.

As part of the Risk Management process, adequate cost and schedule contingencies will be included in the Performance Baseline. Therefore, technical and engineering risks for the FACET project are considered low.

### 2.7.2 Schedule and Cost Risks

The primary risks identified for the FACET Project are the schedule and cost risks. The risks are associated with several factors, in particular, procurement requirements that may cause delays in acquisition of new components, uncertainty about the condition of existing components and systems, and factors that are outside of the scope of the project. For each of these risks, mitigation strategies have been developed that include advanced procurements, early preparatory and system assessment efforts, and close cooperation with all parties involved. Details of the risk analysis and mitigation strategies are available in the Risk Registry and in the Risk Management Plan.

In view of the mitigations already developed for the identified risks, the cost and schedule estimates are judged to be of low risk in terms of completing the project on schedule and within the cost range. As part of the Risk Management process, adequate cost and schedule contingencies will be included in the Performance Baseline.

## 2.8 Stakeholder Input

The primary stakeholder in the FACET project is the HEP advanced accelerator R&D community. This community has been involved in the design and planning of the project, and it is expected that FACET will continue to attract university, national laboratory and international users. Through its existing outreach and community programs, the stakeholders will be kept informed about initiation of and progress toward completion of the project. An Experimental Advisory Program Committee will be organized, and through it the stakeholders will remain engaged in determination of the experimental program.

The design of FACET has been developed by the scientific and technical staff at SLAC, working in conjunction with members of the advanced plasma acceleration community and other potential users of the facility. This combination is best equipped to define the optimal performance parameters for the facility to be able to carry out the science of interest in a cost-effective manner.

Throughout the design and planning process for FACET, every effort has been made to maintain communications with DOE, with the prospective user community, and with the management of SLAC. Design improvements have been implemented to address community and management input. In particular, following an earlier review of the FACET proposal, a new sailboat chicane has been designed to provide simultaneous delivery of both electron and positron bunches to the plasma. This will allow studies of plasma acceleration of a positron bunch by an electron drive bunch. Communication with solid state scientists and researchers working on dielectric wakefield acceleration resulted in adjustments to the experimental area design to make it more suitable for different kinds of experiments with ultra-short focused bunches.

## 2.9 Acquisition Strategy

The DOE Stanford Site Office (SSO) will implement the FACET project under the existing M&O contract (DE-AC02-76-SF00515) at the SLAC National Accelerator Laboratory. The contractor (SLAC) will manage and administer the project under the overall direction and oversight of the DOE Federal Project Director.

The FACET Project is funded in the framework of the American Recovery and Reinvestment Act (ARRA), and as such has special obligations for the use of funds and special reporting requirements. The implementation of ARRA principles for the FACET project are specified in the next section.

Detailed Advance Procurement Plans (APPs) will be developed together with the SLAC procurement office, for all procurements exceeding a defined cost threshold or those determined to be critical path, regardless of dollar value. APPs will detail major procurement milestones and any unique procurement considerations associated with requirements. If foreign vendors are considered as part of the source selection process, appropriate Buy American Act decisions, determinations and approvals will be made in accordance with the flow down requirements of the prime contract, the DOE approved SLAC purchasing system, and the American Recovery and Reinvestment Act as described below.

Based on the schedule risk analysis, a list of Advanced Procurements and Advanced Activities has been developed, to be initiated prior to CD-3. These items are described below.

### 2.9.1 Implementation of ARRA Requirements

Being funded within the framework of the American Recovery and Reinvestment Act (ARRA), the FACET Project has special obligations for the use of funds. The American Recovery and Reinvestment Act specifies that ARRA funded subcontracts should be competitive fixed-price subcontracts. The project will use this method of procurement to the maximum extent possible. Components procured from commercial vendors will be analogous to those that have been procured for accelerator beamline hardware throughout the high energy physics scientific community. The design of FACET components, to the maximal extent possible, will be done in a way to minimize the use of non-domestic materials or components, except in cases where performance, cost or compatibility with existing systems at SLAC may be compromised.

Within the ARRA framework, the FACET Project also has special reporting requirements. Simultaneously with FACET, SLAC will be implementing several other ARRA projects. The SLAC financial management systems will segregate all ARRA-funded project work from non-ARRA funds. Weekly followed by monthly reporting on FACET and all SLAC ARRA projects will be conducted in a uniform manner.

Further details of the implementation will be described in future editions of this document.

### 2.9.2 Advanced Procurements

The Advanced Procurements have been identified based on the schedule risk analysis. The AP items include several new components to be manufactured by industry. Due to the need to meet that ARRA Buy American requirement, the AP list also includes any identified foreign procurement items.

# 3 FACET Scientific Case

The FACET project is proposed to meet the Department of Energy Mission Need Statement for an Advanced Plasma Acceleration Facility. FACET will be an experimental facility that provides short, intense pulses of electrons and positrons to excite plasma wakefields and study a variety of critical issues associated with plasma acceleration. SLAC is the only place in the world with the high peak current, high energy electron and positron beams required to continue the development of beam driven plasma wakefield acceleration. With FACET, the SLAC linac will support a unique program concentrating on second-generation research on plasma wakefield acceleration. This program will achieve several key steps on the roadmap to a plasma wakefield linear collider and will assure continued US leadership in accelerator physics.

The FACET facility will involve relocation, refurbishment, and upgrading of accelerator components at SLAC that will provide beams at a new experimental region in Sector 20 of the SLAC linac tunnel. This new facility will allow a continuation of the plasma wakefield research that has been conducted in the past at the Final-Focus Test Beam (FFTB). The FFTB was the main facility supporting plasma acceleration research as well as a broad range of other R&D activities over the past decade. The FFTB was initially constructed to demonstrate the demagnification required for a linear collider final focus, as well as to verify beam optics codes and tuning procedures. Later, when combined with new bunch compression techniques, the FFTB opened up many new and exciting areas of research in beam and plasma physics, ultra-short-pulse x-ray generation, advanced accelerator techniques, specialized diagnostic techniques, solid state physics, and high energy density science.

The FFTB experiments have demonstrated many basic features achievable with plasmas including high gradients and beam transport. This provides clear evidence of the promise of beam-driven plasma wakefield acceleration. At FACET, the research will concentrate on second generation issues that must be addressed for plasma wakefield acceleration to have an application to high energy physics. These include accelerating both electron and positron beams to high energies with a narrow energy spread, small emittance, and efficient energy extraction from the plasma wake. These are challenging questions at the forefront of advanced accelerator research. Answering these questions will require strong collaborations between university and laboratory groups that can attract some of the brightest students in the field of beam physics. The SLAC linac together with FACET will provide high energy, high peak current, low transverse emittance electron and positron beams and the corresponding experimental infrastructure to continue plasma wakefield accelerator research. FACET is the only facility worldwide with the beams needed to continue the development of the beam-driven plasma wakefield accelerators that hold so much promise for high energy physics.

## 3.1 The FACET Facility

Ultimately, new accelerator concepts must be explored experimentally and appropriate facilities are critically important. For the case of plasma-based accelerators, the correlation between state-of-the-art facilities and rapid experimental progress is clearly illustrated in Figure 3-1. In just fifteen years, laser-driven plasma accelerators have advanced from making 10 MeV beams with ~100% energy spread to GeV bunches with a few percent energy spread. The steady increase in maximum energy was enabled by the rise of multi-terawatt laser facilities around the world in Japan (KEK), Great Britain (RAL), France (LOA) and the United States (LLNL, U. of Michigan, U. of T. Austin and LBNL). The progress on beam-driven plasma accelerators has been even

more remarkable with the maximum energy gained in the plasma increasing from a couple hundred MeV to over 40 GeV in just two years. In this case, progress came entirely from the capability of the SLAC linac to produce and deliver increasingly high intensity, very short bunches to experiments in the Final Focus Test Beam (FFTB) Facility.

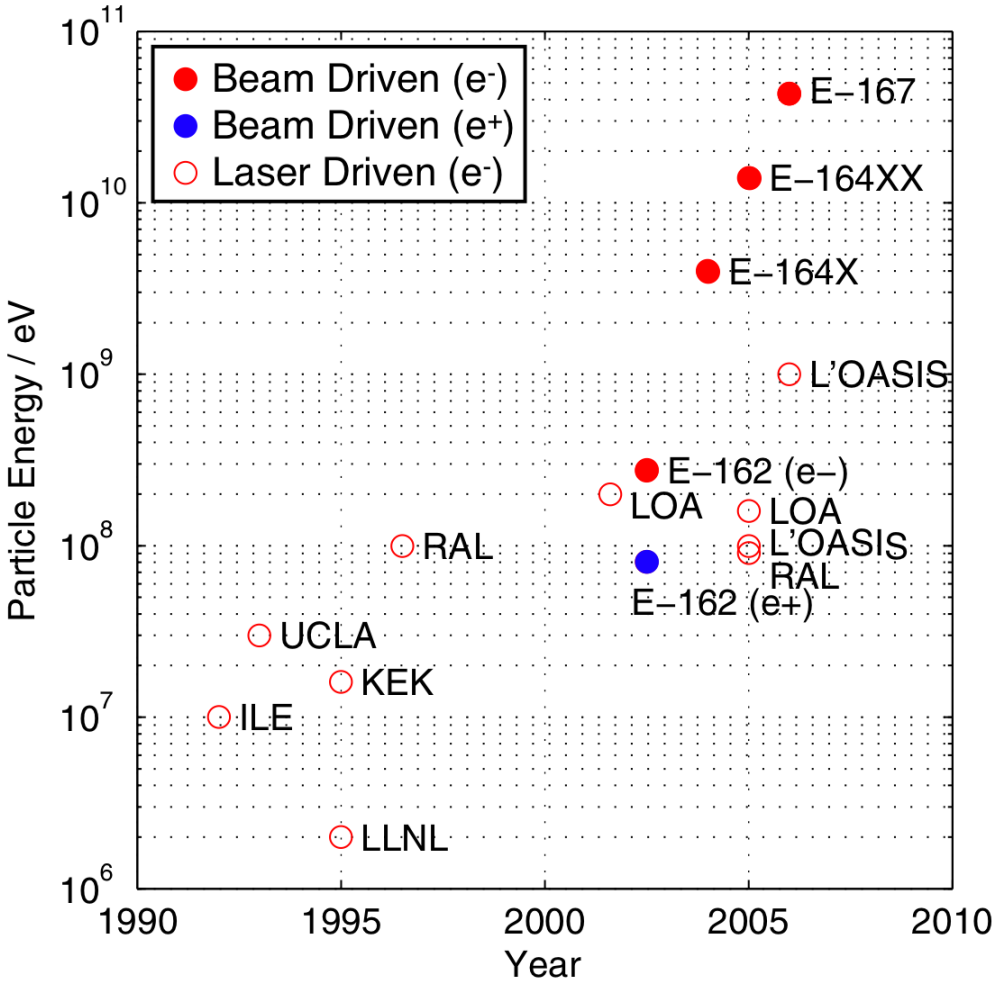


**Figure 3-1.** The maximum energy achieved by plasma-based accelerator experiments (laser and particle beam driven) versus time. All experiments have been with electrons except for the SLAC E-162 experiment.

The SLAC FFTB was a superb facility for experiments requiring beams with high energy, high peak current, and low emittance. These are exactly the beams needed for studying beam driven plasma wakefields. The electron and positron beams available at the FFTB were unique in the world because of the optics of the FFTB and, more importantly, the SLAC linac itself. The opportunities at the FFTB attracted university scientists and led to collaborations with the necessary breadth of expertise. The experiments performed there could not have been performed anywhere else, and the results have received worldwide interest.

The emphasis at FACET will be plasma wakefield acceleration. However, the high-power beams are unique and there will be other important science opportunities, both for high-energy physics and basic energy sciences. It is therefore anticipated that FACET will have a user component to its science program, over and above the plasma wakefield acceleration research.

## 3.2 The Plasma Accelerator Research Program at FACET

The basic concept of the plasma wakefield accelerator involves the passage of an ultra-relativistic electron bunch through a stationary plasma [3]. The plasma can be formed by ionizing a gas with a laser [4] or through field-ionization by the Coulomb field of the relativistic electron bunch itself [5]. This second method allows the production of meter-long, dense ($10^{16}$ – $10^{17}$cm$^{-3}$) plasmas suitable for the PWFA and greatly simplifies the experimental set-up. In single bunch experiments the head of the bunch creates the plasma and drives the wake. The wake produces a high-gradient accelerating field that in turn accelerates particles in the back of the bunch. The system effectively operates as a transformer, where the energy from the particles in the head is transferred to those in the back, through the plasma wake. The physics is unchanged if there are two bunches rather than a single bunch; energy from the leading drive bunch is transferred to a trailing witness bunch.

The FACET experimental program relies heavily on the sophisticated laboratory apparatus and techniques for conducting beam and plasma experiments that were developed by a strong collaboration between university and laboratory groups during the FFTB experiments. Much of this experimental hardware will be relocated to FACET and the collaboration will develop it further as necessary to conduct the next generation of experiments.

## 3.3 Current Status of Plasma Wakefield Accelerator Experiments

In the past seven years, plasma wakefield accelerators have emerged as a leading approach to advanced accelerators, thanks to progress on a number of fronts [6]. The SLAC/UCLA/USC E-162/164/167 collaboration has been the leading group pioneering this research (see Appendix A in [7]). Experiments, conducted by this collaboration at the FFTB facility at SLAC, have shown that plasmas can accelerate and focus both electron and positron high energy beams. In addition, they have demonstrated a variety of new effects, such as the collective refraction of a charged particle beam at a plasma-neutral vapor interface, the generation of betatron x-rays from a few keV to tens of MeV energy, and the acceleration of electrons from the plasma itself with extremely high acceleration gradients. Striking results have come from experiments using a short ($\sigma_z \sim 15$ μm), high peak-current electron beam that field-ionizes a neutral lithium vapor to produce the plasma. Accelerating wakefields in excess of 50 GeV/m have been sustained in an 85 cm-long plasma. This gradient is roughly 3,000 times that in the SLAC linac, and the wakefield in an ~1 m-long plasma accelerated some of the 42 GeV electrons to energies approaching 100 GeV.

## 3.4 Next steps in the Plasma Wakefield Accelerator Program

The most basic tools for plasma wakefield accelerator research are the high-energy density particle beams required to drive large amplitude wakes and the long high-density plasma sections that support the wakes. Section 3.4.1 will detail how FACET will make the high-energy density electron and positron bunches. Section 3.4.2 will explain how the unique properties of these drive bunches aid in creating long, uniform high-density plasmas. Sections 3.4.4-3.4.7 will show how FACET will move beyond the single-bunch experiments performed in the past at the FFTB, and accelerate a discrete bunch of electrons with narrow energy spread and high efficiency. Sections 3.4.9-3.2.9 describe the plans at FACET for the as yet unexplored field of high-gradient positron acceleration in both positron and electron beam driven wakes.

### 3.4.1 Producing High-Intensity Drive Bunches

The dramatic increase in the maximum particle energy produced by beam-driven plasma wakefield accelerators (Figure 3-1) is a direct result of the advent of high-intensity drive bunches at SLAC. There are two factors involved in achieving the high intensities needed for large amplitude wakes—a high peak current and small transverse size.

The high peak current will be achieved in FACET by making use of a threefold compression process similar to that used for the FFTB experiments. Longitudinal compression is accomplished by manipulating the longitudinal phase space of the electron bunches, which has a constant area after the exit of the North Damping Ring (NDR). Achieving the short bunches necessary to drive large amplitude wakes requires raising the beam energy and energy spread. The nominal FACET compression process is described below and illustrated in Figure 3-2.

Longitudinal bunch compression is accomplished by creating a large energy spread correlated with position along the bunch, and then providing an energy dependent path length that results in the bunch "tail" catching up with the "head". Accelerating to higher energy then reduces the relative energy spread to a level acceptable for the final focus system. The maximum beam energy available is given by the length of linac available. LCLS will operate the last kilometer of the SLAC linac with 14 GeV beams, and the FACET beam energy is thus limited to the 23 GeV reached at Sector 20.

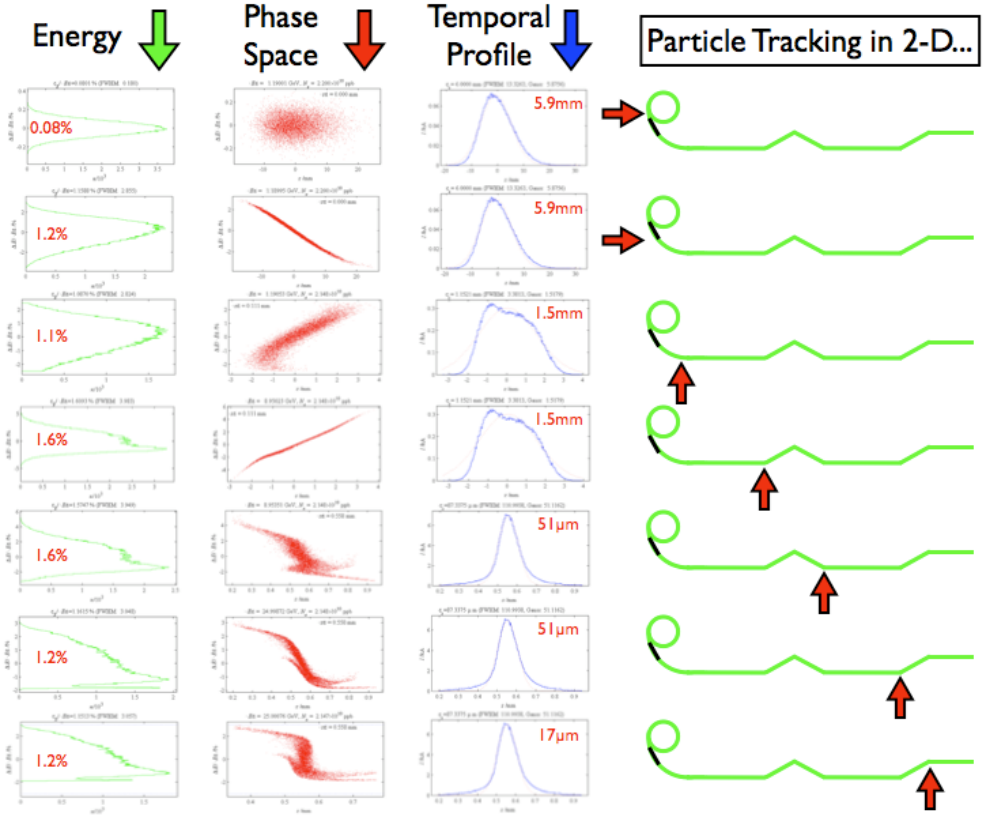


**Figure 3-2.** Illustration of the evolution of longitudinal phase space of the compressed FACET beam showing the three stage compression process.

The key advance for the short bunch program at SLAC happened in the summer of 2002 when a bunch compressor chicane was added at the 9 GeV point, roughly one-third of the way down the 3 km SLAC linac. The new chicane enabled bunches to be delivered to experiments that were fifty times shorter than before – or 12 μm rms. In a three stage process similar to that used for the FFTB, the FACET bunches will be compressed to a predicted minimum of 17 μm rms. A 6 mm-long bunch exits the North Damping Ring of the accelerator with an energy of 1.19 GeV and is given a correlated energy spread in an RF cavity run at the zero crossing phase, which leaves the mean energy unchanged. The resulting correlated energy spread, coupled with the non-zero momentum compaction factor of the ring-to-linac transport line, compresses the bunch to 1.2 mm before it enters the main linac. The phase of the accelerating structures in the linac is set to add an additional energy correlation as the bunch is accelerated to 9 GeV. As a result, at the entrance of the chicane, the tail is more energetic than the head. The magnetic chicane then compresses the bunch to 50 μm. Longitudinal wakefields in the remaining 1 km of linac impose an additional energy correlation, which is used to compress the bunch a third and final time to the minimum value of about 17 μm in FACET.

The bunch length and current distribution will be adjusted by changing parameters in the main linac. A final focus system will then deliver beams with a transverse size similar to those available in the FFTB of about 5 μm rms. The resulting combination of high-energy, small transverse size, short bunch length and high peak current create a beam ideal for driving large amplitude wakes in a beam driven plasma wakefield accelerator.

### 3.4.2 Plasma Production by Field Ionization

Producing a large energy gain requires short, high-density beams propagating through uniform high-density meter-long plasmas. When the current density of the electron bunch is high enough, the Coulomb field of the relativistic electron bunch can also create a plasma in a tube of vapor through field ionization. The plan is to use lithium vapor in the FACET experiments. With a sufficiently dense bunch, the ionization is accomplished by the leading particles of the first or drive bunch, so the majority of that bunch and any trailing bunches encounter a fully ionized plasma. Field ionization has several advantages over other techniques. Most notably it allows for the production of long, uniform, high-density plasmas with no timing or alignment issues. Plasma production by field ionization is one of the most promising techniques for producing the uniform high-density plasmas envisioned for future machines where the plasma length can be a meter or more.

The lithium vapor is created in a heat pipe oven [4] where the neutral lithium vapor density and length are controlled through the pressure of the helium buffer gas and the heating power in the oven. The buffer gas confines the hot lithium at both ends. Lithium has a relatively low ionization potential for the first electron (5.4 eV), allowing ionization sufficient for wakefield generation over a broad range of beam parameters. The larger ionization potential of the second electron (75.6 eV) ensures that the plasma density does not evolve significantly along the bunch due to secondary ionization. The plasma density is then equal to the lithium vapor density. This combination of short bunch length for multi-GeV/m gradients and the large beam density necessary to create the long high-density plasma is not available anywhere else in the world.

### 3.4.3 Computer Simulations

Current and proposed experiments operate in a regime where linear plasma theory is not valid. To help interpret the experimental data and design new experiments, this collaboration has developed extensive computer simulation capabilities that allow one-to-one modeling of the experiment in this nonlinear regime. Two numerical codes are used, OSIRIS [8] and QuickPIC [9]. OSIRIS is a 3-D, fully electromagnetic, relativistic, parallelized particle-in-cell (PIC) code that has been benchmarked against other codes and model problems that can be solved analytically. QuickPIC is a 3-D, PIC code that uses a quasi-static approximation to decrease the computing time. OSIRIS and QuickPIC include the effects of field ionization and electron beam energy loss due to radiation from oscillations in the ion column. OSIRIS and QuickPIC are now the standard tools for simulating the beam plasma interactions in our experiments and have successfully described many of the observed phenomena in a quantitative manner [10,11,12,13]. These codes can therefore be used with confidence to design the experimental program proposed at FACET.

### 3.4.4 Two-Bunch Experiments

Plasma wakefield accelerators have now demonstrated the ability to sustain very large gradients over meter scale distances. The large amplitude wakefield has been both created and sampled by a single bunch, resulting in a large, continuous energy spread in the particles emerging from the plasma. A PWFA-LC must accelerate a separate witness bunch with finite energy spread. Demonstrating this capability requires crafting two distinct bunches separated by a fraction of a plasma wavelength (~100 μm). Until now, there has been no technique capable of both producing the short, high peak current drive bunches required to drive a large wake while simultaneously creating a following bunch to sample and load the accelerating portion of the wake.

A notch collimator installed in the Sector 10 bunch compressor chicane will be used to create the two bunches needed for these next generation plasma experiments at FACET. The concept of a notch collimator is as follows. The electron or positron bunch entering the bunch compressor chicane necessarily has an energy spread that is highly correlated with position along the bunch. In the middle of the magnetic bunch compressor chicane, the beam is dispersed in energy in the bend plane. Since it is dispersed in energy, the correlated energy spread dictates that it is also dispersed in time. Thus, collimating a different portion of the bunch energy spectrum, or position at this location, will collimate a different portion of the bunch in time. By placing a collimator of appropriate variable geometry at different locations along the bunch, a wide variety of drive/witness bunch configurations can be created. One example that produces two bunches with a charge ratio, spacing and bunch length suitable for two-bunch experiments is shown in Figure 3-3. This technique can be used to generate an electron drive bunch with an electron witness bunch or a positron drive bunch along with a positron witness bunch.

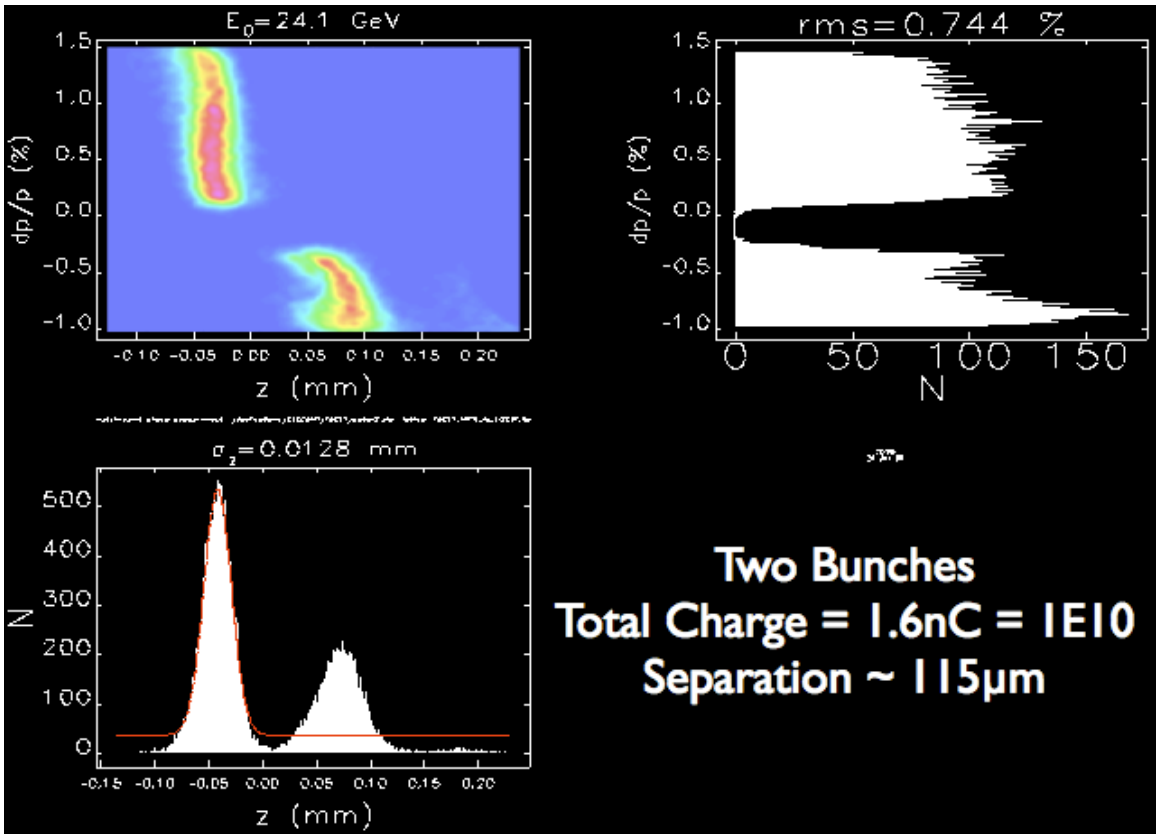


**Figure 3-3.** Simulated longitudinal phase space of drive and witness bunches at the FACET focal point. The bunches were created for FACET PWFA experiments using a notch collimator.

The collimation process is modeled in 6 dimensions (x, x', y, y', t, p) with a combination of tracking codes linked together by MATLAB. ELEGANT [14] is used to track the beam from the exit of the North Damping Ring to the middle of the Linac Bunch Compressor Chicane (LBCC) in Sector 10. The particles are then converted into an appropriate input for EGS4 [15] via the program SHOWER [16]. The notch collimator and the vacuum region around it are simulated with EGS4. The EGS4 output is then converted and loaded back into ELEGANT for tracking to the exit of the chicane and on to the FACET focal point. The notch collimator concept has the ability to craft several bunches from a single initial bunch and has been recently demonstrated experimentally [17].

### 3.4.5 High Gradient Acceleration Experiments

Accelerating a witness bunch with narrow energy spread and high efficiency is one of the primary goals of the FACET program. For plasmas to be useful in future colliders, they must provide not only high gradients, but also high energy transfer efficiency and small energy spreads. For example, a low charge witness beam can have a narrow energy spread because the beam does not extract much energy from the plasma wake, leaving it unperturbed. That is, the witness bunch produces a wakefield that is small compared to that of the drive bunch. However, this process is by definition inefficient. A high charge witness beam on the other hand produces a

significant wakefield, extracts substantial energy from the plasma wake of the drive beam and changes the plasma wake significantly. This is a necessary condition for high-energy extraction efficiency. Obtaining high efficiency and low energy spread requires judicious choice of the beam parameters and placement of the witness bunch and the drive bunch. The witness bunch must be separated from the drive bunch by just the right amount such that the witness bunch wakefield compensates for the increasing gradient of the wake from the drive bunch, thereby producing a total wakefield that is constant over the length of the witness bunch. The FACET program will take advantage of the two-bunch capability outlined in Section 3.4.4 to address these two issues for the first time. The remainder of this section will focus on the narrow energy spread, while the following section (Section 3.4.6) will focus on efficiency.

The two-bunch capability will provide a number of particles to beam load the plasma wake sufficiently to make the wake amplitude constant over the witness bunch length, and minimize the bunch energy spread. Experiments at FACET will systematically study the physics of the beam loading of plasma wakes. The witness bunch delay and charge will be varied and the corresponding energy gain and energy spread measured. These two parameters will be optimized for the maximum energy gain with the minimum energy spread.

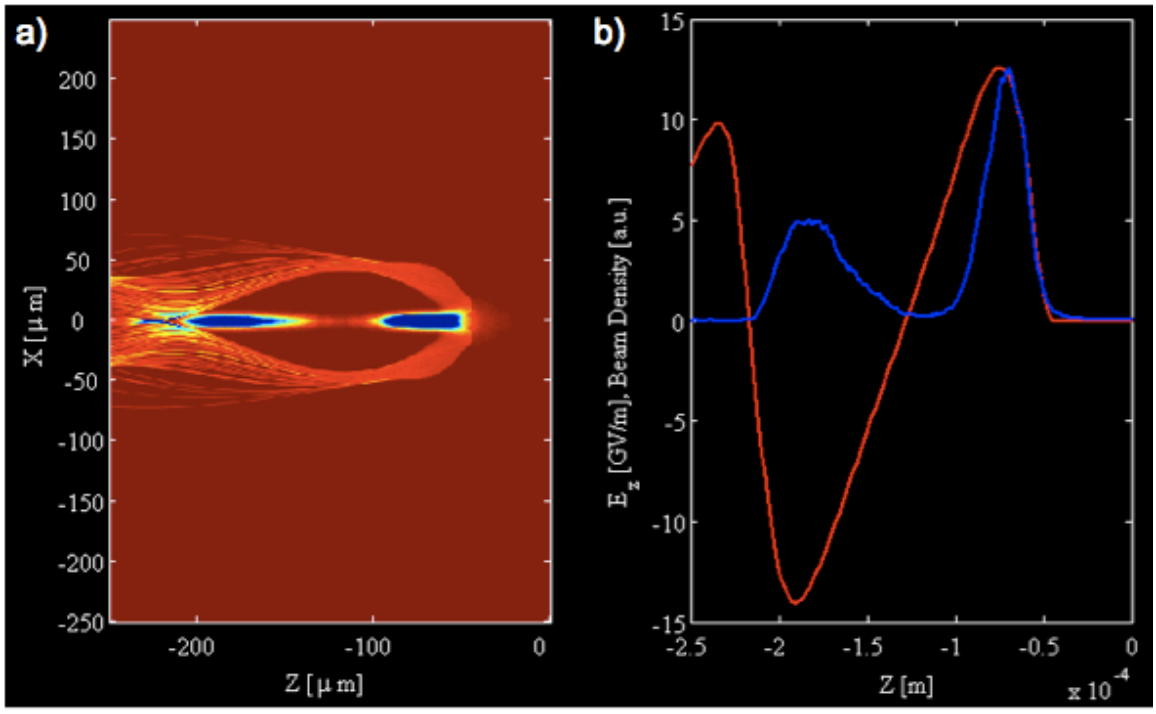


**Figure 3-4.** QuickPIC simulations showing a PWFA utilizing a drive/witness bunch configuration from the notch collimator to produce a high energy witness bunch with a relatively narrow energy spread of a few %. (a) The plasma electron response (red) to the drive beam (blue) propagating from left to right. (b) The drive and witness beam profile (blue) shown in Figure 3.4 is plotted with the resulting longitudinal electric field created by the plasma wake (red). For these simulations the drive bunch length was 14 μm, the witness bunch length was 20 μm, the bunch separation was 115 μm and the plasma density was 5.4 x $10^{16}$ e- cm-3.

### 3.4.6 Efficiency

Accelerating a second bunch with narrow energy spread will open the door to a set of measurements concerning the efficiency of the plasma wakefield accelerator. When the drive beam excites a wakefield in the plasma, if the wake is not sufficiently loaded by a second bunch, the wake will continue to oscillate behind the witness bunch. These additional oscillations correspond to energy left in the plasma that will eventually heat the plasma electrons. On the other hand, if the wake is fully loaded, the plasma electron oscillation will last for only one-half of a period and terminate after the second bunch. Such a scenario would maximize the efficiency (~95%) at the expense of a large energy spread in the second (accelerated) bunch.

The efficiency can be separated in two parts: efficiency for the transfer of energy from the drive bunch to the plasma wake, and from the plasma wake to the witness bunch. The latter is optimized through beam loading. The former is optimized by maximizing the transformer ratio $R$, defined as the ratio between the peak accelerating field and the peak decelerating field of the wake (within the drive bunch). In the linear plasma wakefield theory for a single drive bunch with a symmetric Gaussian current profile, the transformer ratio is smaller or equal to two. However, in linear theory with a Gaussian bunch, various transverse slices of the drive bunch lose energy at different rates so that some slices will lose all their energy before the others. The non-uniform energy loss will lead to less than optimal energy transfer efficiency. This is one motivation for operating in the nonlinear blowout regime where the longitudinal fields are independent of radius.

Simulations predict that, when in the nonlinear regime, bunches with Gaussian longitudinal profiles can demonstrate a beam-to-beam energy transfer efficiency of ~35% within the plasma while maintaining an energy spread of a few percent in the accelerated bunch. The two bunch experiments discussed above will demonstrate this experimentally by measuring the total charge and energy spectrum of the accelerated bunch to quantify the energy transferred from the drive bunch. Demonstrating high efficiency while simultaneously delivering a narrow energy spread bunch from a plasma accelerator operating with multi-GeV/m gradients will set the beam driven plasma accelerator apart from other advanced concepts as being the only package with a demonstrated chain of efficiency that offers a path to the multi-megawatt beam powers required to do physics in the TeV energy range.

The efficiency can be improved by using a bunch with a longitudinal current profile tailored such that all longitudinal slices lose energy at the same rate (except for the very first ones). This is accomplished by ramping up the current along the bunch, and the optimum longitudinal shape is triangular [18]. In that case, the peak decelerating wake field remains constant at a low value along the drive bunch, while the peak-accelerating field left behind the bunch keeps increasing with the bunch length. The transformer ratio then scales as $\pi$ times the number of plasma wavelengths covered by the bunch, and can be much larger than two. More sophisticated bunch profiles can lead to even larger enhancements of $R$. We propose to investigate higher transformer ratios by manipulating the phase space of the bunch along the three compression stages of the linac after the initial two bunch experiments with Gaussian beams. The compromise between optimum efficiency and beam quality will be studied and characterized.

### 3.4.7 Emittance Preservation

The high-gradient electron acceleration experiments are performed in the nonlinear "blow-out" regime of the PWFA [19]. In this regime, the beam density $n_b$ is larger than the background plasma density $n_p$ ($n_b \geq n_p$), and all the plasma electrons are expelled from the bunch volume. As a result, the focusing force of the pure ion column is linear with radius and constant along the bunch, and the peak accelerating gradient can exceed the value predicted by linear theory. However, because of the strong focusing force of the ion column, the beam may experience many betatron oscillations along the plasma [20,21]. For example, in the E-167 experiments, the betatron wavelength for the 42 GeV electrons was 1.3 cm in the $2.7 \times 10^{17}$ cm$^{-3}$ plasma, corresponding to about 65 beam betatron oscillations over the 85 cm plasma. Therefore, in a future PWFA collider application it will be desirable to match the beam to the ion column in order to avoid large changes in the beam exit angle caused by possible small variations in plasma density or incoming beam parameters.

The matching condition for a beam with a relativistic factor $\gamma$ and normalized emittance $\varepsilon_N$ focused to a transverse size $\sigma_r$ is $\gamma m_p \sigma_r^4/\varepsilon_N^2 = 1/2\pi r_e$. Considering the normalized emittances typical of future collider designs, 2,000/50 nm in the horizontal and vertical planes respectively, the transverse beam sizes matching the ion column with a density of $10^{17}$ cm$^{-3}$ are roughly 0.5 μm and 50 nm at 500 GeV and scale inversely with the fourth root of the beam energy. These beams need to be injected into the plasma cell aligned to the drive beam trajectory within a fraction of the beam size. The experiments at FACET will not reproduce such small beam sizes but will verify the basic sources of emittance dilution including hosing, filamentation, and sources of transverse coupling.

The density of a bunch with these matched sizes and $10^{10}$ electrons exceeds $10^{20}$ cm$^{-3}$ ($n_b >> n_p$). The assumption that the massive plasma ions are at rest for a few plasma periods is valid until $n_b/n_p$ approaches $m_{ion}/m_{electron}$; this assumption is then no longer valid. In this case, the drive or the witness bunch will impart such a large transverse momentum to the plasma ions that they will be focused onto the axis within one plasma wake period. The focusing of the plasma ions will create nonlinear focusing forces that will vary along the bunch, and will result in significant emittance growth of the accelerated bunch.

A number of methods have been proposed to try to mitigate the effect of plasma ion motion on the beam quality [22]. These include using atoms heavier than lithium for the plasma, *e.g.*, argon or xenon; using an input beam with a phase-space correlation to compensate for the nonlinearity of the focusing force; using a plasma with a radial density gradient similar to that used to guide laser pulses. However, a solution has yet to be demonstrated. It is therefore important to find ways to minimize the effect of ion motion both with numerical simulations and in experiments. The effect of plasma ion motion could be observed by measuring betatron oscillations [20] while varying the $n_b/n_p$ ratio or in a plasma lens experiment where the beam charge and transverse size could be varied from $n_b > n_p$ to $n_b >> n_p$. These types of experiments are ideally performed with the beams that will be available at FACET that can be focused to small transverse sizes, combined with very high peak currents, to reach densities much larger than the plasma density.

### 3.4.8 High Demagnification Plasma Lens

Plasma lenses, with their extra-large focusing strength, may be a natural complement to high-gradient, plasma-based accelerators. Beam focusing by plasmas has been demonstrated both for

electrons [23] and positrons [24,25]. However, these experiments showed low demagnification ratios (< 5) and relatively large focused transverse sizes (>1 μm at 28.5 GeV), while a high-demagnification leading to sub-micron sizes would be required for collider applications.

There are a number of very interesting experimental topics to be studied with plasma lenses at FACET. First, in an under-dense lens with a beam density larger than the plasma density, the lens is formed by expelling the plasma electrons from the bunch volume, thereby creating a pure ion column with linear radial focusing strength (free of geometrical aberrations). The dynamics of the lens formation must be studied in detail. The same two bunch capability described in Section 3 would provide a drive bunch to both create the plasma and expel its electrons, and a following witness bunch that is cleanly focused. Second, when in the focusing process the beam transverse size becomes comparable to the average distance between plasma particles (≈ plasma density$^{-1/3}$), the focusing field becomes random and may limit the ultimate transverse size achievable. Third, as the electron beam is focused its peak space charge field increases with its density and may become large enough to set the plasma ions into motion, thereby degrading the quality of the focused beam. Fourth, contrary to a magnetic lens, the focusing strength can be made to increase adiabatically along the lens itself [26] in order to reduce the lens length and beam final size, as well as to minimize the synchrotron radiation loss (Oide radiation). The combination of a well characterized high energy, high density electron beam, plasma source, specialized instrumentation and techniques developed for the plasma acceleration research are critical components to any plasma lens program and make FACET a natural facility for conducting this research.

### 3.4.9 Positron Acceleration

Positron acceleration is not as well studied and understood as the acceleration of electrons at the present time. The conceptual PWFA-LC in [7] uses an electron drive beam to generate the accelerating field for the positrons, but other concepts, like the single- and multi-stage afterburners, employ a positron drive beam [27,28] in all cases, and accelerating high average power positron beams in high-gradient plasma wakefields requires operating in the nonlinear regime. The initial studies of positron acceleration will have the goals of understanding the underlying physics of the positron/plasma interaction and establishing an appropriate drive beam configuration. To obtain good efficiency, it will be necessary to operate in a regime where nonlinear and relativistic plasma effects are important. In this regime, positron and electron beams are fundamentally different, because plasma electrons are repelled by an electron beam but attracted by a positron beam.

In the electron beam driven plasma wakefield accelerator concept the plasma electrons are blown out by the dense incoming electron bunch. The resulting bubble, containing only plasma ions and free of plasma electrons, has attractive properties as an accelerating structure. Specifically, it can support multi-GeV/m gradients with an accelerating field constant in radius. Further, the bubble provides a near ideal focusing channel for the accelerating beam that simultaneously focuses in both transverse planes with a gradient proportional to the density and linear in radius. For the positron beam driven plasma wakefield accelerator, the situation is more complicated. A dense positron bunch propagating in a plasma does not expel the plasma electrons, rather it draws them in. In fact, the beam can draw plasma electrons in from a volume proportional to the cubic skin depth of the plasma, creating plasma electron densities many times the initial neutral density. The influx of plasma electrons into the beam volume can give rise to

fields that are both stronger and more dynamic than with an electron drive beam. Nevertheless, there are scenarios where a positron beam driven PWFA can be operated successfully.

The Experiments in the FFTB demonstrated for the first time the acceleration of positrons in plasmas using the long positron bunches ($\sigma_z \approx 700$ μm) available at SLAC prior to 2003. However, the measured acceleration gradients were only of the order of 70 MV/m [29], while measurements at higher densities showed halo formation and emittance growth [12].

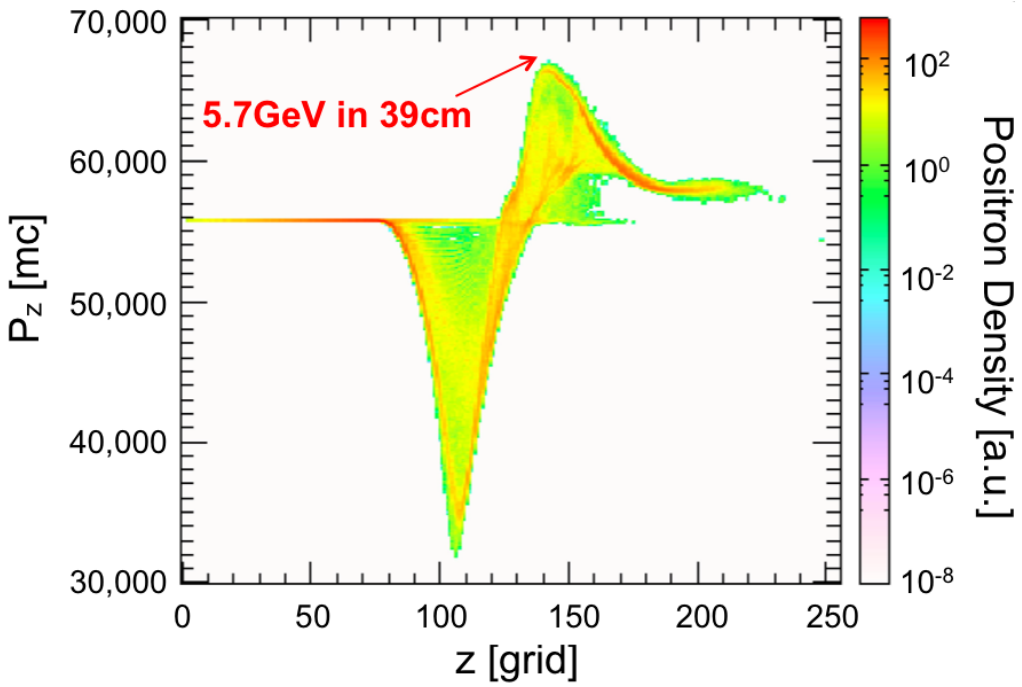


**Figure 3-5.** Simulated longitudinal phase space of a compressed positron beam after propagation through 39 cm of field-ionized plasma showing a maximum energy gain of 5.7 GeV.

Numerical simulations suggest that short positron bunches with parameters similar to the electron bunches can excite wakefields with amplitudes of the order of 5 to 10 GV/m as shown in Figure 3-5. The compressor at Sector 10 will be modified to allow for the compression of positron bunches as well as electron bunches. Then the initial positron acceleration experiments at FACET will test positron acceleration by using a single high-intensity positron bunch to simultaneously create the plasma and excite a large amplitude wake. As with the final FFTB experiments the single bunch will sample all phases of the wakefield giving a complete picture of the large and dynamic fields involved. Understanding the viability of any plasma afterburner concept requires experimental investigation of the positron beam driven PWFA operating in the nonlinear, high-gradient regime. As the only facility in the world with the capability to deliver high-energy, compressed and tightly focused positrons, this work can only be done at FACET. Subsequent experiments will study two bunch positron acceleration using the Sector 10 notch collimator to demonstrate acceleration of positrons with high gradient, good efficiency and low energy spread. After these studies, positron acceleration using an electron drive beam will be investigated as well as the use of hollow channel plasmas to improve the performance of the positron acceleration techniques.

### 3.4.10 Positron Acceleration in Electron Driven Wakes

In addition to positron acceleration using a positron drive beam discussed in the previous section, the acceleration of positrons in the high-gradient plasma wakefield excited by an electron beam will also be investigated. This approach offers the advantage of not requiring the large facilities necessary to create positron drive beams with tens of megawatt average power.

Testing this idea experimentally involves merging independent bunches of positrons and electrons produced and accelerated in the SLAC main linac. At the plasma entrance, the merged beams would need to be on the same transverse orbit, with the positron bunch trailing the electron bunch by roughly one plasma wavelength (~100 μm). Initial experiments at FACET will use a simpler approach to generate positrons *in situ* within an electron beam driven plasma wake by focusing the electron beam into a small tungsten wire located right inside the plasma [30]. Here, the electron pulse generates an electromagnetic shower, consisting of secondary electrons, positrons and photons. If the wire is thin enough, the emittance of the primary electron beam is not seriously degraded, and it can still drive a nonlinear plasma wake containing a blow-out region. Such a plasma wake includes a region where the electromagnetic fields are both focusing and accelerating for positively charged particles. Simulations suggest that this region could be used to trap positrons from the shower, and accelerate them to relativistic energies (Figure 3-6).

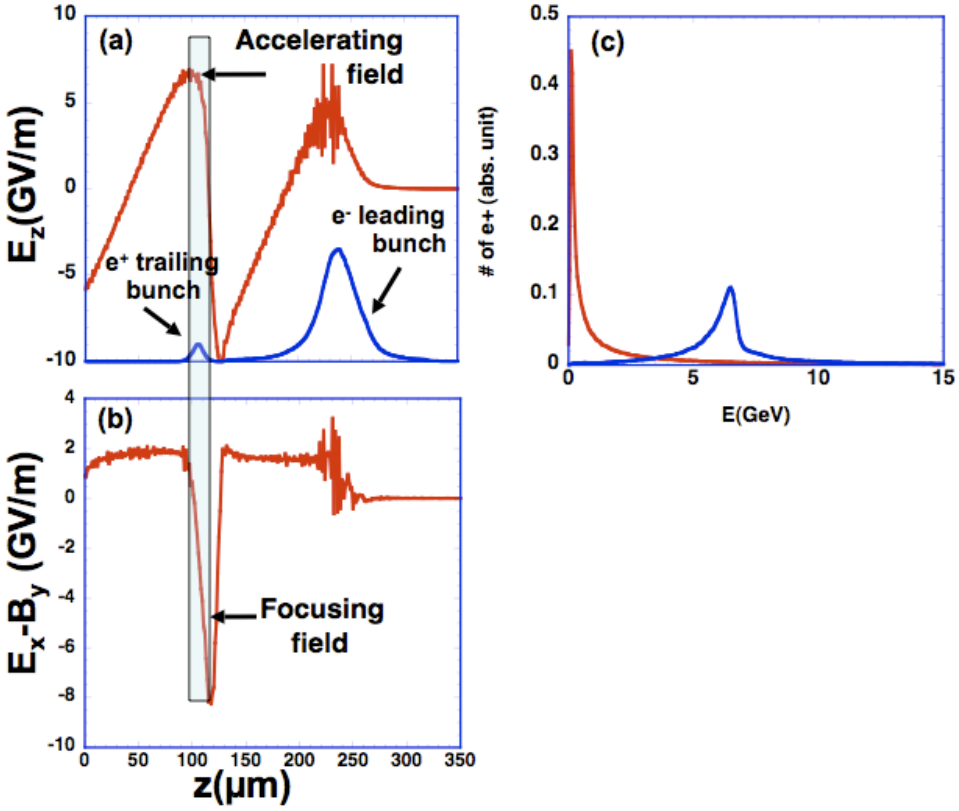


**Figure 3-6.** 3-D OSIRIS simulation results showing an electron beam driven plasma wakefield at a distance 9.5 cm into the plasma: (a) longitudinal wakefield ($E_z$) lineout propagating along the z axis, and (b) transverse wakefield ($E_x$-$B_y$) lineout along z at x=4.6 μm; and (c) Energy spectra of the positron beam load after s=0.02 cm (red line) and s=1 m of plasma (blue line). The bunches shown in (a) propagate to the right. The green rectangle overlaying (a) and (b) indicates the location where the wakefields are both focusing and accelerating for positrons and where the positron beam load is placed.

This idea, of generating positrons *in situ* within an electron beam, is speculative and in the early stages of development but, if successful, it would allow one class of positron acceleration experiments to proceed before the completion of the symmetric bunch compression chicane in Sector 10 and it would allow the demonstration of positron acceleration using electron beam driven wakes before the upgrade of the Sector 20 chicane discussed below.

If the initial experiment accelerating positrons in electron beam driven wakes is successful, it will strongly motivate developing a system where accelerating positrons in electron beam driven wakes could be tested with a high charge electron drive beam and a high charge positron beam. This would require accelerating and compressing individual electron and positron beams in the SLAC linac. This is possible because beams can be extracted from the electron and positron damping rings on the same linac pulse [31]. The electrons and positrons will have to be separated by ½ RF wavelength (5 cm) in the SLAC linac to accelerate both to high energies, and then brought together with appropriate spacing to systematically study positron acceleration in electron beam driven wakes. It is possible to do just this by modifying the FACET Sector 20 chicane to simultaneously accommodate both electron and positron beams and bring them together after a combined path length difference of 5 cm. This upgrade to the FACET facility is described in more detail in Sections 4.1.4 and 4.10.1.

### 3.4.11 Hollow Plasma Channels for Positron Acceleration

Plasma acceleration in plasma channels has been a holy grail for plasma accelerators for some time now and for several reasons. For laser wakefields the channel guides the laser, overcoming diffraction limits. For particle beam-driven plasma wakefields, channels and particularly hollow channels have been shown to offer potentially higher beam quality [32]. Numerical simulations show that plasma wakes generated by positron beams can be maximized by using a hollow plasma channel with a radius approximately equal to one plasma skin depth. The channel provides a timing mechanism for the "sucked-in" plasma electrons, preventing the phase mixing that reduces the positron wake amplitude. Since there are no charges in the hollow plasma channel, the transverse oscillations are suppressed. The beam transverse size can be larger than would be necessary to match the beam to the plasma, allowing for a higher beam current, and for a tighter focusing of the beam after the plasma exit. Plasma channels may provide an opportunity to maximize both the center-of-mass energy and the luminosity of an electron-positron plasma-based collider.

Creating hollow channel plasmas in the field-ionized regime is a challenge, yet it illustrates precisely why University-National Lab collaborations are critical to the success of FACET. Ideas exist to manipulate the neutral vapor radial profile [33], but these ideas are in their infancy and require a sustained program with the promise of eventual testing to be fully explored. While the experimental program is proceeding at FACET, colleagues at UCLA and USC with extensive experience in plasma source development can refine these ideas through laboratory testing and, once successful, bring them to FACET for testing with the accelerator. Challenging problems also bring opportunities for new collaborations to form or existing ones to expand. One example of this is the recently approved Phase 1 SBIR project 'Hollow Channels for Positron Plasma Wakefield Acceleration' [34]. Phase 2 of this SBIR program will culminate with testing the developed hollow channel plasma at FACET.

## 3.5 Dielectric Wakefield Accelerators

Future accelerators with ultra-high fields will not be based on conventional metallic resonant cavities, because the power necessary to excite such structures becomes excessive. This forces consideration of shorter wavelength linac structures. Existing linacs, which have tens of MV/m accelerating gradients in the 1 to 10 cm wavelength range, would be naturally scaled to mm and sub-mm wavelengths for GV/m operation. It would be advantageous to operate in the THz region, $\lambda \sim 0.3$ mm, but here the problem is the power source because no conventional sources exist with the power needed to achieve GV/m fields. Therefore, the emphasis has been on beam-driven wakefields to address the need for higher electromagnetic power at THz frequencies. In a dielectric wakefield accelerator electromagnetic power is radiated by an ultra-short, intense "driving" electron bunch propagating in a high impedance environment formed by a hollow dielectric fiber. This power is then used to accelerate another "witness" bunch just as in the case of the plasma wakefield accelerator.

Sufficient available power for high gradients depends on having high peak currents, a small inner radius of the hollow dielectric fiber, and, therefore, a drive beam with small transverse emittance to propagate through the fiber. The required beam can only be provided by FACET making FACET unique for exploring dielectric wakefield acceleration.

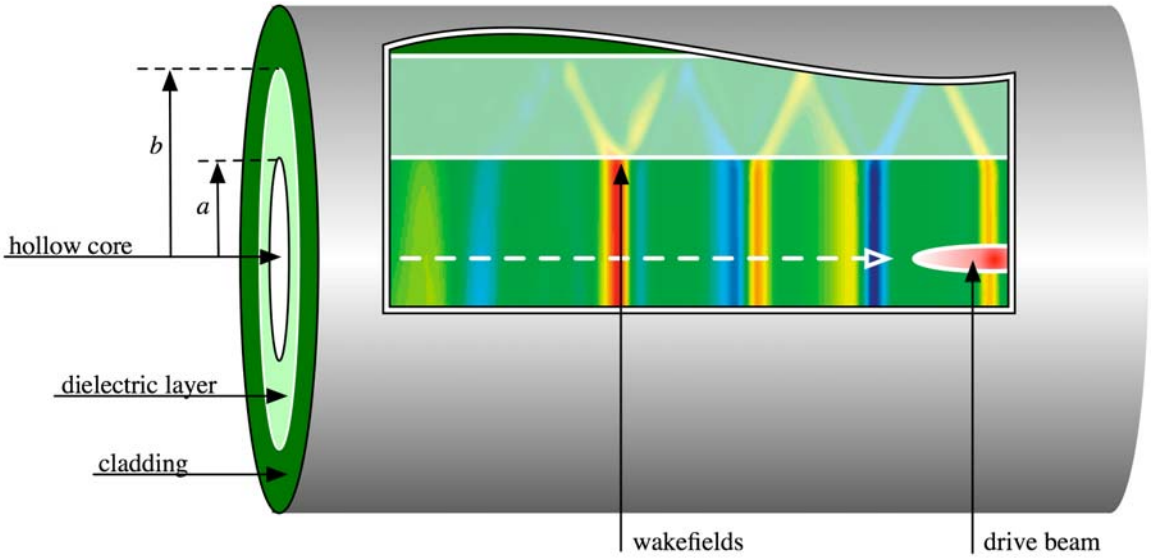


**Figure 3-7.** Conceptual drawing of the dielectric wakefield accelerator. A "drive" beam excites wakefields in the tube, while a subsequent "witness" beam (not shown) would be accelerated by the reflected wakefields (bands of color).

### 3.5.1 The Hollow Dielectric-Tube Dielectric Wakefield Accelerator

Wakefield-driven accelerating-schemes can offer high gradients and conceptually simple geometries. The Dielectric Wakefield Accelerator (DWA) based on a hollow dielectric tube is one such approach (Figure 3-7). A short (<1 ps) drive-bunch traversing the tube creates Cerenkov wakefields that propagate towards the dielectric boundary at the Cerenkov angle, and are reflected back towards the center axis, where a second bunch arrives and is accelerated [35].

The dielectric wakefield accelerator solves the THz-power problem by using radiated fields from short electron bunches, leveraging high-precision fabrication technology from developments in fiber optics, and provides a straightforward means of producing large on-axis accelerating fields. These fields may be used most straightforwardly by accelerating a trailing on-axis bunch, or by directing the radiated fields to an off-axis, higher impedance structure (step-up transformer [36]). Note that these mechanisms work equally well with electrons or positrons.

### 3.5.2 Work to Date

With the above considerations in mind, an experiment (T-481) carried out at the FFTB was designed to assess the survivability of dielectric tubes subjected to high fields generated by short electron-bunches. Tubes, produced from commercially available hollow $SiO_2$ fiber-optics, were cut, polished, baked to remove the cladding, and metallized on the outer surface. An array of 10 tubes, each 1 cm in length, was placed in a precision holder with multiple V-shaped grooves cut in parallel. The holder, which was optically pre-aligned to the nominal electron beam path, could be moved transversely to the beam path, allowing placement of any of the tubes along the beam axis. A vacuum chamber housed the holder and various beam diagnostics. Tubes of both 100 μm and 200 μm ID were exposed to a number of beam shots, with the induced wakefield tuned by variation of bunch length. CCD array cameras were placed to observe the tube-end from the top and side (relative to the beam path). The side camera image was digitized and recorded, along with relevant electron beam parameters, for offline analysis.

The main results of the T-481 collaboration include [37]:

- Demonstration of beam control (trajectory, bunch length, etc.) adequate for a dielectric wakefield accelerator;
- Generation of surface fields in excess of 20 GV/m; and,
- Measurement of breakdown fields in excess of 1 GV/m.

These results were obtained in a 2-day long run in the FFTB, and it would have been impossible to obtain them without the expertise and instrumentation developed in the plasma wakefield research. To extend these studies further, it is necessary to provide more direct experimental measures of the electromagnetic wake properties.

### 3.5.3 Next Steps

Following the success of T-481, the next round of experiments would involve three phases of development based on the FACET beams [38]. The first phase would be a detailed breakdown study including exploration of a large range of design parameter space, materials, and cladding designs; and, quantifying the fields by measurement of the coherent Cerenkov radiation. The second phase would attempt to directly observe acceleration and deceleration of particles in 10 cm length fibers. The third phase—once FACET is well characterized and fully operational—would involve significant acceleration, building on the results and expertise gained in the initial two phases, by using tubes around one meter in length.

The specific goals of the proposed dielectric wakefield accelerator studies at FACET can be listed:

- **Coherent Cerenkov Radiation (CCR) measurements**: Investigations of coherent Cerenkov radiation in the THz spectral range will serve as a measure of the fields in the dielectric, and as a bunch length diagnostic.

- **Materials**: In T-481, only fused silica tubes were tested; additional materials including CVD-fabricated diamond [39] will be explored.
- **Coating**: The thin metallic coating used on the tubes in T-481 proved inadequate to withstand ohmic heating due to induced currents. Use of dielectric cladding will be explored at FACET.
- **Varying tube diameters**: T-481 used off-the-shelf fused silica tubes which were available in 100 μm and 200 μm IDs, and fixed 350 μm OD. Several custom diameters would be fabricated, allowing the breakdown limit to be explored at fixed beam parameters.
- **Varying tube length**: Short, 1 cm tubes were used in T-481. The FACET experiments will use lengths from 1 to 10 cm with the ultimate goal of pursuing a 1 m long dielectric wakefield accelerator module. They will also allow the dependence of breakdown on time of exposure to high gradient wakefields.
- **Direct observation of beam changes:** Longer fibers will allow for the direct measurement of momentum change to the beam due to wakefield acceleration and deceleration, and may also produce notable changes in the transverse centroid due to transverse wakes.
- **Preparation**: Alternative fiber preparation techniques will be considered and tested. Different methods of cladding removal and tips polishing (*e.g.* diamond cleaving) to eliminate debris contamination in the tube bore will be employed.

### 3.5.4 Future Research

The measurements from these initial FACET experiments would significantly advance the state of knowledge on dielectric wakefield accelerators. By having characterized the breakdown threshold for multiple materials, having measured the coherent Cerenkov emission, and having shown direct energy exchange with the beam, these experiments would prove the viability of dielectric-tube wakefield accelerators with GV/m accelerating gradients.

The next phase measurements would increase the dielectric accelerator length to the meter scale and demonstrate substantial, high-gradient acceleration of beams. The β*s are significantly less than a meter, and it will be necessary to focus the beam transversely. Small bore permanent magnet quadrupoles can have high enough gradient for building a FODO array that will extend over the length of the fiber and confine the beam. Acceleration of 1 GeV or more would be measured with the dielectric fiber contained in such a FODO channel. This would open the possibility of colliders and compact, high-energy machines based on dielectric-tube wakefield structures.

## 3.6 Linear Collider Accelerator and Beam Instrumentation R&D

A TeV-scale Linear Collider aims, through clean and precise measurements, to uncover the physics behind the discoveries expected at the LHC, complementing the LHC's capabilities. This ambitious program challenges the current state of the art of both collider detector technologies [40] and accelerator instrumentation. Developing the acceleration hardware for beam manipulation and instrumentation needed for the required precision beam diagnostics, and nondisruptive collimation requires ongoing experiments with linear collider-like beams, proof of

principle demonstrations, and eventual production module tests. FACET will be an ideal venue for much of this work.

A variety of linear collider related beam tests were conducted at the FFTB, where the small spot sizes achieved enabled important material damage studies and spurred development of novel beam instrumentation such as the Shintake interferometric spot size monitor [41]. The FFTB was decommissioned in 2006, but tests continued in End Station A in 2006-08 using a 28.5 GeV beam, parasitic with PEP-II operation. The ESA programs addressed a variety of physics and R&D questions and included a suite of linear collider instrumentation experiments involving prototype energy spectrometers, prototype RF beam position monitors, and studies of collimator wakefields, the interaction point backgrounds, and bunch length diagnostics.

FACET offers a variety of possibilities for linear collider accelerator, beam handling and instrumentation R&D, in particular for those requiring electron or positron beams with large charge, good quality and small spot sizes. Precise collimation of the beam halo is required in a linear collider to prevent beam losses near the Interaction Region that could cause unacceptable backgrounds for the detector. The tight apertures of the collimators, however, cause wakefields that can result in beam deflections and increased emittance. Design studies and ESA experiments allowed optimization of the material and shape of the spoilers for the collimation system, so that wakefields generated by these collimators would be controlled. The next essential step will be a beam damage test. The experimentally measured safe beam density on the collimators will determine the length, performance and cost of the whole collimation system. The FACET beam with large charge and small size beams will be ideally suited for these critical tests. The collimator beam damage tests will likely require iteration on design and further beam measurements of the collimator wakefields. Such measurements can also be conducted at FACET.

The International Linear Collider (ILC) beam dump uses a 10bar water vortex flow to absorb 18 MW of beam power. It has a window that is a millimeter thick that separates the beam lines from the dump water. This window is of crucial importance for the reliability of the ILC design. Experimental studies at FACET will allow determination of the appropriate metal or alloy, the safe beam density, and the optimal shape of the beam dump window.

A variety of tests relevant for particle detectors and development of the linear collider physics options could also be done at FACET including studies of a small scale laser cavity for a photon collider. Various beam instrumentation such as synchrotron radiation, optical transition, diffraction radiation, beam halo and precision RF cavity position monitors can be also developed and tested at FACET.

In summary, the full-intensity, high-energy electron and positron beams available at FACET, with bunch length and size of tens of microns provide unique opportunities for developing linear collider accelerator hardware and beam manipulation techniques, diagnostic equipment, and conducting various beam damage studies. FACET will thus support and have important impact on any linear collider development program.

## 3.7 Crystal Collimation R&D

The availability of good quality, high energy electron and positron beams at FACET offers a unique opportunity to study crystal channeling of electron and positron beams. Crystal channeling and volume reflection phenomena are being actively studied now, both theoretically

and in experiments at the Tevatron, RHIC and the SPS [42], primarily for hadron beam applications. For lepton beams, the physics of interaction with crystals involves radiation, and for electrons also the enhanced interaction with nuclei and atomic electrons. One of the phenomena recently considered theoretically is the volume reflection radiation [43] of electrons and positrons in bent crystals. The process features high power radiation, larger angular acceptance in comparison with channeling radiation, and weak dependence on the sign of the charge. These properties can make it suitable to be used as a driving principle of the collimation system of high energy e+/e- collider, or as a new type of compact photon source. FACET will allow studying these phenomena and investigating applicability to a future linear collider, in particular for improvements of the collimation system.

## 3.8 THz Radiation and Science Opportunities in BES

In addition to the unique capability of FACET beams for accelerator R&D, the facility will also enable a much broader science opportunity through the high intensity electric and magnetic fields associated with the high quality beams. These fields, in fact, closely resemble half-cycle terahertz (THz) electromagnetic waves, but orders of magnitude stronger than those created by laboratory tabletop sources. Such an intense source will open up many new opportunities across a range of solid state physics.

In recent years there have been significant scientific advances in solid state physics and chemistry induced by terahertz radiation. Applications as diverse as semiconductor and high temperature superconductor characterization, tomographic imaging, label free genetic analysis, cellular level imaging and chemical and biological sensing have thrust terahertz research from relative obscurity into the limelight. Conventional laboratory sources are typically limited to peak electric fields of the order of 1 MV/m. In contrast, the fields surrounding relativistic electron beams exceed 1 GV/m. Such field strengths rival those experienced by valence electrons in materials (~1 V over the size of an atom) and their application can therefore create new states of matter previously not observable. Because the pulse length around 1 ps is considerably longer than the Bohr precession time of a valence electron (about 1 fs) in the atomic field, THz fields act like DC fields on the electron cloud and may thus distort the atomic electron cloud and even cause atomic motions which may be used to initiate chemical reactions. For these reasons, we see unique and exciting opportunities for new advances with the capabilities of the FACET beams to produce the most intense sources of terahertz radiation known today.

### 3.8.1 Relativistic Electron Beams as a Source for THz Radiation

The fields surrounding a relativistic electron bunch are shown schematically in Figure 3-8 (left). Each electron carries electric and magnetic fields that, due to relativity, are confined to a plane perpendicular to the electron motion. The total fields surrounding an electron bunch are the sums of the individual contributions, which can be divided into two regimes corresponding to coherent and incoherent superposition.

In the coherent superposition regime the total field is the sum of individual contributions from single charges and the associated fields are very large (Figure 3-8). Qualitatively we expect a picosecond field pulse to lead to a frequency spectrum extending to 1 THz (energy of 4.14 meV and wavelength of 300 μm), which is very similar to a pure half-cycle THz photon pulse,

except near zero frequency. The resulting THz field pulse from an electron bunch can be separated from the electron bunch as an electromagnetic wave by either bending the electron beam in a magnetic field or sending it through a foil, where the absorbed fields will be re-radiated as true photons. A relativistic electron beam also contains an incoherent field component. This is confined within the bunch, where the fields of the individual electrons may be out of phase.

The contributions of the coherent and incoherent fields can be calculated by the Weizsäcker-Williams method, which describes an electron beam in terms of virtual photons. The virtual photon spectrum of a typical 30 GeV electron bunch is shown in Figure 3-8 (right). The incoherent virtual photons appear as X-rays, but with a much reduced field ($E$ proportional to $\sqrt{N}$) and intensity (proportional to $E^2 \sim N$) compared to the THz component with intensity $\sim E^2 \sim N^2$.

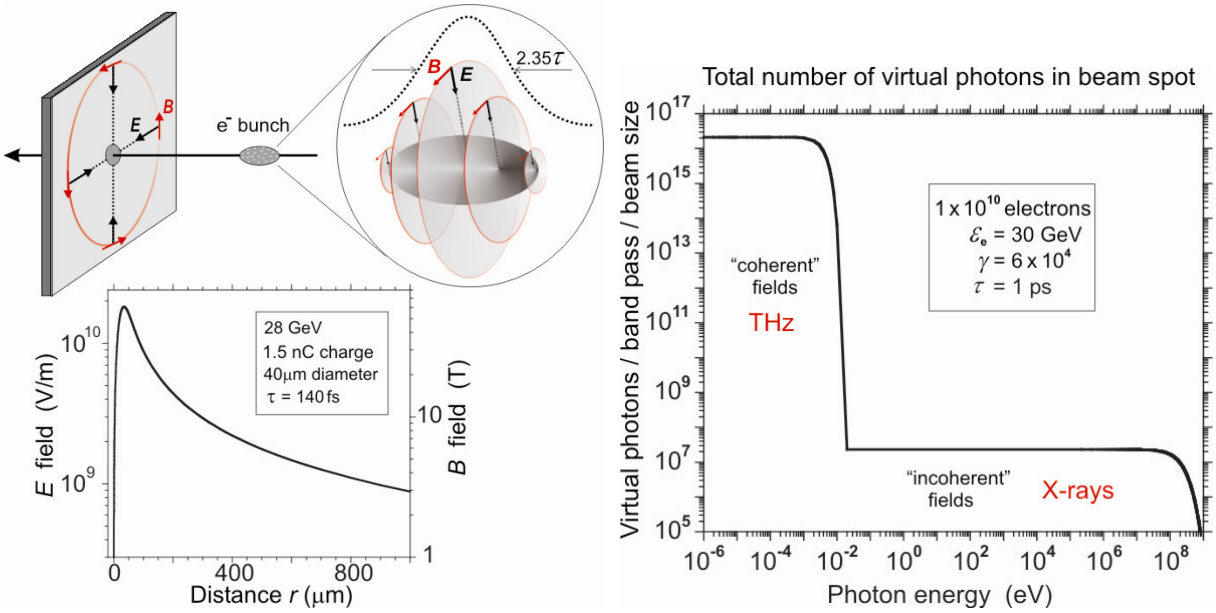


**Figure 3-8.** (left) Typical experimental geometry and characteristic spatial and temporal orientation of the electric and magnetic fields for a relativistic electron bunch incident on a stationary sample. The *E*- and *B*-field strengths versus distance from the beam center are also shown for a 28 GeV beam energy and a Gaussian $\tau$ = 70 fs longitudinal and $\sigma_r$ = 20 μm transverse bunch size. (right) The total virtual photon spectrum within a Gaussian beam radius of a 30 GeV electron beam with $\tau$ = 1 ps and bunch charge of $N = 10^{10}$ electrons.

### 3.8.2 Application to Studies of Magnetism

Recently, it has been recognized that terahertz radiation is an ideal tool for the study of spin dynamics, which is essential for the basic understanding of magnetism as well as for its technological applications [44, 45, 46]. Ultrafast changes of the magnetization induced, *e.g.*, by a laser pulse, will lead to the emission of terahertz radiation that probes the time dependence of the spontaneous magnetization [46, 47]. However, in some of the last experiments conducted at the FFTB it was also demonstrated that the terahertz radiation accompanying compressed highly

relativistic electron bunches can also be used to create very large electric and magnetic fields in metals [48]. This technique holds considerable interest and future promise.

The setup for the FFTB experiment is similar to that shown in Figure 3-8 (left), where a uniformly magnetized metal sample is placed in the relativistic electric and magnetic fields of the beam. A powerful electric and magnetic field pulse is created in a thin film of magnetic metal by a relativistic electron beam traversing the sample. As discussed previously, such electromagnetic field pulses of 100 fs – 2 ps duration are very similar to half-cycle pulses of terahertz photons [44]. The electric field of the bunch generates a magnetic anisotropy, and the resulting anisotropy field leads to a spin precession (in addition to the one introduced by the magnetic field alone), which can be detected in the magnetic switching pattern.

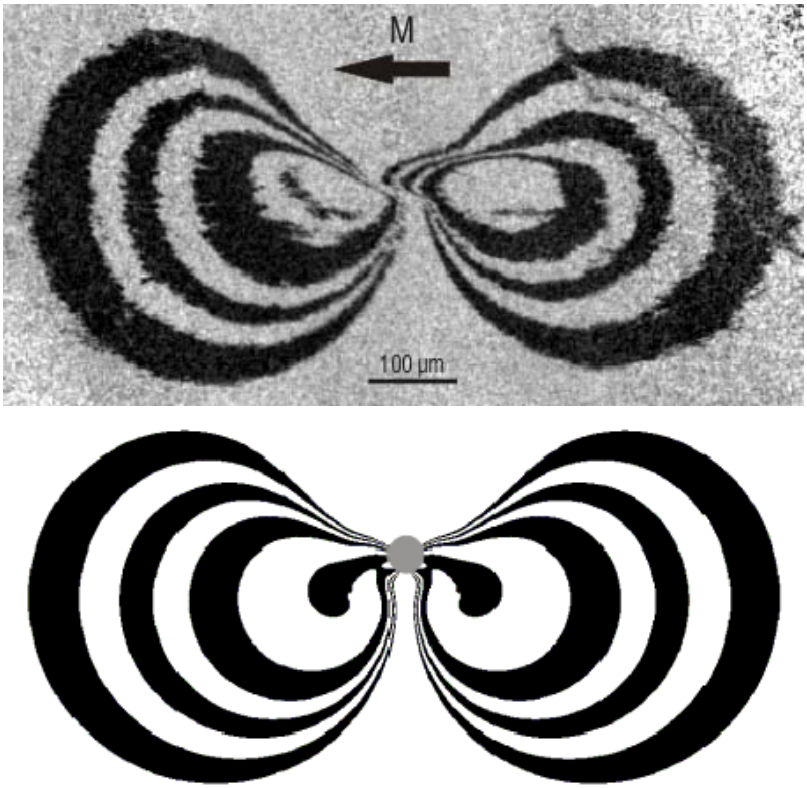


**Figure 3-9**. Observed (top) and calculated (bottom) magnetic patterns for a single compressed electron bunch of $\tau$ = 70 fs traversing a thin film sample along the surface normal. The observed pattern was recorded by spin sensitive scanning electron microscopy (SEMPA). In the light grey regions, *M* points into the preset direction as shown, while in the dark regions *M* has switched into the opposite direction. The lower pattern is calculated with the Landau-Lifshitz-Gilbert (LLG) equation including the torque generated by the induced anisotropy field due to the *E*-field of the bunch. This pattern reveals the characteristic flattening of the upper switching boundaries, created by the presence of the *E*-field inside the metallic sample. Without a penetrating electric field, this feature would be absent. The location of beam impact and width of the bunch is indicated in grey.

Using spin precession as a diagnostic tool, we were able to observe the resulting generation of a large new type of magneto-electronic anisotropy in a ferromagnetic thin film subjected to such ultra-fast (70 fs) and ultra-strong ($\geq 10^9$ V/m) electric field pulses, as shown in Figure 3-9.

This simple experiment provides the first clear evidence of a new type of magnetic anisotropy, generated by an E-field induced distortion of the valence states. Applications of magnetic materials are based on the control of magnetic anisotropies, in particular the creation of suitable atomic arrangements to manipulate the magnetic anisotropy energy. Generally, the electromagnetic fields lead to multiple ultrafast switching of the magnetization and moreover modify the electronic structure. It is safe to predict that in future applications pulses from terahertz lasers can replace the relativistic electron bunches and thus terahertz radiation will be one of the primary tools for the study and application of ultrafast magnetization switching and spin dynamics.

### 3.8.3 Investigation of Ferroelectric Switching Dynamics

The development of faster, higher density, non-volatile storage mechanisms using ferroelectric materials depends on how small one can make a functional ferroelectric domain, and how fast it can be switched in an applied electric field, with corresponding ultrafast atomic-scale displacements within the unit cell. Intense femtosecond time-scale THz fields, as will be produced at FACET, will enable control and characterization of the intrinsic dynamics associated with ferroelectric devices, and provide a new way of visualizing the processes that fundamentally determine the properties of real devices.

Ferroelectrics are materials with a dipole moment within each unit cell that is correlated across the entire crystal, giving rise to a net polarization that can be reoriented by an applied field. These are important as storage devices, as infrared sensors, and as micro-electromechanical systems. The most technologically relevant ferroelectric materials, characterized by a switchable macroscopic polarization, involve the perovskite oxide structures, for example $BaTiO_3$ or $PbTiO_3$. Figure 3-10 shows the low and high temperature phases of the perovskite oxides which, on cooling below the Curie temperature (e.g. 493$^o$C for $PbTiO_3$), undergo a tetragonal distortion leading to the development of a spontaneous polarization. The phase transition is driven by a phonon softening of optical phonon modes (which may be directly driven under THz excitation), and has been studied using a variety of Raman, x-ray and inelastic neutron scattering techniques [49, 50, 51].

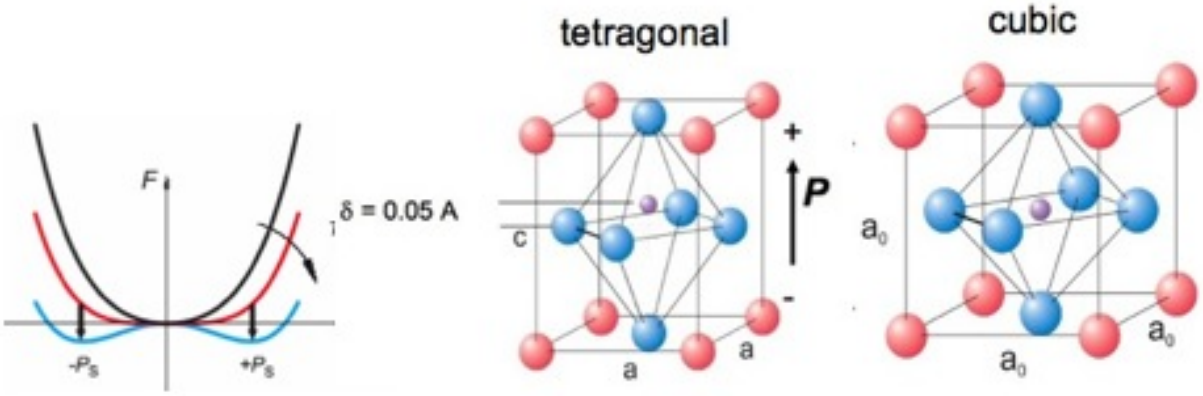


**Figure 3-10.** (left) Model free energy changes as the temperature is reduced towards the Curie temperature. (right) Unit cell structural changes associated with the development of the ferroelectric state.

Using the FACET electron beam resolves many difficulties and limitations encountered in previous experiments utilizing laboratory scale sources. Experiments at FACET would involve exposure of samples to the short pulsed electric field from beam bunches, and then the resulting domain pattern is imaged with piezoelectric force microscopy techniques. The magnitude, direction and the pulse length of the applied field can be very accurately controlled with the FACET beam. The field will be very uniform up to micrometer distances; but will be changing in magnitude and direction over larger areas, thereby allowing investigation of polarization dynamics as a function of field magnitude and direction in just one exposure. The dependence of polarization dynamics on pulse length from 100 ps down to 100 fs can be studied by changing the compression of the electron bunch.

We can anticipate the following distinct regimes of ferroelectric switching that can be probed in an experiment with FACET e-beams:

1. Domain wall creep limited regime–for fields well below the pinning field $E \le E_0 \sim 50$ MV/m and pulse lengths longer than the characteristic switching time $t \ge t_0 \sim 70\,\text{ps}$. Studying the domain size as a function of field magnitude and pulse length will allow an accurate measurement of the pinning field and switching time avoiding the difficulties associated with electrodes in [52].
2. Nucleation limited regime – for fields larger than the pinning field $E \ge E_0 \sim 50$ MV/m and pulse lengths shorter than the characteristic switching time $t \le t_0 \sim 70\,\text{ps}$. This regime cannot be accessed by any of the currently existing experimental techniques. In this regime the propagation of the domain wall will be "ballistic" and limited by the energy dissipation rate.
3. Intrinsic switching regime–for fields much larger than the pinning field $E >> E_0 \sim 50$ MV/m and pulse lengths much shorter than the characteristic switching time $t << t_0 \sim 70\,\text{ps}$. In this regime polarization switching is not limited by extrinsic (impurities, defects etc) domain nucleation mechanisms, but occurs through a coherent (homogeneous) single-domain reorientation, similar to the well-known switching of single-domain magnetic particles. Very little is known about this interesting regime in ferroelectrics.

FACET will provide a non-contact means of coupling in intense, femtosecond electric fields in order to definitively study the ferroelectric switching process. Electric fields larger than the coercive field will be easily generated and coupled into a variety of samples. We will be able to investigate the ability of samples to repetitively switch by using synchronized electrical pulses coupled in through an electrode structure that reset the sample after each electron bunch/field excitation pulse. An electrode structure will also enable us to partially bias the sample, with the THz pulse providing the final push. We expect that these kinds of studies will define the limits on which future ferroelectric devices may be expected to function, and should aid in the development of faster and more reliable devices.

### 3.8.4 Applications to Studies of Semiconductor Devices

The clock frequency of modern microprocessors is in the GHz range. However, the speed of amplifiers for state-of-the-art fiber optical communication approaches 100 GHz. Future devices will be smaller. As the dimensions shrink, parasitic capacitances as well as the gate length shrink, leading to even faster devices. At the same time, the thickness of the gate oxide is reduced to only a few nanometers. Applying a voltage to the gate leads to large electrical fields in the range of many 10s of megavolts per meter. Therefore, it is essential for the future of microelectronics to study materials under extreme electrical fields. The THz radiation from the FACET electron beam is an ideal tool to study electronic properties of materials on the femto- to pico-second time scale under extreme electrical fields. This combination makes the THz field unique to study materials for future electronic devices.

We anticipate a program of THz scattering experiments with semiconductors and insulators. The THz field will modify the electronic structure of the materials and lead to self-modulation of the THz field. In addition, time resolved laser spectroscopy using a THz pump pulse will allow us to investigate carrier generation and dynamics caused by the electrical field of the THz pulse in the time domain. The THz field can be modified by lithographically defined micro antennas on the sample, leading to even stronger electromagnetic fields by concentrating the THz radiation to a small area. It will be extremely interesting to study the limits of electronic conduction in metals and semiconductors.

### 3.8.5 Applications to Studies in Chemistry

There are a vast number of economically important processes that rely on reactions at surfaces and interfaces, such as catalysis in chemical and energy production. The microscopic understanding of reactions at surfaces requires an in-depth knowledge of the dynamics of elementary processes on an ultrafast timescale. The intermediates that appear in each elementary step are present only for a short period of time and at extremely low concentrations. Therefore they are often undetectable under steady-state conditions. As a consequence, it has been extremely challenging to visualize the underlying reaction mechanism and dynamics of processes at surfaces.

One approach to the study of an ultrafast excitation is to initiate a chemical reaction and then probe the progression of the reaction. Excitation of phonons, frustrated rotational and translational motions of molecular adsorbates plays an important role in processes at surfaces that are driven by kT, *i.e.*, temperature. These mechanisms account for nearly all the processes of essential societal and economical interest. Femtosecond visible laser pulses have been used to trigger the reaction. Laser pulses heat the electrons, leading to a very high transient electronic temperature followed by the subsequent energy transfer to phonons and frustrated vibrational modes. As vibrational temperature rises, the reaction is initiated and the time evolution is followed through products released into the gas phase [53, 54, 55]. At the moment, there exists no direct way to pump surface reactions by exciting the motion of the nuclei of an adsorbed molecule on an ultrafast timescale.

The ultra short electron bunches in FACET open up the opportunity to develop new methods for triggering the motion of nuclei. Assuming an electron pulse width of 100 fs, broadband radiation will be obtained with cut-off frequencies as high as 10 THz, which matches the frustrated vibrational motions of adsorbed species on the surface. Therefore a temperature

jump over an ultra short time scale is possible by exciting frustrated vibrational motions using an ultra short electron bunch. There are no other excitations that generate any large amount of charged hot carriers, making for a clean experiment.

Not only is the frequency of the pulse of major interest, but also the directional electric field. One of the important developments in the last decade has been the direct control and manipulation of atoms and molecules as exemplified by the movements of individual atoms and molecules on solid surfaces by means of scanning tunneling microscopes (STM) [56]. The manipulation is achieved through application of a strong electric field, typically >1x10$^9$ V/m (or >0.1 V/atom) as illustrated in Figure 3-11. Electric field pulses with durations in the 100 fs – 1 ps range and comparable field strengths can be used to drive chemical reactions [57].

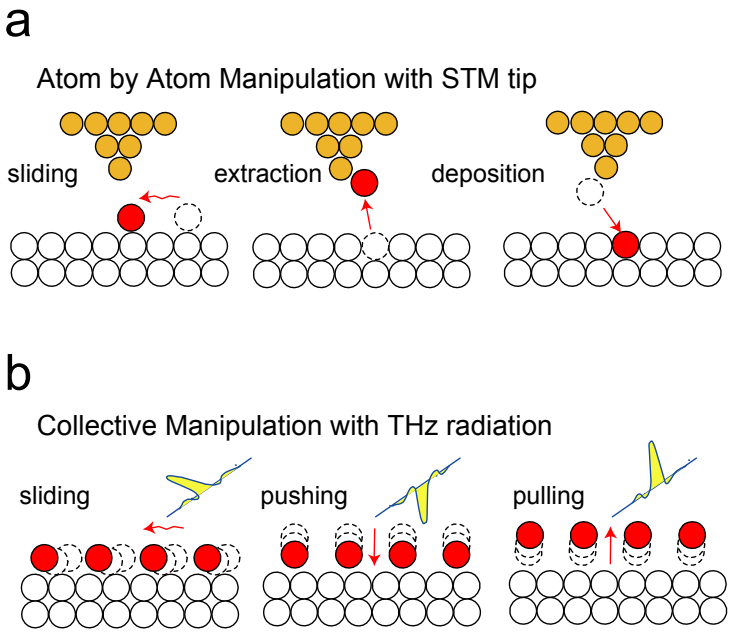


**Figure 3-11.** a) Atom by atom manipulation with a STM tip [55]. b) Collective manipulation with strong photon field with half cycle electric field pulse in different directions to the surface.

One experimental approach is to prepare monolayers of adsorbed molecules on single crystal metal surfaces and position the sample near an electron beam to initiate the chemical reaction. When the electron beam passes by, a strong electric field is produced close to the surface for an ultra short time period, *i.e.*, ~100 fs, resulting in exposure to broad band THz radiation. The THz temperature jump or the strong electric fields will stimulate processes on surfaces. In order to detect whether a surface reaction has occurred, the angular direction of desorbing products can be analyzed using a mass spectrometer. In the temperature jump process, the absorbed THz radiation dissipates among several degrees of freedom and the angular distribution of desorption products should show a simple cosine distribution similar to that observed for conventional thermal desorption experiments. On the other hand, if the desorption is induced by the strong electric field, the desorbing products are expected to be strongly peaked in a direction related to the direction of the molecular motion being excited in the excitation process. FACET will therefore provide a unique tool for studying surface processes over a wide range of reactions that are of primary societal and economic interest.

THz radiation may also be used to turn on and off electrochemical reactions. Fuel cells are used to produce electricity, in a process where a proton produced from hydrogen is electrochemically combusted on the surface of a catalyst that is immersed in an electrolyte solution. There is an ionic layer formed in the electrolyte solution near the catalyst surface, denoted the electrochemical double layer. This double layer is essentially a capacitor, with an extremely strong E-field inside the electrochemical double layer of the order of 1 GV/m [58]. The ultra short electric field pulse from FACET, with comparable field strength, provides a means to change the electron affinity in the electrochemical double layer over very short time durations. The electron affinity change will result in a variation of the electron transfer rates across the interface and can turn on and off the electrochemical reaction. A demonstration that THz radiation can stimulate the electrochemical process would be possible by studying the oxidation of a Pt electrode covered with CO in an acid solution. The reaction yield of a THz radiation stimulated process would be evaluated by comparing the electrochemical oxidation current of samples with and without THz irradiation. Once again, the unique properties of the FACET beams would be crucial to this area of research.

# 4 Technical Description of FACET

## 4.1 Introduction

FACET is a new experimental facility located in Sector 20 of the linac tunnel, upstream of the point where the LCLS injector joins the linac. It will support experiments requiring tightly focused and compressed beams of electrons or positrons. The FACET installation in Sector 20 consists of a bunch compressor, a final focusing section, an experimental area and a beam dump. FACET will also include modification of the bunch compressor in Sector 10, to compress positron bunches as well as electron bunches.

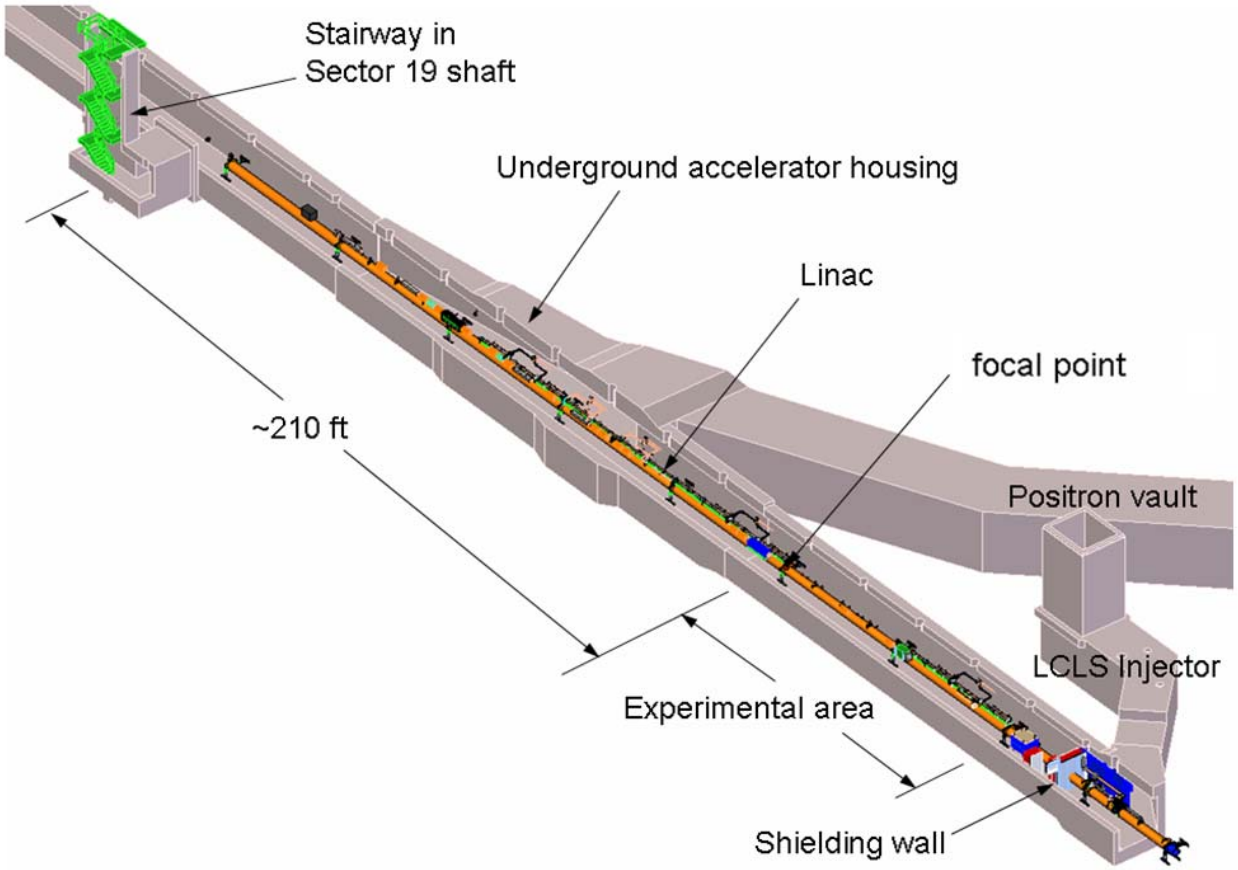


**Figure 4-1.** Cutaway view of the underground linac tunnel in the Sector 20 FACET region.

A cutaway drawing of the linac tunnel in this region is shown in Figure 4-1. Cross-sectional views of the linac housing upstream of the final focus and at the position of the FACET focal point are shown in Figure 4-2 and Figure 4-3. The existing light pipe is part of the linac alignment system and will be left in place for this purpose, although the accelerator and its associated support structure and waveguides will be removed in the area of the focal point. Also shown are two quadrupole magnets on the overhead bypass lines previously used to transport beams of electrons and positrons to PEP-II.

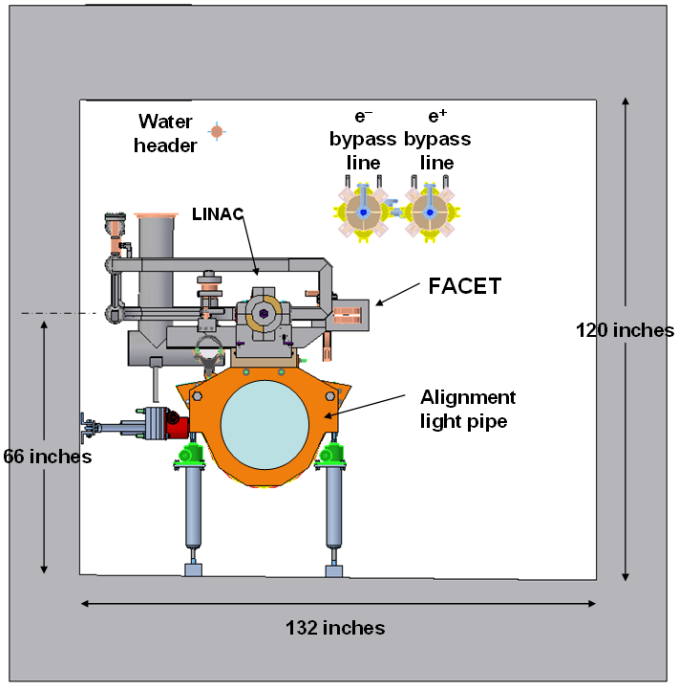


**Figure 4-2.** Tunnel cross section upstream of the FACET chicane region. The linac and its support structures are shown above the alignment light pipe and the e+ and e- bypass lines that transport electrons and positrons to the PEP-II HER and LER rings.

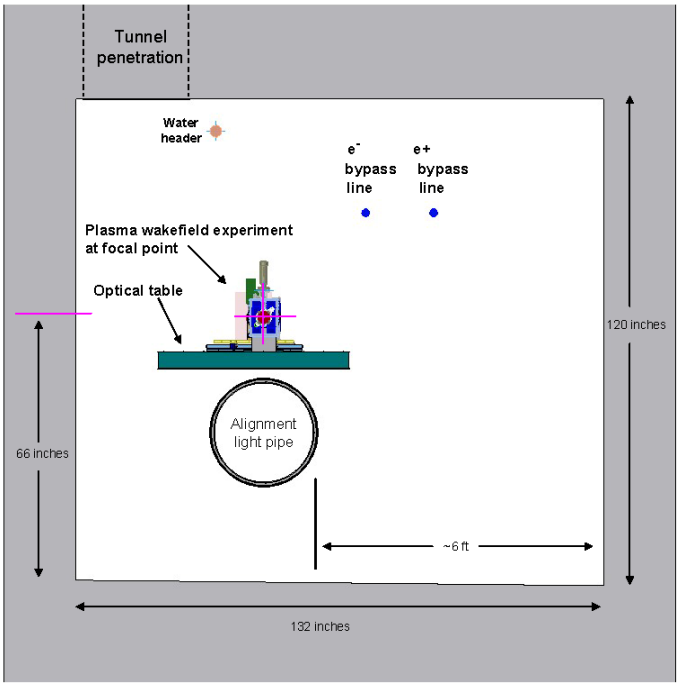


**Figure 4-3.** Tunnel cross section at the position of the FACET final focus. For illustration of the size of the experimental area, a four-foot wide optical table is shown which serves as a mounting platform for a lithium oven, centered on the FACET beam position, for the plasma wakefield acceleration experiment.

The linac beam trajectory, the light pipe, and the electron and positron bypass lines to PEP-II are visible in Figure 4-4, a photograph taken in the linac housing near the proposed FACET focal point. Penetrations extending up to the Klystron Gallery above are located at twenty foot intervals along the tunnel, providing convenient access for pipes, conduits, and cables. Existing cable trays visible in the upper right corner of the photograph can accommodate the anticipated experimental requirements.

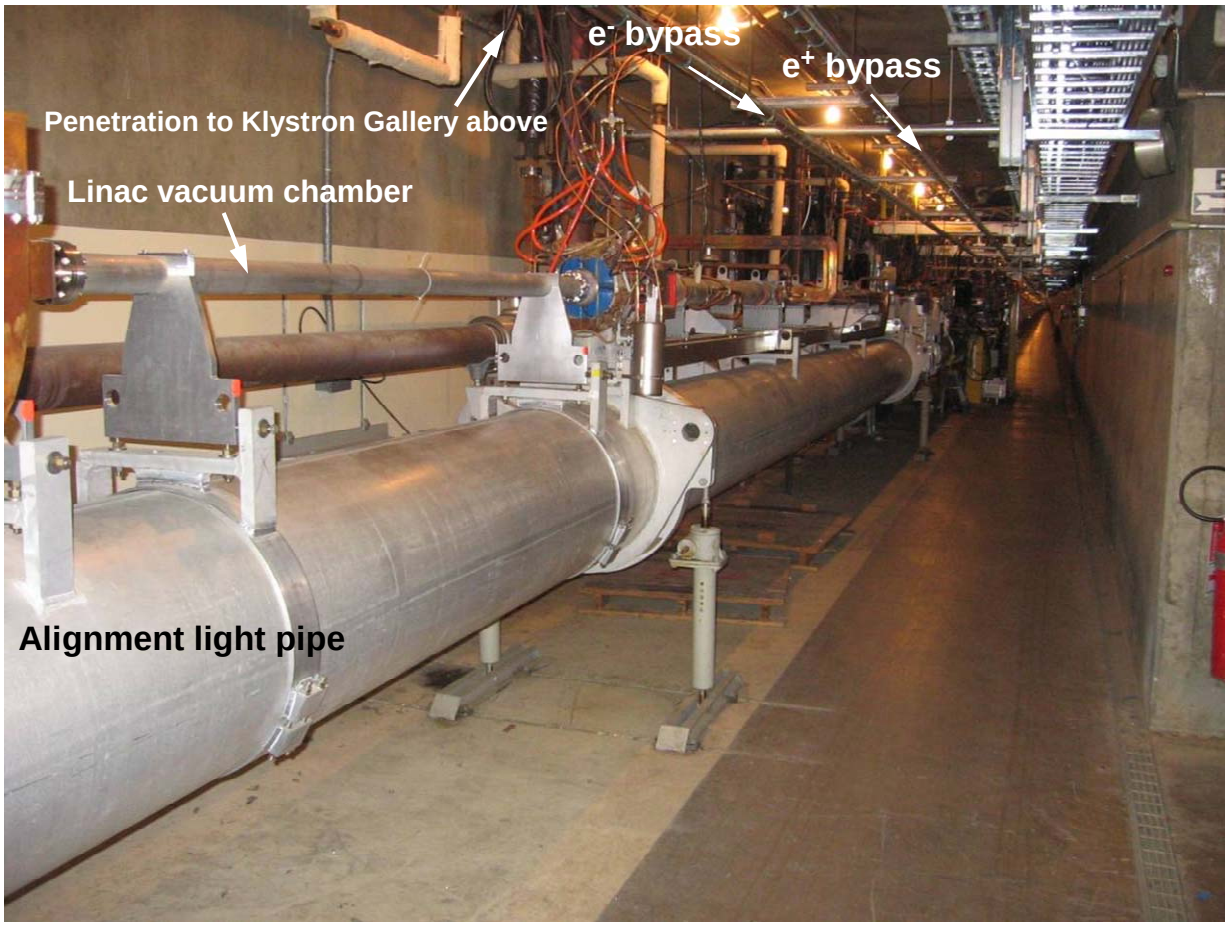


**Figure 4-4.** Sector 20 FACET region in the linac tunnel. The linac beam passes through the vacuum pipe directly above the large laser alignment pipe. The electron and positron transport lines are visible overhead on either side of the row of light bulbs, and a convenient cable tray runs along the upper right.

### 4.1.1 Modes of operation and parameters

The FACET project will provide beamlines hardware and systems allowing operation with either an electron bunch or a positron bunch delivered to the Sector 20 experimental area. A future upgrade will allow simultaneous delivery of both the electron and positron bunches to Sector 20. The next sections describe details of FACET operation in these modes.

**Table 4-1.** FACET beam parameters

| | |
|---|---|
| Energy | 23 GeV with full compression and maximum peak current. |
| Charge per pulse | 2 x $10^{10}$ (3.2 nC) $e^-$ or $e^+$ per pulse with full compression. |
| Pulse length at IP ($\sigma_z$) | 25 μm with 4 % fw momentum spread with full compression and 40 μm with 1.5 % fw momentum spread with partial compression. |
| Typical spot size at IP ($\sigma_{x,y}$) | 10 to 20 μm nominal. |
| Repetition rate | 30 Hz |
| Momentum spread | 4 % full width with full compression; (3% FWHM);<br>< 0.5 % full width without compression. |
| Momentum dispersion at IP<br>(η and η') | 0 |
| Drift space available for experimental apparatus | 2 m from last quadrupole to focal point; approximately 23 m from the focal point to the beam dump. |
| Transverse space available for experimental apparatus | 3 x 3 m |

### 4.1.2 Electrons to Sector 20

The linac accelerator facility was modified and upgraded in the 1980's to generate and accelerate beams of electrons and positrons for the SLC program at repetition rates of up to 120 pulses per second [59]. This facility has been in nearly continuous use to provide short intense bunches of electrons and positrons for PEP-II, as well as for the FFTB and ESA programs. A few years ago, a compressor chicane system was added in Sector 10 to provide a method for compressing electron bunches to unprecedentedly short length with corresponding high peak current to support new research programs in the FFTB facility [60].

The proposed Sector 20 FACET facility will take full advantage of the linear accelerator and all these improvements. Pulse repetition rates up to a maximum of 120 pulses per second can be accommodated with the existing control and timing systems. For most applications, 30 pulses per second repetition rate is likely to be the most cost effective mode.

The linac systems up to the Sector 20 experimental area will operate independently of any LCLS activities, and experimenters will be able to enter the linac housing in this area while the LCLS is operating.

### 4.1.3 Positrons to Sector 20

FACET can deliver either electrons or positrons to the proposed new experimental area in Sector 20. The production of positrons involves first accelerating an electron beam to Sector 19, where it is directed onto a target to produce positrons. The positrons are then returned to the South Damping Ring (SDR), where they are stored until the next linac pulse.

The existing pulse compression chicane in Sector 10 only works with electrons. This is a consequence of the geometry of the chicane, which only allows beams of one charge to pass. To produce a compressed positron bunch requires that the chicane be made symmetric, allowing both electrons and positrons to pass through.

Switching the Sector 20 focusing system between electrons and positrons will require reversing the polarities of some of the magnets, a procedure likely to take about a day or two to complete. This will not be practical as a routine quick-switch operation; however, switching polarities can be done whenever the research program requires the opposite charge, and the work required to switch polarities can be done outside the linac housing without interfering with any other running accelerator program. With the magnet polarities reversed, a positron beam can be focused and delivered to experiments in Sector 20, and the beam parameters will be virtually identical to those that can be achieved with electrons.

The mode of operation likely to be most reliable and economical will involve pulsing the linac at 30 times per second, with 15 pulses accelerating electrons to the production target, interleaved with 15 pulses per second of positrons delivered to the experimenters. Faster rates are possible, including a maximum possible rate of 120 pulses of positrons per second, accelerated on the same linac cycles as 120 pulses of electrons used to make more positrons.

### 4.1.4 Electrons and Positrons

The mode of operation with simultaneous electrons and positrons will only be possible after the FACET upgrade, at which time the positron arm of the sailboat chicane will also be completed.

## 4.2 Sector 20 Beamlines

### 4.2.1 Beamline design

The new FACET lattice will be installed in Sector 20 beginning after quadrupole QLI19-901. A schematic plan view of the magnet layout is shown in Figure 4-5, while Figure 4-1 provides a cross-sectional view of the linac tunnel with existing components and the new FACET beamline. The lattice consists of the chicane section, the Final Focus (FF) section, and the experimental area with a beam dump. The beam Interaction Point (IP) is located 2 m downstream of the last FF quadrupole. The present proposal includes only the lower chicane in Figure 4-5 to provide the transport and bunch compression either for electron or positron beams. All initial experiments can be carried out with this single beamline.

The FACET design is compatible with a future upgrade option, where the upper chicane is added (not part of this proposal) to allow a simultaneous transport of both the electron and positron bunches placed longitudinally adjacent to each other for a drive and witness bunch arrangement. This scheme entails a low charge positron bunch accelerated one-half S-band wavelength ahead of a stronger electron bunch in the linac. The electron bunch is sent through the lower chicane and the positrons through the upper chicane in Sector 20. These chicanes provide the same compression for e- and e+ bunches and the specified path length difference of 52.7 mm. The latter results in the e+ witness bunch emerging from the chicane slightly behind the e- bunch at a position where it can be accelerated by the electron driven plasma wakefield at the IP. The distance between the e+ and e- bunches can be adjusted by variation of the trajectory

in the upper chicane. Both beams are focused to the same round spot size at the IP in the Final Focus section.

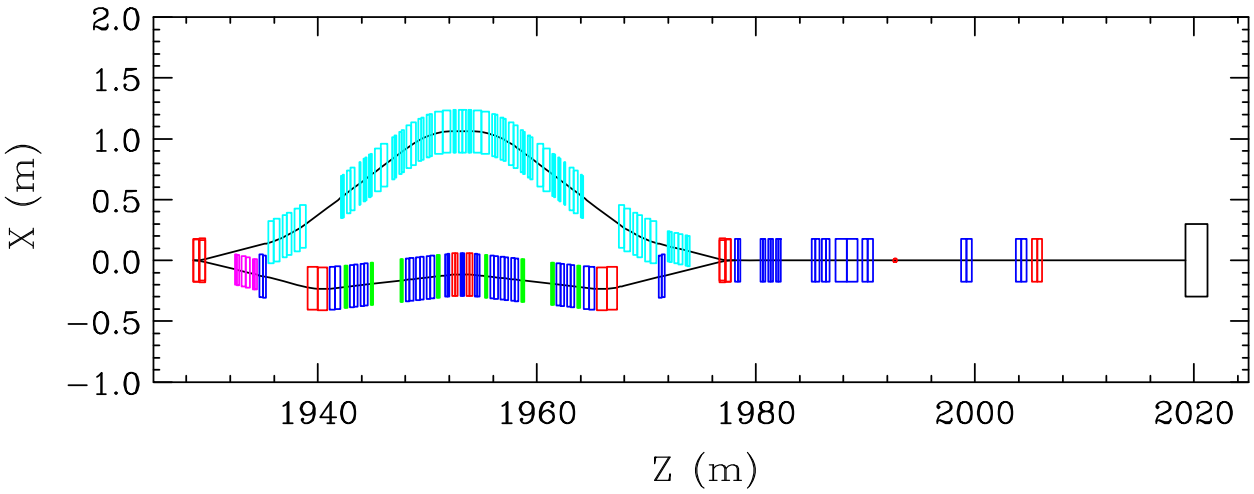


**Figure 4-5.** FACET horizontal layout in Sector 20, where quadrupoles are shown in blue, bends in red, sextupoles in green and the dump in black. The IP is at Z=1992.7 m. The present proposal includes only the lower beamline which can transport and compress either electron or positron beams. The upper chicane (shown in light blue) can be added later for simultaneous transport of electrons and positrons for a drive and witness bunch arrangement.

The Sector 20 lower chicane optics in Figure 4-6 is designed to be compatible with the future upgrade to the upper positron chicane. This places constraints on the geometric configuration as well as on the chicane optical properties. The latter must take into account that the simultaneously transported e- and e+ beams will share quadrupoles in the 2 km linac as well as in the FACET Final Focus and the experimental line. This leads to opposite focusing of the e- and e+ beams in the shared quadrupoles resulting in a special transformation property, where the horizontal matrix $M^-_x$ for electrons is the same as the vertical matrix $M^+_y$ for positrons, and vice versa. This also naturally leads to a matched condition, where the horizontal beta function $\beta^-_x$ for electrons is equal to the vertical beta function $\beta^+_y$ for positrons, and vice versa. In order to preserve this condition in the separate e- and e+ chicanes in Sector 20, they are designed to have the same matrix property, i.e. $M^-_x = M^+_y$ and $M^-_y = M^+_x$. The latter greatly simplifies the e- and e+ beta match in the downstream shared Final Focus, since the e- and e+ beta functions are automatically the same except for the exchange between x and y planes. In addition, the quadrupole and bend magnets in both chicanes are designed to provide the same linear matrix term $R_{56}$ = 4 mm necessary for the final bunch compression, the specified 52.7 mm path length difference, cancellation of the 1st order dispersion, and geometric separation between the e+ and e- magnets. The chicane optics is made symmetric in order to simplify the design and minimize the number of magnet families. Finally, three families of sextupole magnets are included in each chicane to minimize chromatic variation of β functions and 2nd order dispersion at the IP, and reduce the 2nd order momentum compaction term to $T_{566} < 100$ mm. A wiggler section consisting of three vertical bends is included in each chicane to generate a pattern of synchrotron radiation suitable for measuring the beam energy without interfering with the primary program. Beta

functions in the lower and upper FACET lines are shown in Figure 4-6, and the dispersion functions in Figure 4-8.

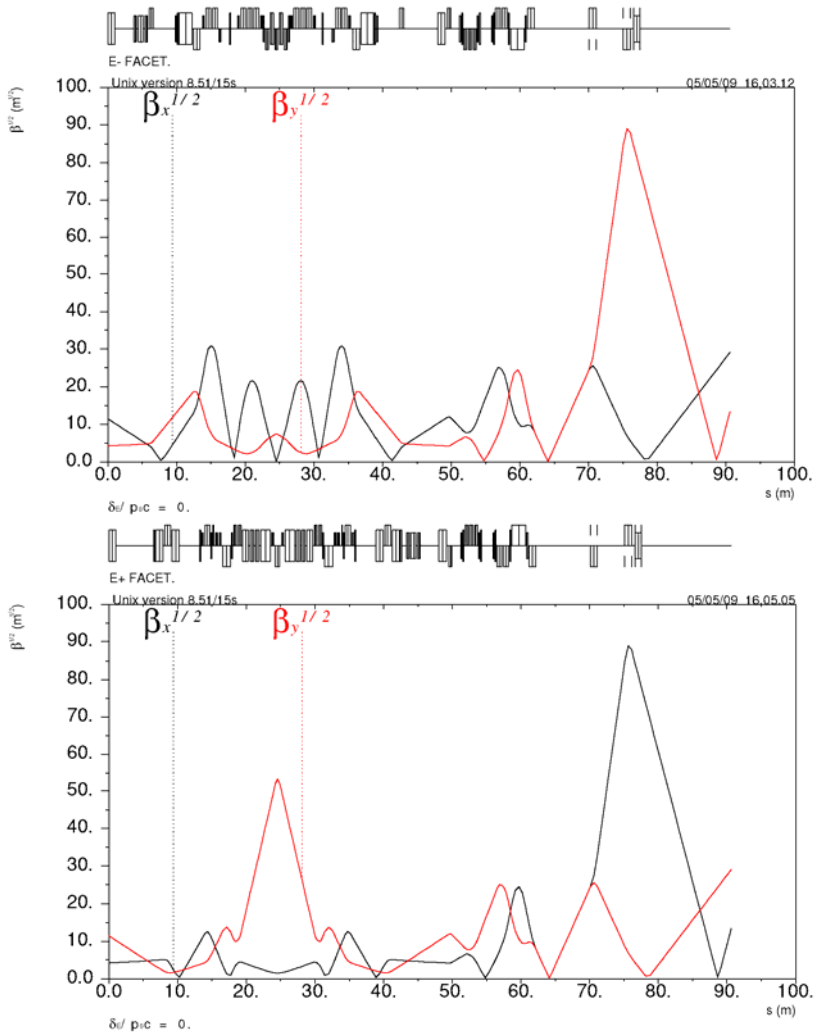


**Figure 4-6.** FACET beta functions in linac Sector 20 for e- (upper figure) and e+ (lower) beams. The IP is at S=64.1 m, where $\beta^* = 6$ cm.

The FACET Final Focus located downstream of the chicanes consists of 5 quadrupoles: a matching doublet and a FF triplet. The triplet focuses the beams to a round spot at the IP. The FF quadrupoles provide sufficient range for tuning of the IP beta functions. This may be needed for optimizing the IP beam spot as well as for matching to the strong plasma focusing.

In this proposal, with only the lower chicane installed, the routinely achieved linac emittance of $\gamma\varepsilon_x = 50$ μm, $\gamma\varepsilon_y = 5$ μm is planned to be used which requires the IP beta functions in the range of $\beta_x^* = 1.5$ cm, $\beta_y^* = 15$ cm for a round spot size. In the FACET upgrade option, with both chicanes installed, the e- and e+ round IP sizes are easier to achieve with round emittances and beta functions, in the expected range of $\gamma\varepsilon_x = \gamma\varepsilon_y = 25$ μm (coupled beam in damping ring) and $\beta_x^* = \beta_y^* = 6$ cm. With this parameters, the ideal 1st order IP beam size $\sqrt{\beta\varepsilon}$

at 23 GeV is within 4-6 μm. This is below the specified 10-20 μm spot size which permits enough room for expected growth due to various aberrations caused by large beam energy spread, synchrotron radiation and errors. The relative contributions from these aberrations depend on the specific beam parameters and optics. Typically, the synchrotron radiation at 23 GeV from Sector 20 magnets increases the horizontal spot by 40-70% depending on e- or e+ beamline, beta functions and emittance. The large 4% energy spread in the final beam may create up to a factor of two growth. The latter is expected to be reduced with further optimization of chromatic correction.

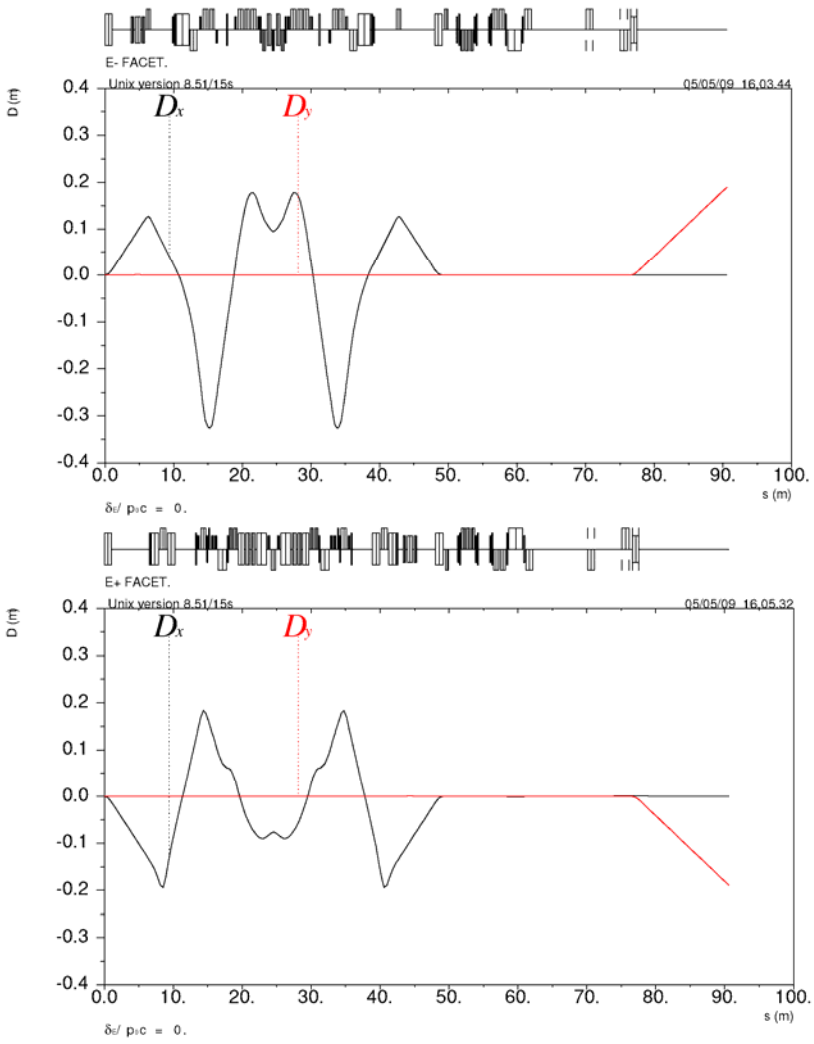


**Figure 4-7.** First order dispersion functions in the FACET linac Sector 20 for e- (upper figure) and e+ (lower) beams. The IP is at S=64.1 m.

Lattice in the experimental and dump line consists of a quadrupole doublet located 6 m after the IP, followed by a vertical bend magnet. The two quadrupoles can be adjusted to focus the extracted beam to a second focal point; and the bend magnet creates a 14 mrad vertical deflection directing the beams to the dump.

The linac Sector 19 will be used for betatron matching to the FACET optics in Sector 20. Six out of eight quadrupoles in Sector 19 will be adjusted to match to the beta functions in Sector 20, while the other two quadrupoles must remain at their nominal strengths since they are part of the positron production line attached to Sector 19. These two quadrupoles provide a fixed deflection for the offset electron beam directed onto the positron target. The changes in Sector 19 will also require adjustment of six quadrupole families in the production line in order to maintain a small beam size at the target.

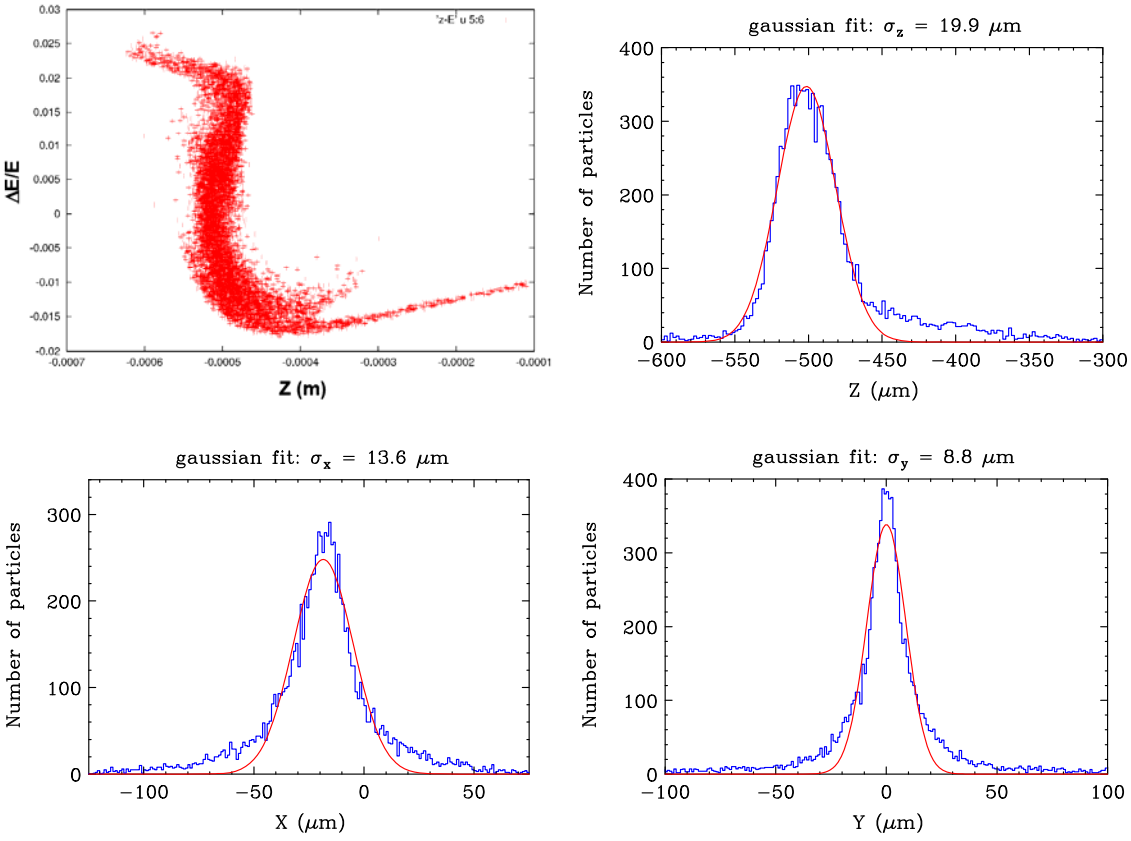


**Figure 4-8.** Beam tracking simulation for the present FACET proposal with only the lower (electron) chicane installed. Longitudinal phase space Δp/p vs. Z (top left), bunch length profile (top right) and transverse X and Y profiles (bottom) at the IP.

Simulation of IP beam distribution for the present FACET proposal, with only the lower chicane installed, is illustrated in Figure 4-8. This was obtained using the code DIMAD [61] by tracking a 23 GeV beam in the ideal Sector 20 lattice taking into account the synchrotron radiation effects. The initial beam at entrance into the Sector 20 was simulated with a Gaussian X-Y spread for normalized emittance of $\gamma\varepsilon_x$ = 50 μm, $\gamma\varepsilon_y$ = 5 μm. The initial longitudinal distribution was realistically simulated using the LiTrack code [62]. In this case, the bunch length was minimized taking into account the momentum compaction in the linac RTL line and in the Sector 10 and 20 chicanes, as well as the effects of wakefield in the linac. The IP beta functions were set to $\beta_x^*$ = 1.5 cm, $\beta_y^*$ = 15 cm. The simulations show that the Gaussian fit rms

bunch length is $\sigma_z$ = 19.9 μm yielding 17.4 kA peak current, and the Gaussian fit rms X-Y sizes are $\sigma_x$ =13.6 μm, $\sigma_y$ = 8.8 μm.

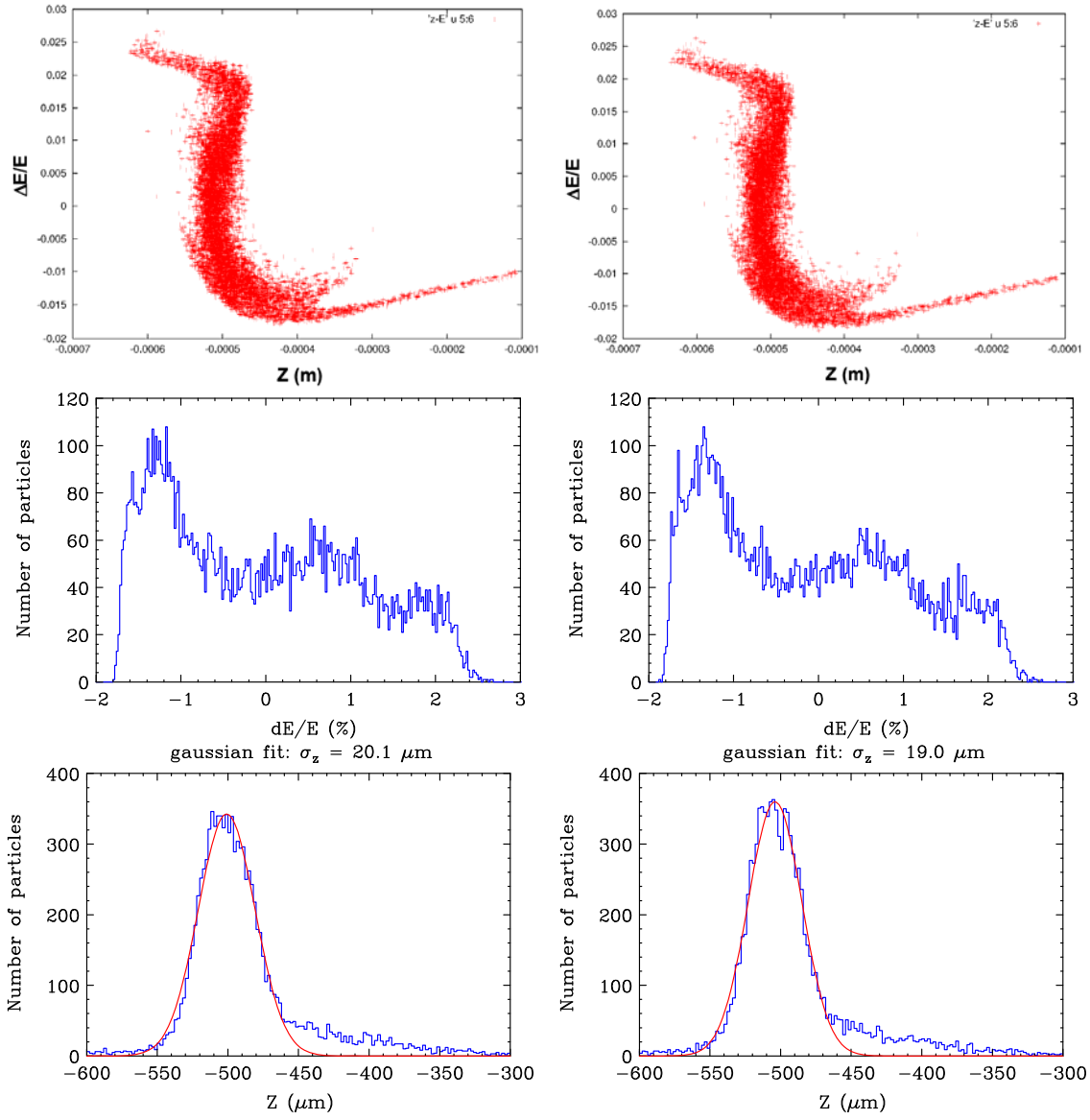


**Figure 4-9.** Simulation of longitudinal beam distribution for the FACET upgrade option with both the electron and positron chicanes installed. Electron drive bunch (left) and positron witness bunch (right), longitudinal phase space Δp/p vs. Z (top row), energy distribution (middle row) and bunch length profile (bottom row) at the IP.

The IP distributions in the FACET upgrade option, when both the e- and e+ chicanes are installed, are illustrated in Figures 4-10 and 4-11. The tracking was done for 23 GeV beams with the initial Gaussian X-Y spread at entrance into Sector 20, normalized emittance of $\gamma\varepsilon_x = \gamma\varepsilon_y$ = 25 μm, IP beta function of $\beta^*_x = \beta^*_y$ = 6 cm, realistic longitudinal distribution from LiTrack, and synchrotron radiation effects. Figure 4-9 shows that both the electrons and positrons are

compressed to ~20 μm bunch length. A Gaussian fit in Figure 4-10 yields the rms IP size of $\sigma_{x/y}$ = 13.2 / 13.6 μm for electrons and $\sigma_{x/y}$ = 23.3 / 12.1 μm for positrons. Further sextupole and chromatic optimization should reduce the X-Y size.

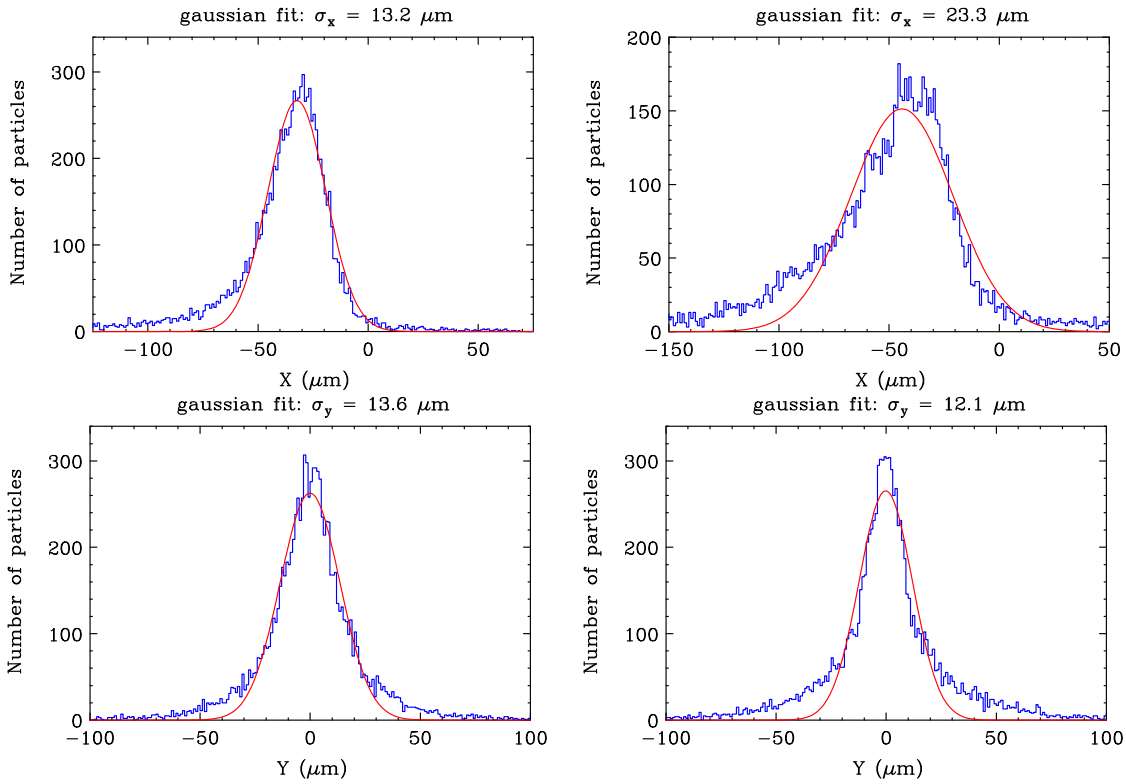


**Figure 4-10.** Simulation of transverse beam distribution for the FACET upgrade option with both the electron and positron chicanes installed. Electron drive bunch (left) and positron witness bunch (right), horizontal (top) and vertical (bottom) profiles at the IP.

Lattice sensitivities to field and alignment errors in the Sector 20 magnets were estimated based on 2% beam size growth at IP from each individual source of error. The obtained tolerances are within an achievable range. The measured field quality in the existing magnets, planned to be used in Sector 20, will be verified.

Separate study was done for the new first and last chicane bend magnets which must accommodate up to ±11.75 mm horizontal trajectories of the separating e- and e+ beams in the FACET upgrade option. The large beam offsets increase the multipole field seen by the beams and therefore make the corresponding field tolerances tighter. The latter were estimated in tracking without synchrotron radiation, based on 2% size growth at the IP from each error. The initial beam at entrance into Sector 20 was simulated with a Gaussian X-Y spread corresponding to the emittance values shown earlier and appropriate model of energy spread for estimating the beam core size at IP. Residual orbit caused by the errors was corrected, therefore most of the IP size growth is due to residual dispersion. The tolerances were calculated taking into account the FACET upgrade option. Assuming these two bend magnets will be built identical, the tightest tolerance found in the electron and positron tracking is applied to both magnets. The resultant

tolerances for a dipole field error and for quadrupole, sextupole, octupole and decapole field components at X = 1 cm for these magnets are:

| $\Delta B_0/B_0$ | $\Delta B_1/B_0$ | $\Delta B_2/B_0$ | $\Delta B_3/B_0$ | $\Delta B_4/B_0$ |
|---|---|---|---|---|
| $4 \cdot 10^{-3}$ | $2.3 \cdot 10^{-4}$ | $2.8 \cdot 10^{-4}$ | $2.2 \cdot 10^{-4}$ | $1.5 \cdot 10^{-4}$ |

The above multipole tolerances are mostly driven by the upgrade positron chicane optics, while the field requirements are looser for the single electron chicane optics in this proposal.

### 4.2.2 Magnets

The FACET optical configuration was designed to make use of existing magnets recovered from the SLC final focus and FFTB as much as possible, see Figure 4-11. Parameters of the quadrupoles, bending magnets and sextupoles needed for the FACET system are listed in Table 4-2. Design of a new bending magnet for Sector 20 is illustrated in Fig. 4-12.

**Table 4-2.** Parameters of Sector 20 magnets and closest match to existing magnets

| Electron Optics @ 23 GeV | | | | | SLC/New Magnet Data | | | | |
|---|---|---|---|---|---|---|---|---|---|
| Name | Name | L | G/D | B/B'/B" | Name | G/D | Data @ 23 GeV | | |
| unique | Optics | (m) | (mm) | (kG-m) | | (mm) | Amp | μΩ | kW |
| B201900T | B1E/P | 1.0400 | 18 | 16.66 | **New** | 23.00 | 648 | 31.58 | 13.26 |
| B202030T | WIG1 | 0.3750 | 20.3 | 5.11 | **51 WG1** | 20.30 | 300 | 183.33 | 16.50 |
| B202040T | WIG2 | 0.3750 | 20.3 | -5.11 | **51 WG1** | 20.30 | | | |
| | WIG2 | 0.3750 | 20.3 | -5.11 | **51 WG1** | | | | |
| B202050T | WIG1 | 0.3750 | 20.3 | 5.11 | **51 WG1** | 20.30 | | | |
| Q202061T | Q1E | 0.5860 | 18 | 540.87 | **0.813Q23** | 20.65 | 117 | 152.06 | 2.083 |
| B202110T | B2E | 1.8120 | 12 | -13.89 | **2D68.5** | 12.70 | -358 | 51.64 | 6.62 |
| Q202131T | Q2E | 0.9730 | 20 | -371.91 | **2.13Q38.31** | 54.00 | -423 | 76.30 | 13.68 |
| S202145T | S1E | 0.2500 | 30 | 15524.15 | **1.625S-A** Mdf core+new coil | 41.28 | 71 | 61.69 | 0.31 |
| Q202151T | Q3E | 0.6936 | 32 | 396.30 | **1.625Q** | 41.27 | 214 | 128.30 | 5.88 |
| Q202161T | Q3E | 0.6936 | 32 | 396.30 | **1.625Q** | 41.27 | 214 | 128.30 | 5.88 |
| S202165T | S2E | 0.2500 | 22 | -35580.91 | **1.625S-A** Mdf core+new coil | 41.28 | -163 | 61.69 | 1.63 |
| S202195T | S3E | 0.2500 | 24 | 21481.53 | **1.625S-A** Mdf core+new coil | 41.28 | 98 | 61.69 | 0.60 |
| Q202201T | Q4E | 0.6936 | 30 | 367.80 | **1.625Q** | 41.27 | 199 | 128.30 | 5.07 |
| Q202211T | Q4E | 0.6936 | 30 | 367.80 | **1.625Q** | 41.27 | 199 | 128.30 | 5.07 |
| Q202221T | Q4E | 0.6936 | 30 | 367.80 | **1.625Q** | 41.27 | 199 | 128.30 | 5.07 |
| S202225T | S3E | 0.2500 | 24 | 21481.53 | **1.625S-A** Mdf core+new coil | 41.28 | 98 | 61.69 | 0.60 |
| Q202231T | Q5E | 0.4078 | 20 | -246.09 | **1.625Q16** | 41.27 | -133 | 87.25 | 1.55 |
| B202240T | B3E | 0.5080 | 14 | 15.44 | **51BI** | 20.65 | 479 | 29.07 | 6.68 |
| Q202251T | Q6E | 0.3000 | 16 | -797.73 | **QX1** | 20.00 | -116 | 59.63 | 0.80 |
| B202260T | B3E | 0.5080 | 14 | 15.44 | **51BI** | 20.65 | 479 | 29.07 | 6.68 |
| Q202261T | Q5E | 0.4078 | 20 | -246.09 | **1.625Q16** | 41.27 | -133 | 87.25 | 1.55 |
| S202275T | S3E | 0.2500 | 24 | 21481.53 | **1.625S-A** Mdf core+new coil | 41.28 | 98 | 61.69 | 0.60 |
| Q202281T | Q4E | 0.6936 | 30 | 367.80 | **1.625Q** | 41.27 | 199 | 128.30 | 5.07 |
| Q202291T | Q4E | 0.6936 | 30 | 367.80 | **1.625Q** | 41.27 | 199 | 128.30 | 5.07 |
| Q202301T | Q4E | 0.6936 | 30 | 367.80 | **1.625Q** | 41.27 | 199 | 128.30 | 5.07 |
| S202305T | S3E | 0.2500 | 24 | 21481.53 | **1.625S-A** Mdf core+new coil | 41.28 | 98 | 61.69 | 0.60 |
| S202335T | S2E | 0.2500 | 22 | -35580.91 | **1.625S-A** Mdf core+new coil | 41.28 | -163 | 61.69 | 1.63 |

| | | | | | | | | | |
|---|---|---|---|---|---|---|---|---|---|
| Q202341T | Q3E | 0.6936 | 32 | 396.30 | **1.625Q** | 41.27 | 214 | 128.30 | 5.88 |
| Q202351T | Q3E | 0.6936 | 32 | 396.30 | **1.625Q** | 41.27 | 214 | 128.30 | 5.88 |
| S202365T | S1E | 0.2500 | 30 | 15524.1504 | **1.625S-A** Mdf core+new coil | 41.28 | 71 | 61.69 | 0.31 |
| Q202371T | Q2E | 0.9730 | 20 | -371.91 | **2.13Q38.31** | 54.10 | -423 | 76.30 | 13.68 |
| B202390T | B2E | 1.8120 | 12 | -13.89 | **2D68.5** | 12.70 | -358 | 51.64 | 6.62 |
| Q202441T | Q1E | 0.5860 | 18 | 540.87 | **0.813Q23** | 20.65 | 117 | 152.06 | 2.083 |
| B203000T | B1E/P | 1.0400 | 18 | 16.66 | **New** | 23.00 | 648 | 31.58 | 13.26 |
| Q203011T | FF1 | 0.4506 | 18 | 375.21 | **0.813Q17.7** | 20.65 | 81 | 122.84 | 0.81 |
| Q203031T | FF2 | 0.4506 | 20 | -352.68 | **0.813Q17.7** | 20.65 | -76 | 122.84 | 0.72 |
| Q203041T | FF2 | 0.4506 | 20 | -352.68 | **0.813Q17.7** | 20.65 | -76 | 122.84 | 0.72 |
| Q203051T | FF2 | 0.4506 | 20 | -352.68 | **0.813Q17.7** | 20.65 | -76 | 122.84 | 0.72 |
| Q203091T | FF4 | 0.6936 | 36 | 299.11 | **1.625Q** | 41.27 | 162 | 128.30 | 3.35 |
| Q203111T | FF4 | 0.6936 | 36 | 299.11 | **1.625Q** | 41.27 | 162 | 128.30 | 3.35 |
| Q203141T | FF5 | 2.0000 | 36 | -320.00 | **QC2** | 52.00 | -314 | 193.15 | 19.00 |
| Q203151T | FF6 | 0.9730 | 40 | -414.33 | **2.13Q38.31** | 54.00 | -472 | 76.30 | 16.97 |

Bend magnets available from the SLC final focus area.

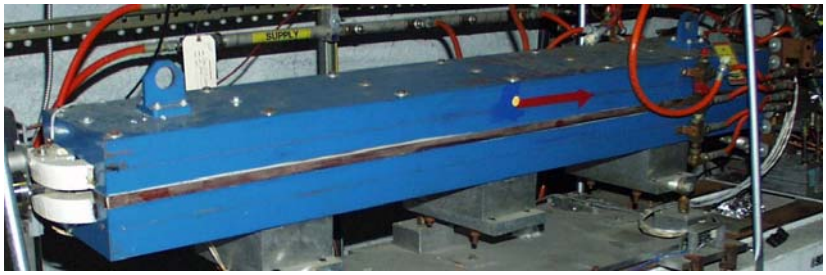

Sixteen quadrupole magnets of this type can be recovered from the SLC final focus system and refurbished for use in FACET. Each is supported by a fully adjustable mover base mechanism.

A large quadrupole magnet appropriate for the FACET final focus has been preserved from the FFTB and may be used with a support base salvaged from SLC.

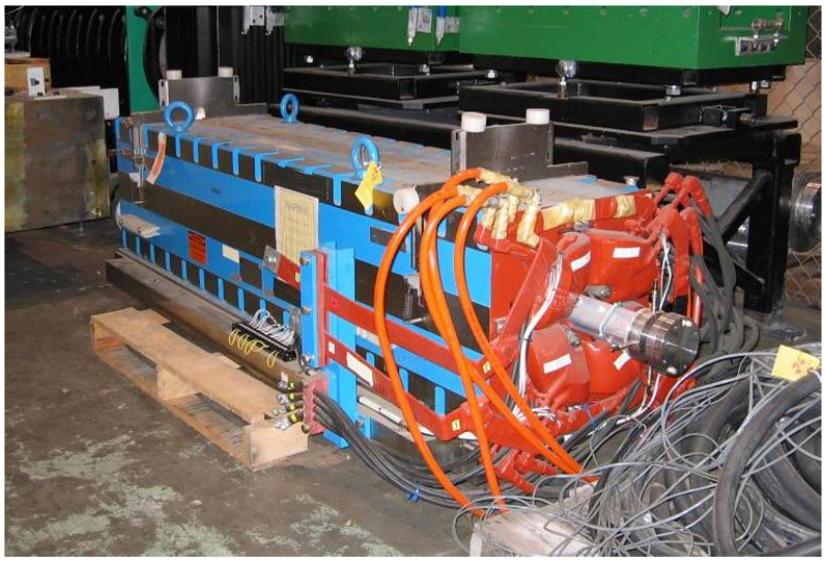

Two other large quadrupoles preserved from the FFTB are well suited for the two positions needed downstream of the IP.


Sextupole magnets needed for the final compressor section will be recovered from the SLC final focus chromatic correction section.

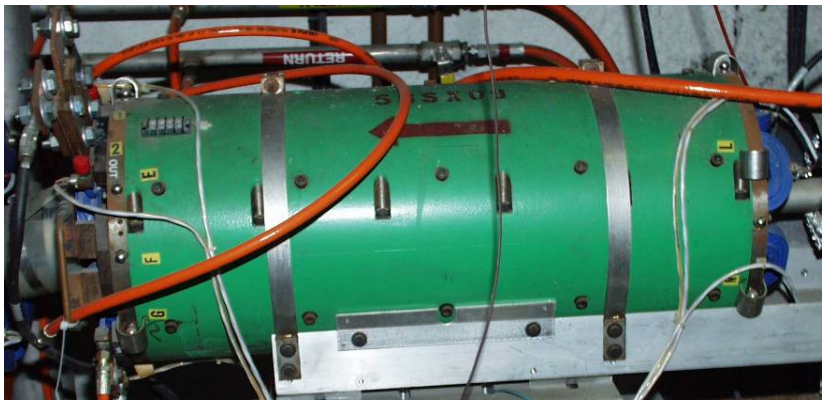

The first few magnets in Sector 20 will be mounted on the existing linac support girder using standard SLAC mechanical designs and refurbished SLC support movers. Eighteen magnets and most of the beam line instrumentation will be supported on refurbished SLC mover bases mounted on pier base supports similar to those used in the SLC final focus system, or on other existing support hardware with appropriate modifications. The pier base supports will have additional braces connected to the tunnel wall where judged necessary for seismic considerations.

A variety of magnet movers are available in decommissioned systems at SLAC and can be refurbished for use in Sector 20.


**FFTB Support**

**SLC Support**

**Figure 4-11.** Photos illustrating existing magnets and supports.

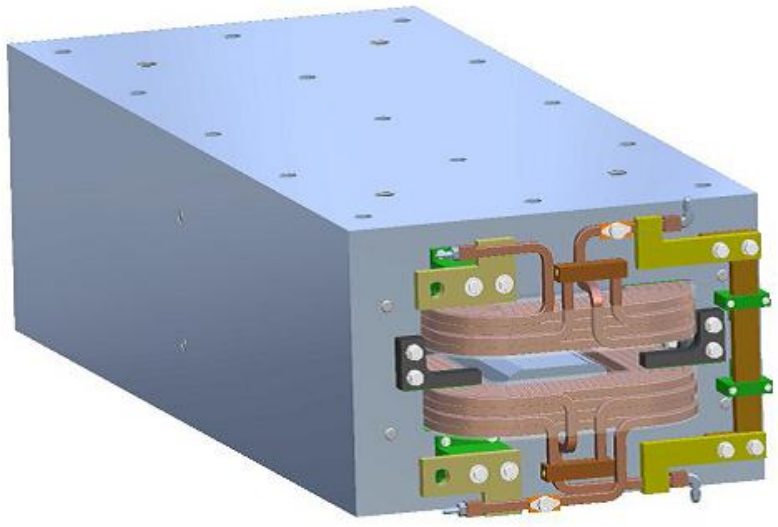

**Figure 4-12.** Design of a new bend magnet for Sector 20.

### 4.2.3 Instrumentation

The sector 20 beam line will be furnished with the standard instrumentation for accelerator operation. Those are beam position monitors, bunch current monitors, beam loss monitors, transverse bunch profile monitors and fixed collimators.

The beam position monitors will have strip lines as pick ups and either salvaged from the SLC final focus or new built after the standard SLC Linac design. The same electronic devices as used in LCLS will be installed to decode the position information and transmitted to the control system. The bunch current monitors and fixed collimators installed in the SLC FF will be reused as well as refurbished screens.

For the PWFE program additional diagnostic will be installed into the sector 20 chicane. In a high dispersion area a wiggler and YAG screen will be installed to measure the bunch energy. To manipulate the bunch profile a set of movable collimators will be used. These will provide to remove the transverse and energy halo from the bunch. Additionally a special "notch" collimator will be installed. It provides the capability to create two bunches from one by collimating a central region from the original bunch. This collimator is designed to change the location and amount of collimated beam to be able to create two bunches with variable bunch current relation and spacing. Between the final chicane bend and the IP, a 1μm thick Ti foil in the beam path produces coherent transition radiation (CTR). The CTR is coupled out of the beamline vacuum to a pyroelectric detector. The amplitude of the signal is inversely proportional to the electron beam bunch length. The signal is fed into the control system for a feedback and a relative measure of the bunch length for quick setup of the linac. A wire scanner and optical transition radiator (1μm Ti foil) close to the IP are used to tune out transverse beam tails and verify the beam has the desired transverse size at the IP. All these devices, except the wiggler that is currently installed in the BSY, were installed in the FFTB and will be refurbished.

### 4.2.4 Vacuum System

Most of the vacuum system for Sector 20 will be assembled from existing magnet and component chambers and will be baked and processed for high-vacuum use. The average beam current is very low and no high-power vacuum chambers are needed. Spool sections salvaged from the FFTB will be modified to fill most of the gaps, with some new adapter flanges, bellows, and tees added. Bend chambers in the chicane section will be polished and coated with copper to mitigate resistive wall effects that could degrade the bunch parameters. A special Y-chamber will be fabricated and installed downstream of the dump magnet to accommodate separated particle beam and photon beam trajectories. Collimators and ion chambers will be installed at a few critical locations to protect downstream components from any unexpected beam loss.

Most of the mechanical supports for the vacuum components will be salvaged from the FFTB or SLC final focus areas or copied from designs from those areas. Vacuum valves will be added near the beginning of Sector 20 and at each end of the experimental area. The existing fast valve at the west end of Sector 20 will be active to protect the linac from any sudden loss of vacuum in the experimental area. Pump power supplies and gauge controllers will be easily accessible in racks in the Klystron Gallery above Sector 20.

The original Sector 20 accelerator pumping system will remain in place and remain active. This will preserve the vacuum integrity of the portions of the original linac remaining in Sector 20, and will be ready, if necessary, to restore the original linac configuration. A set of discrete 55L ion pumps distributed along the beam line will ensure a vacuum level of about $10^{-6}$ torr.

### 4.2.5 Beam Dump

The beam dump design has been optimized for the nominal beam parameters: Eo ~ 23 GeV, N ~ 2E10/bunch, Pulse Rep Rate = 30 Hz : Pav ~ 2.1 kW. Note, the maximum energy is limited to 23 GeV on account of a new dipole magnet in the Sector 20 chicane; otherwise, it would be ~ 28.5 GeV, which is the energy delivered to the positron source located just upbeam of the FACET facility.

The specifics of the dump design are strongly influenced by the shielding requirements to allow occasional access to the experimental region, to minimize activation of the tunnel concrete walls, and to minimize activation of the soil and ground water just outside the tunnel walls. The dump can actually safely and indefinitely absorb the full 120 Hz/28.5 GeV beam, which is ~ 11 kW.

Minimum cooling water requirement for nominal operation and a bulk water temperature rise of $30^{o}$C is w <~ 0.3 gpm; for the maximum possible beam power at the beginning of Sector 20 (11 kW) it is w ~ 1.4 gpm.

The dump is a composite of copper and free-machining tungsten as shown in Figure 4-13. To lower the production of high energy neutrons, the electron beam is deposited and develops the electromagnetic shower in a block of copper of length 18 inch = 45.72 cm = 31.6 Xo. It is 3 inch = 7.62 cm wide; the half width is ~ 2.64 Xo.

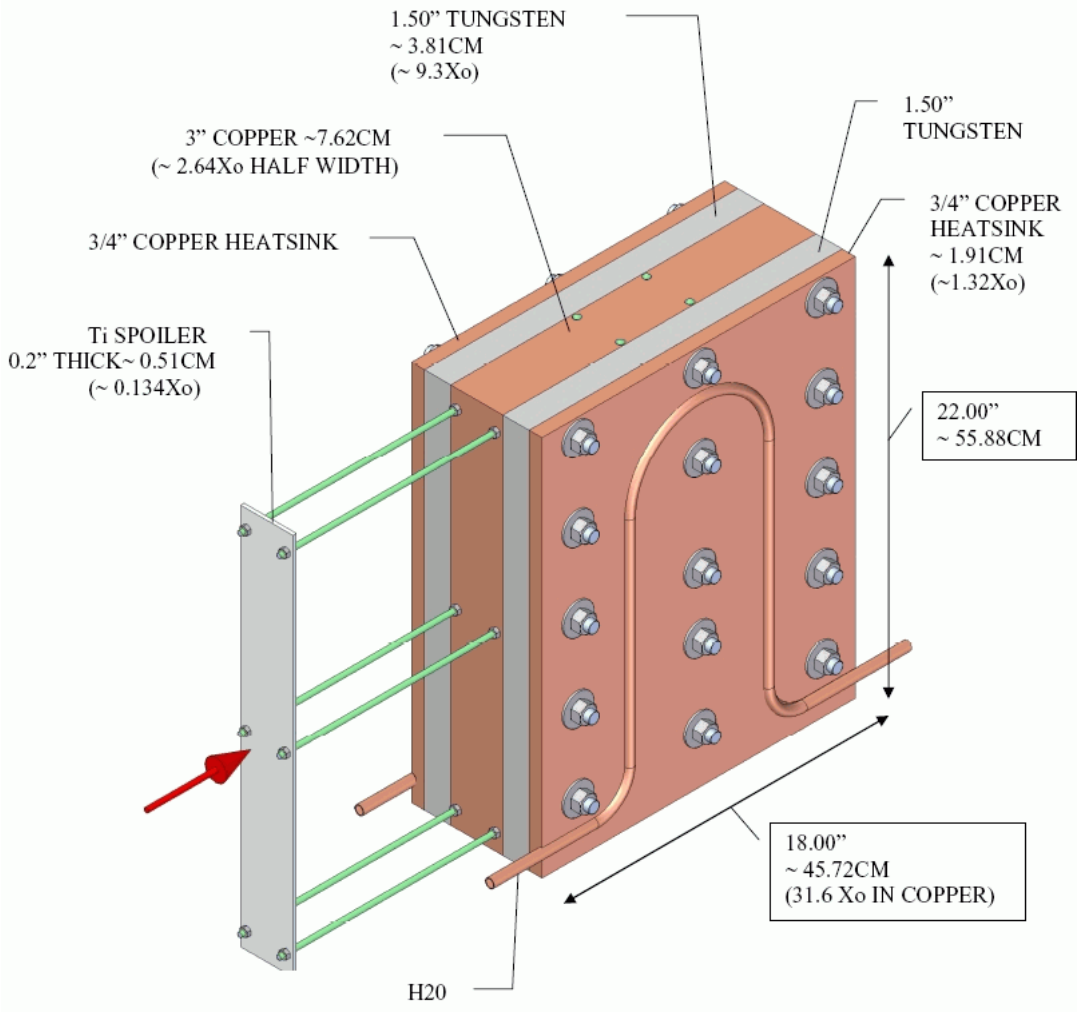


**Figure 4-13.** The core of the beam dump, showing the central copper block and side tungsten slabs as well as the front titanium spoiler.

On either side of the copper block is a 1.5 inch = 3.8 cm = 9.3 Xo slab of free-machining tungsten. Its function is to attenuate the remaining transverse shower and provide an efficient slowing down medium for the high energy neutron flux (since both the polyethylene and the concrete walls of the outer part of the shield are hydrogeneous media that are most effective if the neutrons are thermalized). On either side of the tungsten slabs are water-cooled copper heat sinks. They are ¾ inch = 1.9 cm = 1.32 Xo thick and have copper cooling channels brazed onto them. The central copper absorber block, the tungsten slabs, and the copper heat sink slabs are bolted together. All heat transfer is by thermal conduction to the cooling water passages. The total effective thickness in x-direction is then ~ 14.3 Xo from the beam centerline.

The overall height of the dump is + 11 inch = + 27.9 cm. This allows acceptance of primary energy beams in the center (no experimental use) as well as large energy gains/losses due to plasma wakefield acceleration for either polarity beams. It also provides significant vertical shower attenuation for those particles that are ending-up near the upper and lower maxima. Steel shielding below and above the dump also provides a neutron slowing down medium.

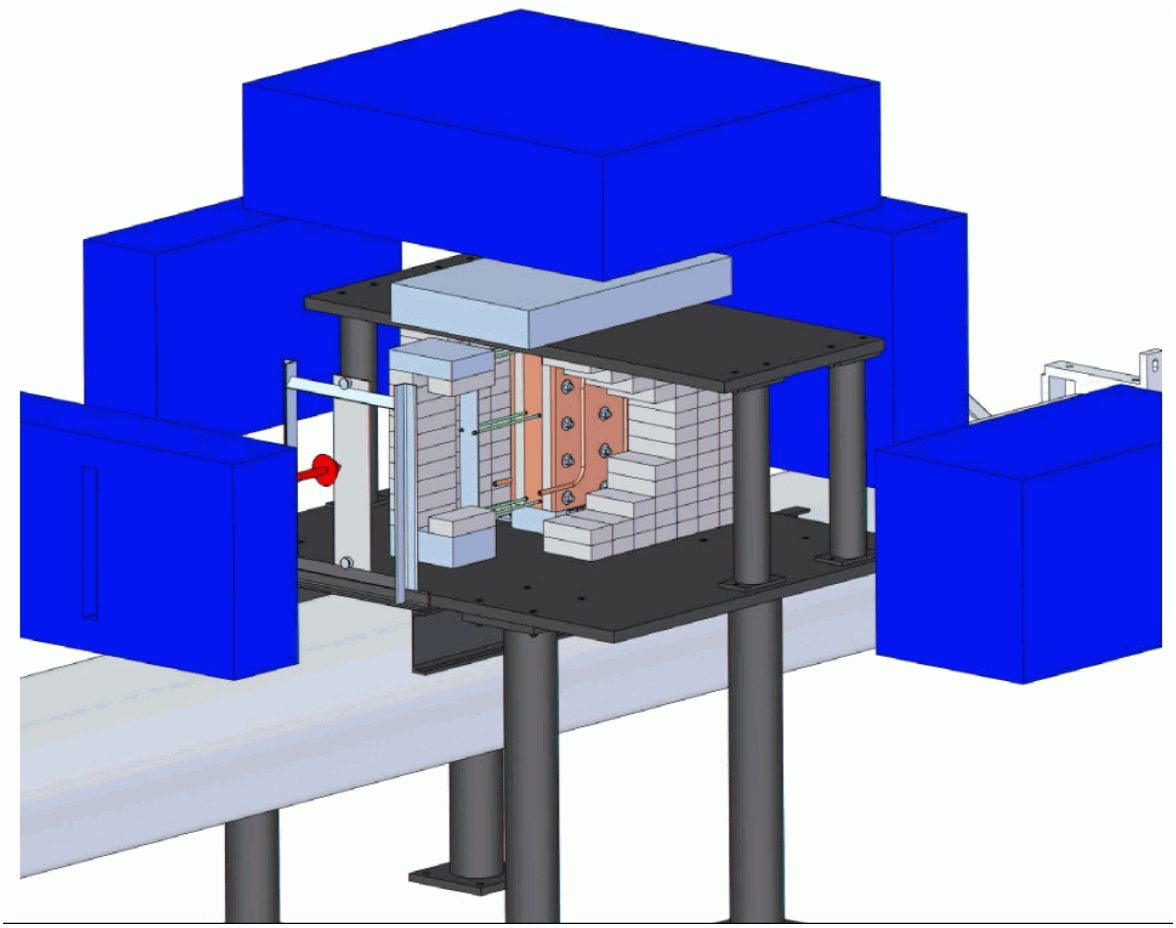

**Figure 4-14.** The expanded outline view of the beam dump, showing the central part, the lead shielding bricks and steel shielding plates, and borated polyethylene shielding outside.

The dump will be preceded by a titanium spoiler of 5mm thickness at a distance of 300mm, since the smallest beam spot size achievable at the dump for coupled damping rings, an emittance of 3 x 3 (SLC units, E-5m of normalized emittance), and perfect alignment through the dump line is of the of the order of $\sigma \sim 50$ μm. The mean square angle of scattering will then increase the minimum transverse beam size to $\sigma_{eff} \sim 120$ μm. This will reduce the single bunch temperature rise at the entrance to the copper absorber block to ~ $10^{o}$C; the consequential thermal stress rise is low enough to guarantee an infinite number of cycles.

On the downbeam end of the dump is a Burn-Through Monitor (BTM) to satisfy the Beam Containment (BCS) requirements. The dump is mounted above the alignment laser light pipe on a support stand, decoupled from the linac as shown in Figure 4-14. There is additional steel shielding on the left or north side of the dump, and either lead or steel shielding on the right or south side. This mini dump cave is surrounded by borated polyethylene shielding to minimize residual activity due to neutron activation.

Ahead of the Ti-spoiler plate is a remotely insertable mask to protect experimenters from residual activity from the dump when there is a need to work on instrumentation just upbeam of the dump.

## 4.3 Sector 20 Experimental Area

The space available for experimental equipment starts at a vacuum valve immediately following the last final focus quadrupole before the focal point. The nominal focal point will be 2 m downstream of this quadrupole; the beam dump will be another 23 m downstream of this point. This drift distance will accommodate a wide variety of experimental arrangements to suit the needs of experimenters and will include a magnetic dump line spectrometer for the outgoing beam. A cross-sectional view of this section of beam line is provided in Figure 4-3.

The Klystron Gallery above the Sector 20 tunnel will house the power supplies for the focusing magnets and the electronics for the instrumentation and control system. The Klystron Gallery also has space in this area for any experimental equipment that must be near to the focal point but be continuously accessible to the experimenters when the beam is on. Existing penetrations at twenty-foot intervals provide paths for direct connections between apparatus in the Klystron Gallery and apparatus in the tunnel directly below.

Figure 4-15 is a conceptual layout of an advanced acceleration experiment involving a plasma oven set up on an optical table at the focal point. With this table in place, experimental apparatus can quickly be installed, aligned, and reconfigured as needed. Also shown are two magnets downstream of the focal point that will be used for measuring the energy of the outgoing beam. They form an image of the focal point at the second focus in the dump line. The optical table and plasma oven are also shown in the tunnel cross section view in Figure 4-3.

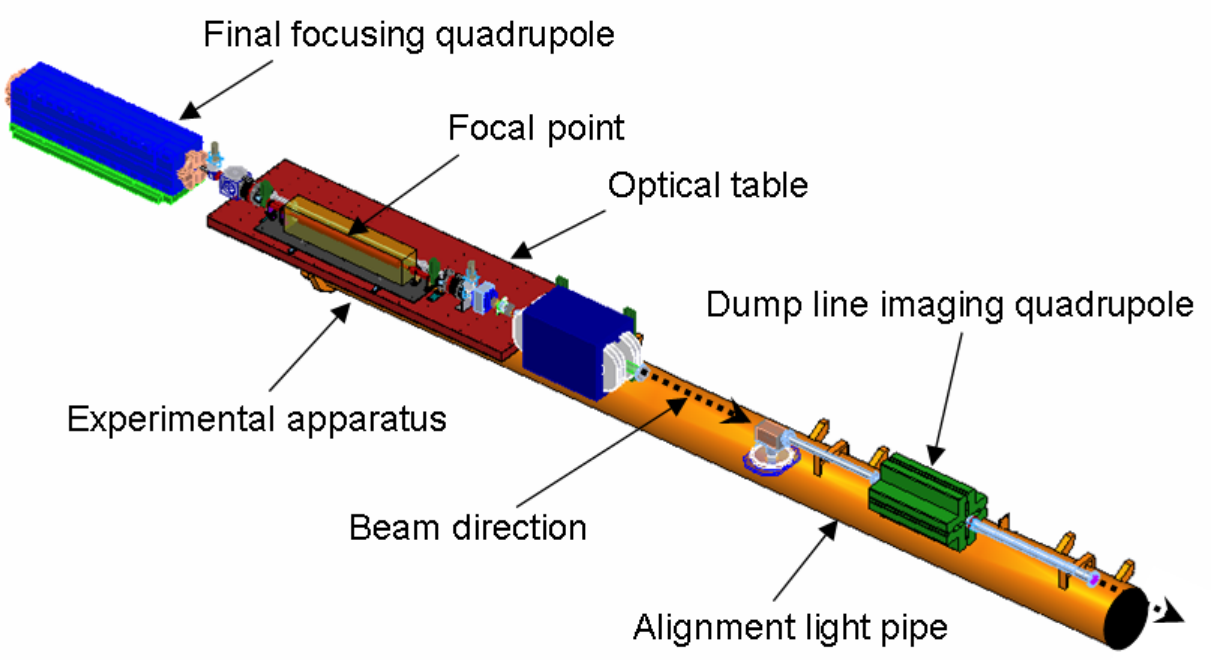


**Figure 4-15.** Proposed arrangement of experimental apparatus for a plasma wakefield experiment. A lithium plasma oven is shown on a general-purpose optical table, followed by magnetic spectrometer apparatus in the outgoing dump line.

## 4.4 Sector 10 Bunch Compressor

### 4.4.1 Beamline Design

A bunch compressor system was installed in the linac Sector 10 in 2002 [63] and was used in conjunction with previously existing accelerator systems to compress electron bunches to less than 100 fs (30 μm) as they were delivered to experiments in the FFTB tunnel. The key components of the electron compressor system are four identical dipole magnets, which together form a symmetric magnetic chicane. Upstream of this chicane, the linac RF system is tuned to introduce a correlation between the electron momentum and longitudinal position within the bunch, such that the higher momentum electrons are shifted toward the trailing end of the bunch. As the bunch passes through the chicane, the electrons with lower momentum follow a longer path, allowing the higher momentum electrons to catch up, and resulting in a significantly shorter bunch. This electron compressor chicane has been used successfully to support several experiments over the past five years.

The existing chicane system works well for electron bunches alone, but cannot be used for positron bunches without significant changes. This is because positrons are produced by first accelerating electrons to the positron production target in Sector 19. To reach this point, the electrons must pass through the Sector 10 chicane. The positrons produced at the target are transported back to Sector 1 and injected into the South Damping Ring for subsequent acceleration through the Sector 10 chicane and on to the experiment area. Switching the polarities of the iron chicane magnets on a pulse-by-pulse basis is not feasible; therefore two separate paths through the chicane area must be considered for the two charges.

In order to provide the positron compression capability for FACET, it is proposed to add a positron chicane placed mirror symmetrically on the opposite side of the electron chicane in Sector 10 as shown in Figure 4-16. This requires two additional bend magnets since the first and the last bends will be shared by the two beams. Since the proposed positron chicane will have the same design as the electron chicane, the electrons and positrons will attain the same bunch length compression.

The existing support structures that were installed for the electron compressor chicane can also support the additional hardware needed for positrons with only minor modifications. New vacuum chambers will be needed to pass the separating and recombining beam paths of the electrons and positrons. Some additional instrumentation will be required to facilitate steering and focusing of the two beams simultaneously.

The first and the last bends will be shared by the electron and positron chicanes. Therefore these bends require a large horizontal aperture of at least 21 cm in order to accommodate the separating beams. Moreover, the very tight sextupole field tolerance in these magnets requires that the bend pole width will need to be over 22 cm. It is also proposed that these magnets have a special pole face design for generating additional focusing as explained below. For the latter reason, two new bends have to be built for these magnet positions. Consequently, the existing outer chicane bends (style name 1D70) will be relocated into the 2$^{nd}$ and 3$^{rd}$ positions in the new positron chicane. The latter is possible because the existing outer bends are identical in design and field quality to the inner bends and therefore satisfy the requirements at these positions.

The present symmetric electron chicane optics with four identical rectangular bends is matched to the upstream and downstream linac optics using adjustment of the adjacent quadrupoles in Sectors 10 and 11. However, if the positron chicane was built the same, it would not automatically match to the same linac optics because of the properties of e- and e+ focusing

in the shared linac as explained in Section 4.2.1. An automatic betatron match of the electrons and positrons would be achieved if the horizontal matrix of the e- chicane is equal to vertical matrix of the e+ chicane ($M^-_x = M^+_y$) and vice versa ($M^-_y = M^+_x$), as in the rest of the linac. However, the matrices of the identical e- and e+ chicanes are naturally the same in each plane ($M^-_x = M^+_x$ and $M^-_y = M^+_y$), but differ in X and Y planes and therefore do not satisfy the matched condition. In the existing design, the consequence of such a mismatch is a factor of 2 enlargement of positron beta function amplitude downstream of the chicane as compared to the matched electron beta functions. Compensation of this mismatch requires at least two focusing elements in each chicane. By design, the chicanes include two small quadrupole correctors placed symmetrically as shown in Figure 4-16. In the symmetric chicane, these correctors can be used as one variable focusing strength. The second focusing element must be added into the chicane. Unfortunately, using another quadrupole corrector seems not practical because it would have to be placed closer to the center of the chicane where a very large aperture is required. The adopted solution is to create the needed focusing by adjusting the edge focusing in the new outer bend magnets. This can be achieved by rotation of one pole face, where the beams are separated, by an angle of 8.895 degrees with respect to the rectangular configuration as shown in Figure 4-17. In combination with the matched quadrupole corrector strength, this will reduce the beta mismatch downstream of the chicane to an acceptable level of a few %.

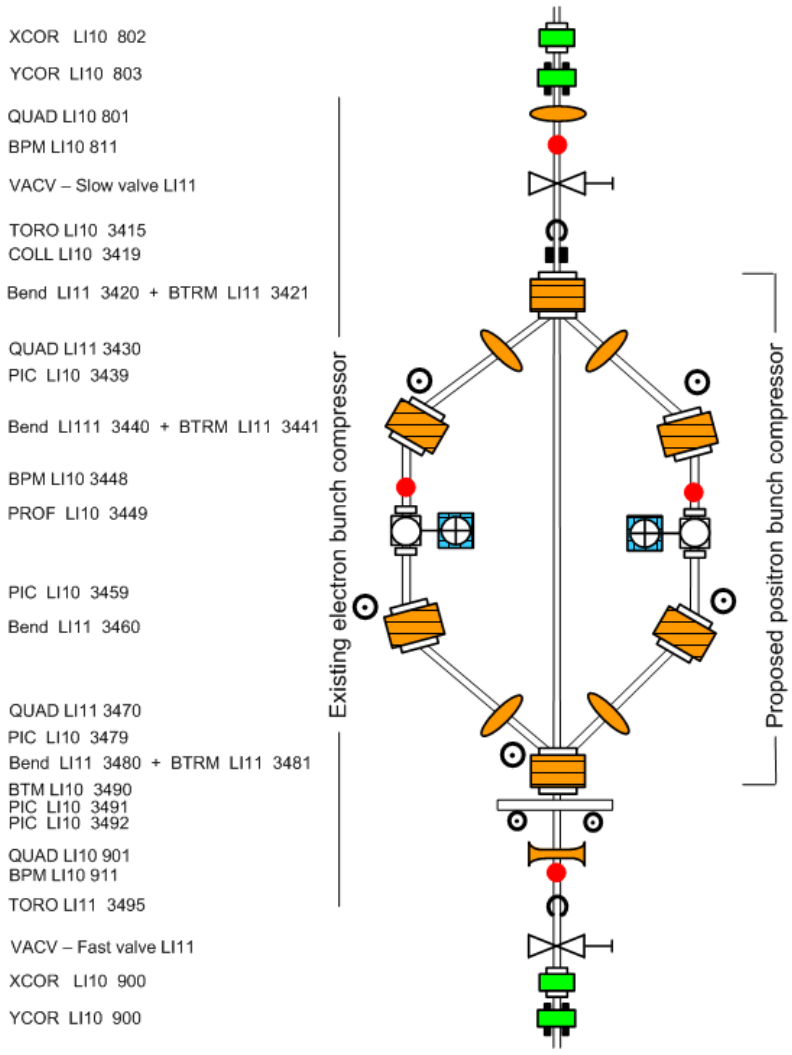


**Figure 4-16.** Sector 10 dual-sided bunch compressor layout.

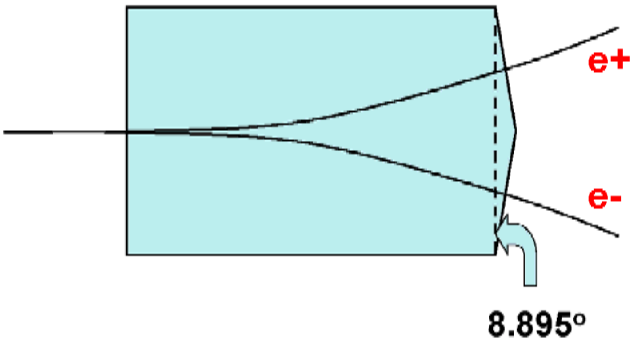


**Figure 4-17.** The pole face configuration in the new outer bend in Sector 10 chicane that creates the necessary focusing for betatron match.

Since the new chicane design is close to the existing design, most tolerance specifications obtained in the very detailed study performed for the existing chicane [63] are applicable to the new design. The major difference is the large ±8.75 cm trajectories of the separating e- and e+ beams in the new outer bends which require tight tolerances on multipole field components in order to avoid large feed-down effects resulting in emittance growth. Secondly, the new chicane beta functions may somewhat differ from the existing design. The tolerances for the new bends were estimated in DIMAD tracking based on 2% emittance growth from each multipole field error. The initial beam at entrance into Sector 10 was simulated with a Gaussian X-Y spread for the expected emittance of $\gamma\varepsilon_x$ = 30 μm, $\gamma\varepsilon_y$ = 3 μm at 9 GeV and rms energy spread of 1.6%. Residual orbit caused by the multipole feed-down was corrected right after the chicane; therefore most of the emittance growth is due to residual dispersion. Assuming that these bends will be made identical, the tightest tolerance is applied to both magnets. The resultant tolerances for a dipole field error and for quadrupole, sextupole, octupole and decapole field components at X = 10 cm for these magnets are:

| $\Delta B_0/B_0$ | $\Delta B_1/B_0$ | $\Delta B_2/B_0$ | $\Delta B_3/B_0$ | $\Delta B_4/B_0$ |
|---|---|---|---|---|
| $1 \cdot 10^{-3}$ | $1.4 \cdot 10^{-3}$ | $2.0 \cdot 10^{-3}$ | $2.2 \cdot 10^{-3}$ | $2.5 \cdot 10^{-3}$ |

These tolerances are very tight, but since the existing chicane magnets were built for the same sextupole tolerance, this level of field quality should be achievable.

An additional modification in the sector 10 chicane is an adjustment of chicane beta functions. It is desirable to make them of the same level with the existing beta functions and identical in the e+ and e- bends in order to attain the same tolerances in both chicanes. This condition can be approximately achieved by focusing adjustment in the adjacent linac quadrupoles. A better match can be done by adding an additional quadrupole in front of the chicane.

### 4.4.2 Magnets

In the Sector 10 modification, the existing dipole magnets in the first and fourth positions of the chicane will be used in the second and third positions on the positron side of the new configuration to form a mirror-image of the electron side. Two new dipole magnets will replace the first and fourth magnets. They will be centered on the linac axis and deflect electrons and positrons in opposite directions. The two new dipoles will require slightly wider pole tips and vacuum chambers than the original ones. Calculations have shown that such magnets can be built and still powered in series with the other dipoles, all the dipoles have solid wire trim coils to allow their integrated strengths to be adjusted to be within 0.1% of each other. The existing magnets have 1.7746m long solid low carbon steel cores, with a gap height of 50 mm, and a nominal field of 1.6 T. One end of the poles of the new dipoles will be shaped as shown in Figure 4-17 to provide the pole face angle of about 9 degrees for both e+ and e- beams, to achieve cancelation of dispersion and control of beta beating.

There are two existing correcting quads, the 2.15Q5.87 style, designed and fabricated in 2002, two more of exactly the same style will be fabricated. There are 2 standard SLAC linac quads, called QC2s and 4 standard linac type 4 correctors in this dual-sided bunch compressor. A full list of magnets showing their lattice names, nominal integrated strengths, nominal operating currents and resistances is given in Table 4-3.

**Table 4-3.** Detailed list of all magnets in the dual-sided bunch compressor in linac sector 10

| Z along beam, meters (Upstream end of magnet) | Lattice magnet name | *Nominal* Integral B.dl T-m or Integral G.dl Tesla (quads) | Engineering name of style of magnet | *Nominal* Operating Current amps | Magnet resistance ohms. At operating temperature | Magnet Max Power (at max op I of 881 A) kW |
|---|---|---|---|---|---|---|
| 1003.58 | B101EP | 2.9193 | 1D70V2 | 848.8 | 0.031 | 24.06 |
| 1008.18 | B102E | 2.9193 | 1D70 | 848.8 | 0.031 | 24.06 |
| 1008.18* | B102P | 2.9193 | 1D70 | 848.8 | 0.031 | 24.06 |
| 1011.48 | B103E | 2.9193 | 1D70 | 848.8 | 0.031 | 24.06 |
| 1011.48* | B103P | 2.9193 | 1D70 | 848.8 | 0.031 | 24.06 |
| 1016.08 | B104EP | 2.9193 | 1D70V2 | 848.8 | 0.031 | 24.06 |
| See their main magnet | Trims on B101EP & B104EP | 0.116 | 1D70TV2 | 7.45 | 2.33 | 0.1427 (at 8 A) |
| See their main magnet | Trims on B102E,102P, 103E,103P | 0.0584 | 1D70T | 9.64 | 1.38 | 0.1377 (at 10 A) |
| 1005.19 | Q101E | -0.09766 | 2.1Q5.87 | 2.1 | 0.47 | 0.047 (at 10A) |
| 1014.47 | Q102E | -0.09766 | 2.1Q5.87 | 2.1 | 0.47 | 0.047 (at 10A) |
| 1005.19* | Q101P | -0.09766 | 2.1Q5.87 | 2.1 | 0.47 | 0.047 (at 10A) |
| 1014.47* | Q102P | -0.09766 | 2.1Q5.87 | 2.1 | 0.47 | 0.047 (at 10A) |
| 1000.73[#] | Q100801T | 2.498 | LINAC QC 1.1Q3.3V2 | 56 | 0.0845 | 1.217 (@120A) |
| 1018.11[#] | Q100901T | -2.723 | LINAC QC 1.1Q3.3V2 | 61.2 | 0.0845 | 1.217 (@120A) |
| Various | 4 existing correctors | | LINAC type 4 | ~3.2 | 2.72 | MCOR PS |

NOTES: * The B102 and B103 dipoles sit offset from the straight ahead beamline, to the left or to the right of the straight ahead line, that is why B102E can have the same Z values as B102P. Ditto the quads Q101 and 102.

[#] The two existing LINAC QC quads are already in a standard string of 8 quads with an LGPS on LI10 of 200A with a booster PS of 25 A for variability.

Except the dipoles- the maximum power value is given at maximum standardizing current.

The support structure under the existing chicane magnets was constructed to be symmetric about the plane of the linac, in anticipation of eventual addition of two more dipoles to compress positron bunches. The new supports and other mechanical devices needed for the compressor system will be direct copies of existing designs.

All six bends in the two chicanes will be powered in series. However, since real magnets may not be exactly identical, trim windings are included on each bend to allow a fine field correction. The quadrupole correctors are included in the chicanes to compensate focusing errors and residual dispersion.

### 4.4.3 Instrumentation

New instrumentation for the positron compressor will be copies of the corresponding devices on the electron side of the chicane. This is a beam profile monitor (fluorescent screen) and a beam position monitor. Most of these devices are available from the FFTB or SLAC final focus system.

### 4.4.4 Vacuum System

The vacuum components needed for the positron side of the compressor chicane will be mirror-image copies of the components on the electron side.

## 4.5 Power Conversion

### 4.5.1 Introduction

The FACET project requires the installation of approximately 45 new dc magnets in Sectors 10 and 20. These magnets can be individually powered or connected in strings. In Sector 20, the FACET installation is divided in sections: an electron line (e-), common magnets, a final focus (FF) section and a beam dump (DUMP) section.

The SLAC Power Conversion Department (PCD) is responsible for the dc magnet power supplies (PS) for FACET. The PCD has a list of all the magnet specifications. From the magnet requirements and their characteristics, (impedances, current, and their exact -Z coordinates), PCD has generated a list of power supplies needed for the Sector 20 installation, which includes now 40 systems. In addition, there will be one new PS required at Sector 10 for the "chicane" magnets.

At Sector 20, the new PS systems will be grouped and installed in the klystron gallery near penetration 20-3. Close to that penetration, klystron 20-3, its modulator and controls will be removed to make more room for the new PS and the racks in which to mount them and their controls. Several existing free-standing PS, dedicated to the existing positron line, could be relocated by a few meters to make the layout more efficient.

About twenty of the new PS will have to be free-standing type, EMHP or other supplies, 30 kW or higher in rating. The rest (about 20) will be rack mounted. This will require about four standard LCLS-type double-bay electronic racks. If either additional floor space is still required or dc cable lengths need to be reoptimized, PCD will place the PS systems for the FF and dump sections near penetration P20-12 or P20-13.

The Sector 20 PS will require about 750 kVA of 480 V 3-phase power, most likely to come from substation K10A. The large power supplies (30 kW and greater) will need fused disconnect switches. Most rack mounted units will need 480 V breakers in their racks. Some smaller supplies (1 or 2 kW) will need 208 V ac 3-phase power, which will require a small step-down transformer powered by the 480 V line.

All the large and intermediate PS (except bulk supplies for MCOR crates) will be individually controlled using standard Ethernet Power Supply Controllers (EPSC). PCD will have the responsibility of building, testing and installing these units. The Controls Department at SLAC will provide the control software and programming, and their integration into the EPICS control system.

Nearly all of these PS will be obtained from installations no longer used, such as FFTB, PEP-II or NLCTA. Only about twenty low-power PS (<1 kW) will have to be purchased.

For trim and corrector magnets, PCD will use MCOR power modules. This will require two MCOR crates, each of which can hold up to sixteen MCOR modules. These will require one 10 kW bulk PS. All these will also be rack mounted.

In addition to the Sector 20 installation, PCD will install a 270 kW power supply at Sector 10 for the chicane magnets. PCD will use an existing PS, which is available from PEP-II, and existing 480 V service from an old 400 kW PS presently in the same position.

The cable plant (both dc and control) installation will be coordinated by PCD with the help of the PCD Cable Shop. Technical descriptions of the cable plant installations are addressed in a different section of the CDR document.

## 4.5.2 Magnet Power Supply General Characteristics

### 4.5.2.1 Large Power Supplies

The large power supplies (LGPS) for FACET are used for magnet systems requiring output power greater than 30 kW, for applications where it is not feasible to combine several 10 kW or 15 kW smaller units. Two types of LGPS will be used for FACET: free-standing (72-270 kW) and EMHP units (up to 80 kW).

4.5.2.1.1 The Free-standing Power Supplies

The free-standing units are unipolar off-line switchmode supplies, with a 6-pulse bridge rectifying 480 V ac, 3-phase input power to yield unregulated 650 V dc [64]. The unregulated 650 V dc feeds one (or two) IGBT H-bridges, which convert the dc into PWM 16 kHz square wave ac. This high frequency ac drives the primary side of a step-down transformer followed by rectifiers and low pass filters. Figure 4-18 is a block diagram of the internal arrangement of such a LGPS.

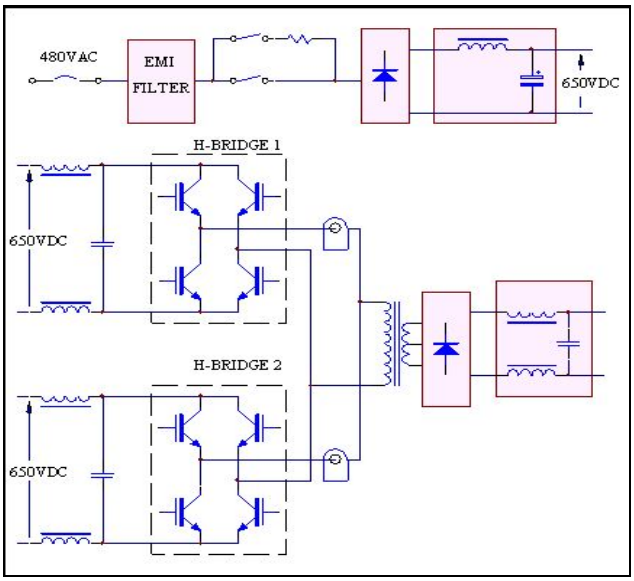


**Figure 4-18.** Large power supply block diagram.

PEP-II installation has eight of these LGPS with output ratings from 72 kW to 270 kW, which were used to power PEP-II quad magnets in the electron-positron collider region. These supplies were redesigned/rebuilt [64] during the 2004 summer shutdown and all the control circuits were replaced. A new PWM control board, programmable logic controller (PLC), and touch panel were installed to improve LGPS reliability, and to make troubleshooting easier. Figure 4-19 shows two of these supplies. These LGPS are water-cooled.

**Figure 4-19.** Two of the large free-standing magnet power supplies in PEP-II.

4.5.2.1.2 The EMHP

The EMHP power supply has a pair of SCR modules connected in reverse parallel in each of the three phases. These modules work in conjunction with the firing circuit and a feedback loop, which works to keep a regulated constant voltage or current output. The feedback loop determines the firing angle of the SCRs ensuring a regulated ac input voltage is applied to the primary of a power transformer. This regulated ac voltage is then adjusted to the proper output level by the power transformer. After being full-wave rectified and filtered, a constant output voltage or current is produced. Figure 4-20 shows the EMHP functional block diagram, and Figure 4-21 a typical EMHP installation. EMHPs are exclusively air-cooled units.

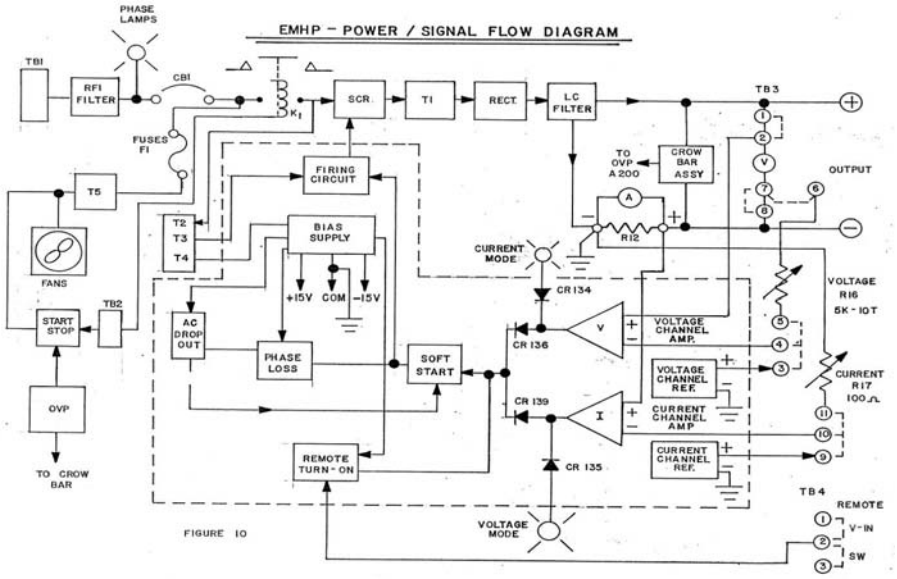


**Figure 4-20.** EMHP block diagram.


**Figure 4-21.** Typical EMHP Power Supply.

#### 4.5.2.2 Intermediate Power Supplies

The intermediate PS for FACET are off-the-line and have a 16 kHz H-bridge inverter driving a step down class H (220 °C) transformer followed by a high frequency rectifier stage and two -40dB/decade low-pass filters [65]. Units with power ratings of 2.4 kW to 4.8 kW have 208 V ac, 3-phase input, with efficiencies greater than 85%. All other higher power intermediate PS have 480 V ac, 3-phase inputs, presenting, at rated current, efficiencies greater than 90%, and a power factor of 0.94. Figure 4-22 shows their basic power topology.

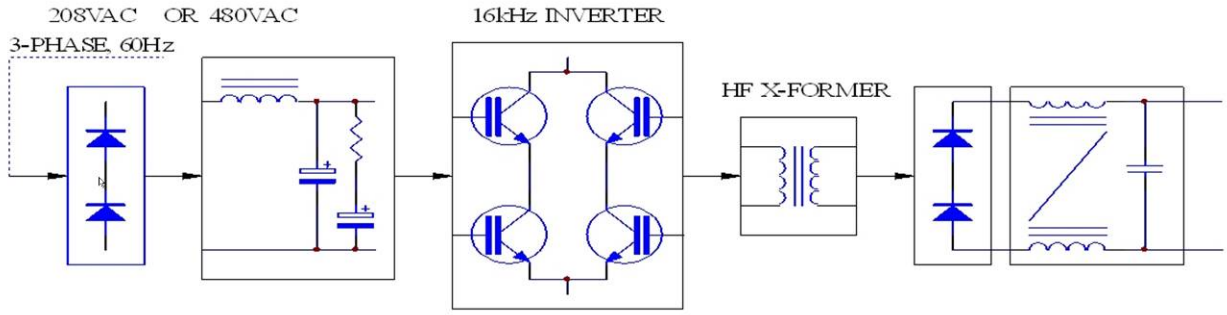


**Figure 4-22.** Intermediate Power Supply Block Diagram.

A 19” standard rack mounted modular design is the best option. This allows operation of an intermediate PS similar to the PEP-II [65], SPEAR3 [66] or LCLS systems [67], thus reducing the required inventory of spare units. The intermediate PS are designed to be series- or parallel-connectable to yield the desired output power, thus keeping a rack-mounted modular design up to about 45 kW of output power. All intermediate PS are air cooled. Figure 4-23 shows a typical intermediate PS installation in double-bay racks.

In terms of mechanical arrangement, the intermediate PS have a rack-mounted design based upon a NEMA1 chassis, and are standard 19” width, and 22” deep. Depending on the rated output power, heights vary from 5.25” (3U), 8.75” (5U), to 21” (12U).

**Figure 4-23.** Typical Intermediate Power Supply Installation.

#### 4.5.2.3 Trim and Corrector Supplies

The PCD will use MCOR modules to power small trim and corrector magnets. MCOR modules are extensively used around SLAC and other laboratories, offering a compact solution for bipolar output currents ranging from 6 A to 30 A [68]. Figure 4-24 shows the standard MCOR module for up to a 12 A output current. Figure 4-25 shows the basic block diagram for a MCOR12 module. The MCOR module has a typical stability of better than 25 ppm/°C, which is sufficient for the corrector magnets requirements, typically 1000 ppm for diurnal variations. Table 4-4 summarizes the basic parameters of a MCOR module.

**Table 4-4.** MCOR System uses and requirements

| | |
|---|---|
| Ratings | 40 V-6 A, or 40 V-12 A or 40 V-30 A |
| Uses | Power 6 A, 12 A, and 30 A correctors, small quadrupoles, and trim magnets that require unipolar or bipolar current |
| Stability versus temp | ≤ 25 ppm / °C, 10 to 100% |
| Short term stability | 30 ppm RMS, 1 s |
| Long term stability | 400 ppm RMS, 10 s at 30 °C |
| Ambient | 4 °C to 45 °C |
| Bandwidth as I source | dc to – 3dB ≥ 10Hz |
| Load | 0.05 H ≤ L ≤ 1.0 H<br>0.1 s ≤ L/R ≤ 1.0 s |

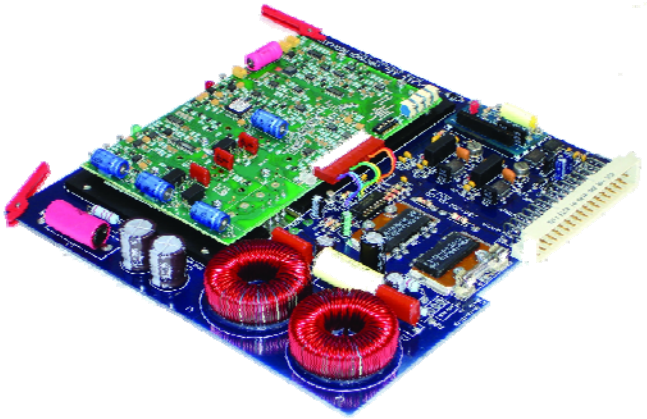

**Figure 4-24.** An MCOR module for 6A, 9 A or 12 A.

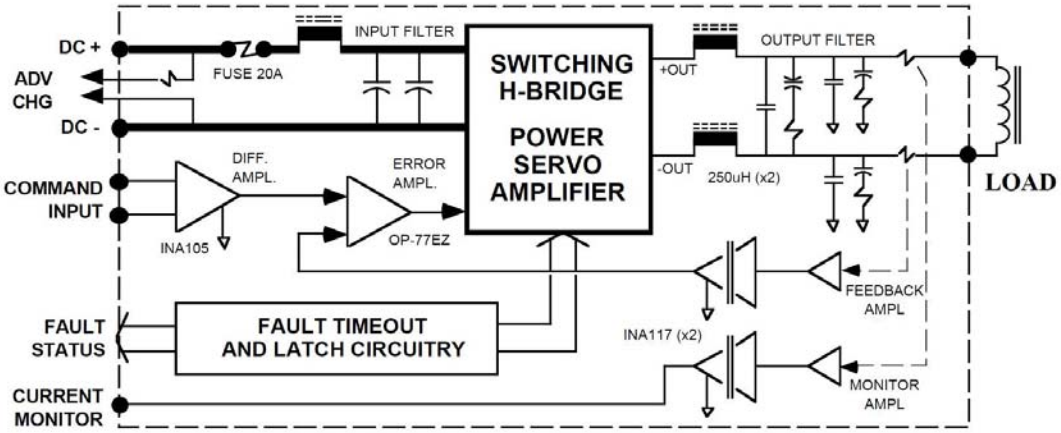


**Figure 4-25.** MCOR Power Module Block Diagram.

### 4.5.3 Magnet Power Supply System Topologies

PCD will keep the standard topology for magnet PS used successfully for installations around the SLAC complex since 1981. For large and intermediate power supplies, PCD will use the Ethernet Power Supply Controller (EPSC) to control the output current loop and interface to the EPICS machine control system. For bend trim and corrector magnets requiring bipolar output, PCD will use MCOR modules.

#### 4.5.3.1 Large and Intermediate Power Supply Systems

The proposed system topology for large and intermediate PS can be seen in Figure 4-26 and Figure 4-27. (PCD is responsible for the specification and installation of elements identified in red). This system topology has been used in projects such as PEP-II [64], SPEAR3 [69] and LCLS [67], which provides the advantage of commonality between several installations, a reduced inventory of spare equipment, and an established knowledge basis by the maintenance and control staff.

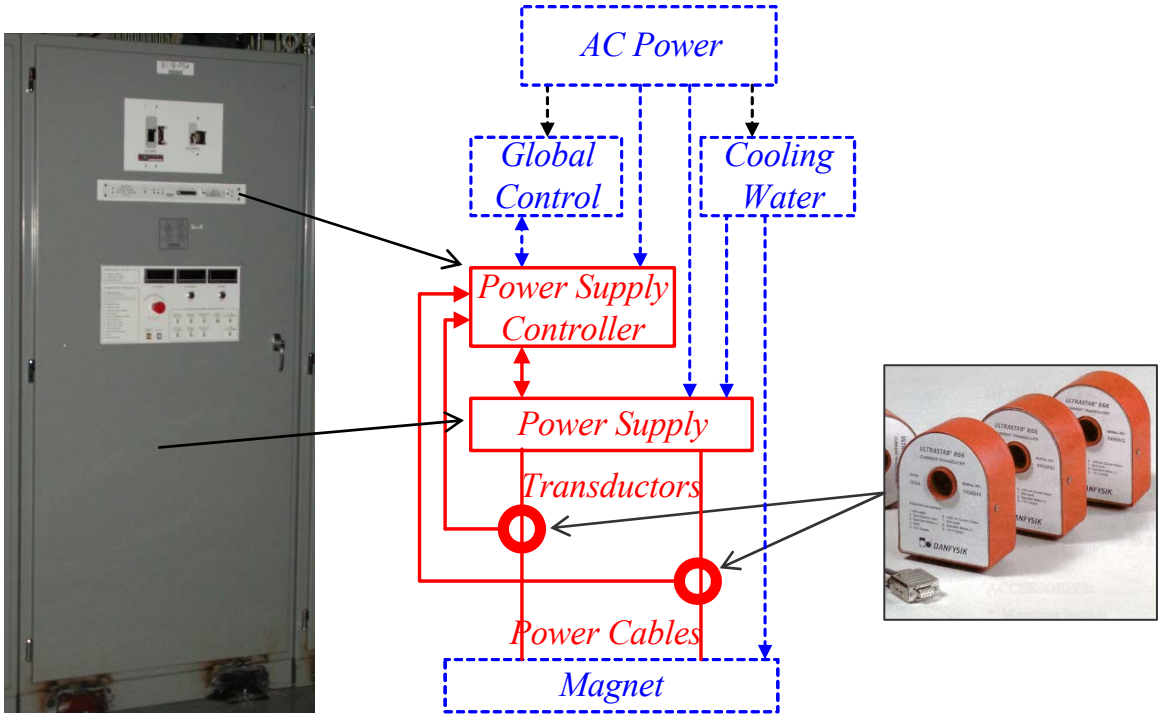


**Figure 4-26.** System Topology for the FACET Large Power Supplies. (Magnet protection not shown).

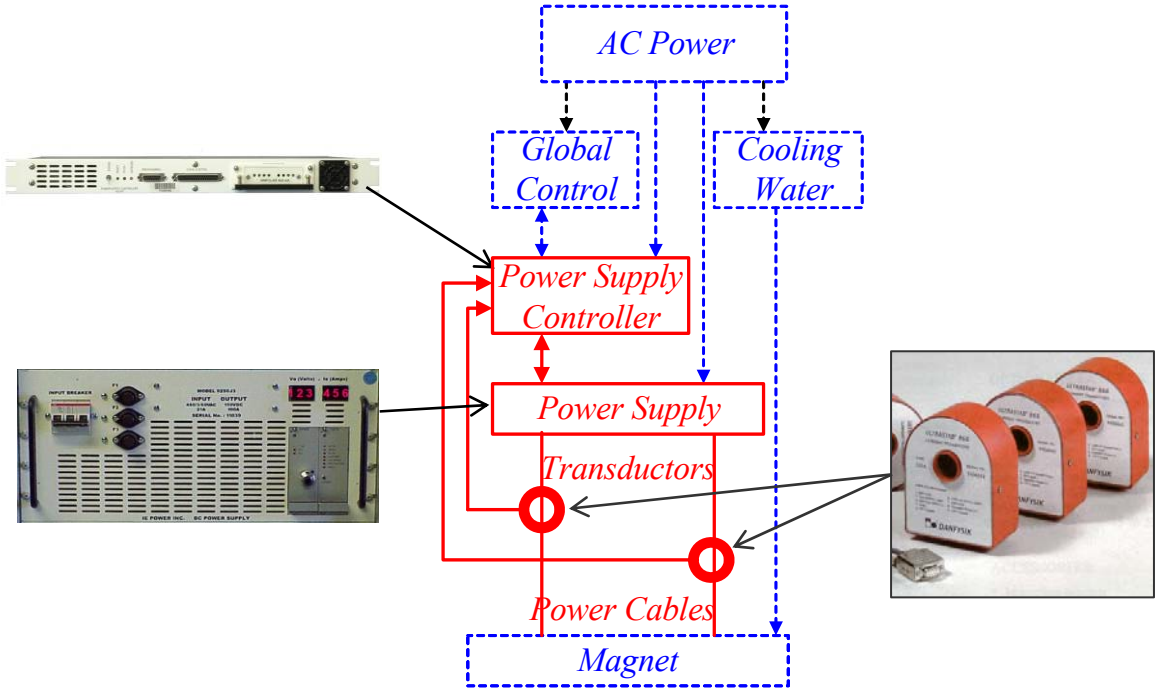


**Figure 4-27.** System Topology for the FACET Intermediate Magnet Power Supplies (Magnet Protection not shown).

A 1U, 19 inch rack-mounted Ethernet-based power supply controller (EPSC) provides precision regulation of magnet current via a closed external current loop. It also monitors power supply's current, voltage, and ground current. It manages the external interlocks, and communicates abnormal conditions to the FACET control system.

The EPSC provides better then 1 ppm current setting resolution, and 50 ppm stability over a 40 °C environment change. It employs a standard analog power supply interface to control standard commercial power supplies of many ratings, types and from different manufacturers.

The output current control loop of each large or intermediate PS will be adjusted to yield an overall output current regulation bandwidth of 10 Hz. This is sufficient to compensate for thermal variations of the magnet and cabling resistance.

#### 4.5.3.2 The Ethernet Power Supply Controller

The Ethernet Power Supply Controller (EPSC) [70] is a replacement for the PEP II Bitbus PS controller. It is interchangeable with a PEP-II chassis, but uses an Ethernet instead of Bitbus protocol. It provides greatly enhanced performance and diagnostics for approximately US$ 3000/unit. Table 4-5 presents the main performance characteristics of the EPSC, and Figure 4-28 shows its internal structure.

The main features of the EPSC are:

- Daughter boards for magnet dependant configuration
- Support for redundant transductor
- Hardware protection, latching and reporting of all system faults by FPGA
- Ramping of power supply output current

**Table 4-5.** EPSC Main Parameters

| Parameter | |
|---|---|
| DAC resolution | 24 bits |
| DAC noise (0.1 to 10 Hz) | 2 μVrms |
| DAC Linearity 0-10V | 2 ppm max |
| ADC effective # of bits | 20 bits |
| ADC readings per second | 60 |
| ADC noise (0.1 to 10 Hz) | 3 μVrms |
| ADC temp stability max | 0.25 ppm / °C max |

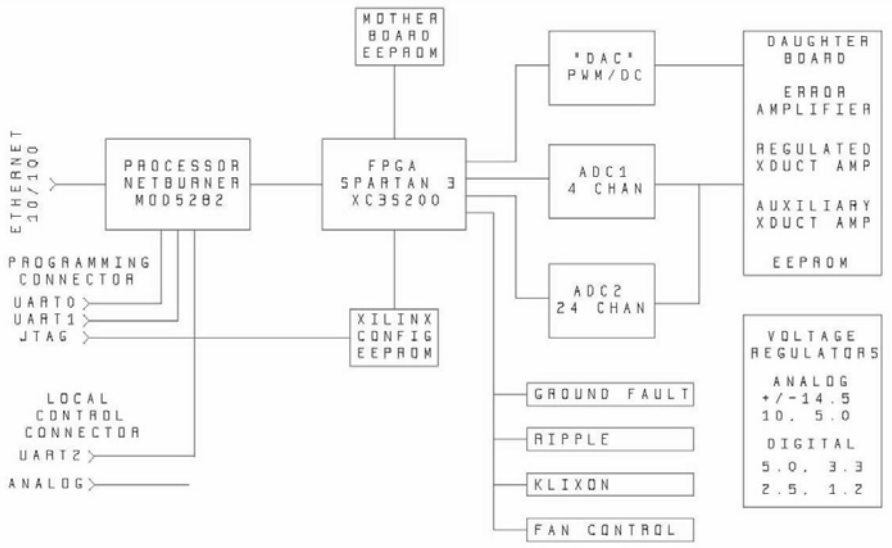


**Figure 4-28.** Internal structure of the EPSC.

#### 4.5.3.3 Bend Trim and Corrector Power Supply Systems

A single Eurocard crate accommodates up to 16 bipolar power modules (MCOR) of different ratings [68]. The physical MCOR crate is a standard 6U by 220 mm Eurocard format, with 17 slots, one for a control system interface card, and sixteen for the MCOR modules. Each MCOR module has a 'personality card', which is mounted directly on to it. This personality card contains passive components that determine the maximum output current limit, the transfer function of command voltage to output current, and the compensation network for the error amplifier section. All cards and modules are accessible from the front of the crate, and connect to the backplane using standard Eurocard connectors. Air cooling for the crate is provided by fan rack sets and plenums, which draw in cool air from the aisle and pass it through the crate and into the rack, thus keeping the rack interior at positive pressure.

A single bulk PS rated 60V and 165A provides regulated voltage to two crates of MCOR modules. Figure 4-29 shows the overall block diagram for a MCOR power supply system for several magnets powered from a single crate.

A programmable logic controller (PLC) controls and monitors the operation of the bulk power supply. The PLC is EPICS-compatible. It provides remote turn-on and turn-off capability, and monitors the output voltages and currents of the three bulk power supplies. It also detects ground current flow.

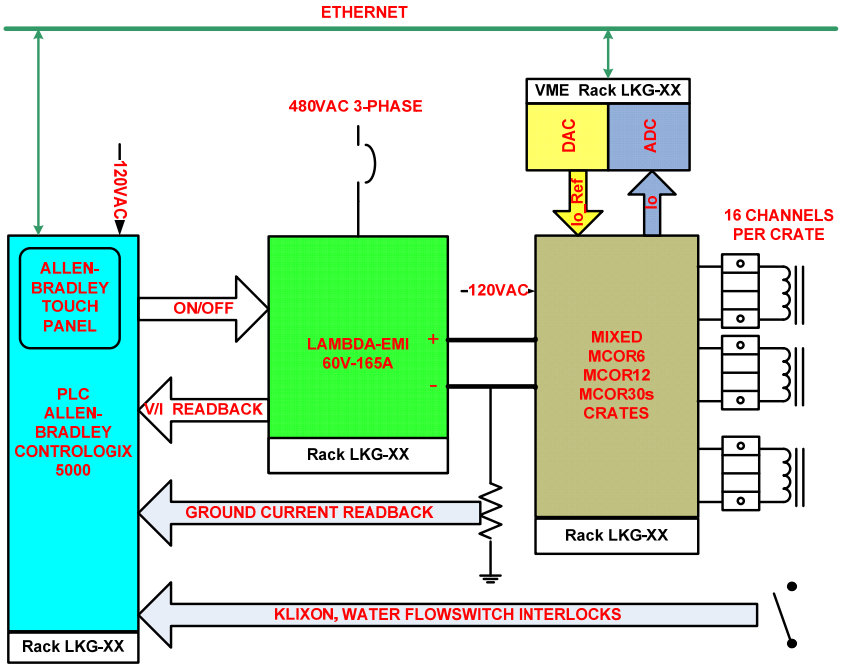


**Figure 4-29.** MCOR Power System Block Diagram.

### 4.5.3.4 Quad Trim Power Supply Systems

Some of the FACET quads located in either the electron or positron chicanes in Sector 20 will need additional trim PS to provide a 10% boost to the quads common current. In this case, PCD will install 1U intermediate PS, which will also be controlled by EPSCs. Figure 4-30 shows a typical PS system arrangement for this application. In this arrangement, a bulk PS provides the baseline current for the entire string of series-connected quads and the boost PS provide the additional 10% current margin needed.

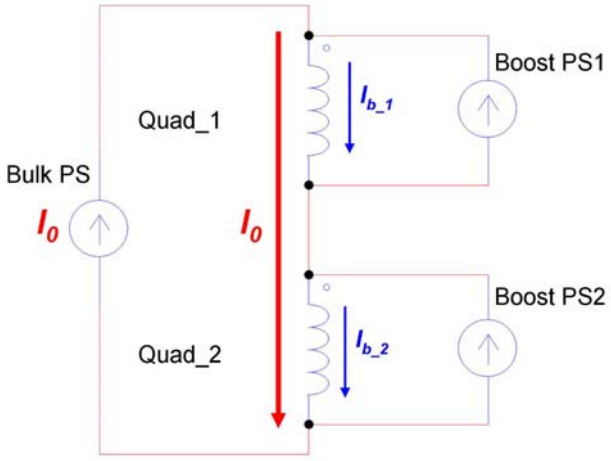


**Figure 4-30.** Quad Trim PS System Topology.

### 4.5.4 Safety

PCD will hold regular safety and project review meetings throughout the program. All electrical equipment and systems will be subject to a comprehensive inspection according to the Electrical Equipment Inspection Program (EEIP) at SLAC. This maximizes the use of nationally recognized testing laboratory (NRTL) listed components and ensures the equipment satisfies the NEC and OSHA safety codes.

Power supply to magnet power cables are flexible stranding, low smoke, zero halogen, construction suitable for cable tray and accelerator housing use. Cable ampacities conform to the NEC2008, Tables 310-16 and 310-17. Cable tray fill conforms to NEC Article 392. Wherever applicable, grounding and bonding requirements conform to NEC2008 Article 250.

The electrical installation and circuit breaker selection will also follow criteria from NFPA70E 2009 edition, Standard for Electrical Safety in the Workplace, especially to minimize the risk of electrical shock and arc flash hazards.

For every individual PS system, PCD will write lockout and tagout procedures per requirements of the Control of Hazardous Energy (CoHE) program at SLAC.

Other standards applicable to the design of magnet PS systems are the SLAC ES&H Chapter 8, Electrical Safety manual and the current edition of the DOE Handbook on Electrical Safety.

**Table 4-6.** Sector 20 magnet power supply requirements

| Magnet Name | PS Requirements | | | Available PS | | | | | # of PS needed |
|---|---|---|---|---|---|---|---|---|---|
| | Volts | Amps | kW | Model | Volts | Amps | kW | V ac | |
| B1_L & R (Com) | 50 | 713 | 36 | EMHP | 60 | 750 | 45.0 | 480 | 1 |
| Wigglers (E) | 60 | 300 | 18 | EMHP | 80 | 375 | 30.0 | 480 | 1 |
| Q1E | 49 | 129 | 6 | ESS | 60 | 165 | 9.9 | 480 | 1 |
| B2E | 45 | 394 | 18 | EMHP | 60 | 500 | 30.0 | 480 | 1 |
| Q2E | 74 | 466 | 35 | EMHP | 100 | 600 | 60.0 | 480 | 1 |
| S1E_L | 11 | 78 | 1 | EMS | 20 | 125 | 2.5 | 208 | 1 |
| S1E_R | 14 | 78 | 1 | EMS | 20 | 125 | 2.5 | 208 | 1 |
| Q3_E | 124 | 236 | 29 | EMHP | 200 | 300 | 60.0 | 480 | 1 |
| S2E_L | 14 | 179 | 2 | ESS | 40 | 250 | 10.0 | 208 | 1 |
| S2E_R | 15 | 179 | 3 | ESS | 40 | 250 | 10.0 | 208 | 1 |
| S3E_L | 20 | 108 | 2 | ESS | 30 | 165 | 5.0 | 208 | 1 |
| S3E_R | 21 | 108 | 2 | ESS | 30 | 165 | 5.0 | 208 | 1 |
| Q4E | 173 | 219 | 38 | EMHP | 200 | 300 | 60.0 | 480 | 1 |
| Q5E | 31 | 146 | 5 | Inv | 40 | 250 | 10.0 | 480 | 1 |
| B3E | 34 | 527 | 18 | EMHP | 50 | 1000 | 50.0 | 480 | 1 |
| Q6E | 14 | 127 | 2 | ESS | 30 | 165 | 5.0 | 208 | 1 |
| Magnet Name | PS Requirements | | | Available PS | | | | | # of PS needed |
| | Volts | Amps | kW | Model | Volts | Amps | kW | V ac | |
| QFF1 | 18 | 89 | 2 | EMS | 20 | 125 | 2.5 | 208 | 1 |
| QFF2 | 37 | 84 | 3 | EMS | 40 | 125 | 5.0 | 208 | 1 |
| QFF4 | 49 | 178 | 9 | Inv | 80 | 195 | 15.6 | 480 | 1 |
| QFF5 | 69 | 345 | 24 | EMHP | 80 | 375 | 30.0 | 480 | 1 |
| QFF6 | 43 | 519 | 22 | EMHP | 60 | 750 | 45.0 | 480 | 1 |
| QS1 | 44 | 495 | 22 | Inv | 60 | 500 | 30.0 | 480 | 1 |
| QS2 | 44 | 495 | 22 | Inv | 60 | 500 | 30.0 | 480 | 1 |
| B5D36 | 33 | 400 | 13 | EMHP | 40 | 450 | 18.0 | 480 | 1 |
| BDMP2 | 34 | 400 | 13 | EMHP | 40 | 450 | 18.0 | 480 | 1 |

## 4.6 Controls

### 4.6.1 Introduction

The FACET proposal (White paper) states that FACET control will be based on the legacy SLC control system (SCP), since that system was successfully controlling the Linac up to the time PEP-II was terminated in April of 2008. Precursor experiments to those proposed for FACET, run in the Final Focus Test Beam, were all controlled by the legacy system, based on CAMAC, micros, and VMS. The experimenters were comfortable with that system, and the experiments were largely very successful.

FACET will use the existing source (electron gun at CID), damping rings, electron compressor in Sector 10, and positron target. An additional positron compressor is planned for Sector 10, and some enhanced capabilities are required for some planned FACET experiments. Approximately 80 meters of new beamline equipment will be installed at the experimental end of FACET (Sector 20), replacing the current equipment.

In the intense LCLS construction and commissioning period since the shutdown of PEP-II, several relevant control system changes have occurred:

- New suite of advanced Unix-based tools.
    - This suite of tools has largely supplanted the VMS-based tools. Both physicists and operators now have facility with the new approach.
- Controls group skill set is now EPICS and Unix. All new implementations have been done with EPICS, not the legacy system.
    - These changes have a major impact on our ability to make changes to the legacy system, although we have done what we can to retain some capability.
- An important ongoing Linac Upgrade Project
    - This AIP project is on track to remove the dependencies of the LCLS portion of the Linac on VMS, "micros", and Multibus. The current expected completion date of this project is mid-2010.

For both the construction and operation of FACET, it is deemed crucial that there be a clean operational separation between LCLS and FACET. As will be discussed, this has important implications for the Timing, Machine Protection, and Personnel Protection systems.

### 4.6.2 Control System Approach

Since there is not time available to complete the ongoing Linac Upgrade project for the LCLS piece of the Linac, and then extend this upgrade to the FACET Linac regions, the only option is to bring up the legacy control system basically as it was at the time of the PEP-II shut-down.

Therefore, the overall approach for FACET is to use the LINAC basically "as was", and to implement the renewed Sector 20 in EPICS, with very minor exceptions in both cases. All EPICS implementations are clones of existing LCLS implementations. One big advantage of this approach over mixing SLC and EPICS solutions in Sector 20 is that it minimizes cross-system (SLC/EPICS) communications. This approach also reflects 1) the reality of needing to run with the legacy system; 2) the leveraging of recent LCLS software developments; 3) the

most efficient use of the software group to support FACET, and 4) preparation for a near-term control system upgrade. This approach is illustrated in Table 4-7.

**Table 4-7.** Systems, counts and implementation

| Subsystem | SLC/EPICS | Count |
|---|---|---|
| | | |
| S10 Magnets | SLC | 6 |
| S20 Magnets | EPICS | 62 |
| S10 BPM | SLC | 1 |
| S20 BPM | EPICS | 20 |
| Toroids | EPICS | 6 |
| Profile Monitors | EPICS | 3 |
| Wire Scanners | EPICS | 4 |
| Timing EVG (master) | EPICS | 1 |
| Timing EVR (slave) | EPICS | 40 |
| Experimental Support | EPICS | 3 IOCs |
| Vacuum | EPICS | 7 gauges |
| Collimators | EPICS | 6 |
| MPS extension | SLC | 20 signals |
| Networking | n/a | |
| SLC Database prep | SLC | |
| SLC Feedback loop | SLC | |
| PPS | New | |
| BCS | New | |

### 4.6.3 Control System Implementation

This section briefly outlines the implementation strategy for the elements of the control system.

#### 4.6.3.1 Experimental Area

Several VME IOCs will be in place to support the changing instrumentation needs of the experiments; a reasonable cable infrastructure will be provided to support foreseeable requests. Many signals will require pulse-ID tagging for accurate correlation with machine parameters; EPICS timing support will be provided, in the form of EVR modules. There will also be a need to interface with third-party equipment, likely PC-based, as was the case in PEP-II; EPICS provides a good interface to such equipment.

#### 4.6.3.2 PPS/BCS (Personnel Protection and Beam Containment)

Ongoing and impending projects are addressing the separation of FACET and LCLS areas in the Linac from the Safety System point of view. The goal is to allow work in the FACET area while LCLS runs, and to eliminate, as far as possible, any interference between the two programs.

There may also be some small amount of BCS work required within FACET around the Sector 10 chicane and Sector 20 beamlines.

#### 4.6.3.3 MPS (Machine Protection)

The 1553-MPS - that was used during the PEP-II era - is still in place and functioning; this will be the MPS system for FACET. The remaining nodes in the LCLS area are being decommissioned now and being replaced with the new Link-node MPS; the 1553-MPS algorithm will be modified accordingly. The older TIU (Tone Interrupt) system, which is still in use for much of the Linac, needs some maintenance, but will run "as was". It may be necessary to add a few more signals to MPS in the new Sector 20 chicane, which will require no significant hardware, but rather only wiring, perhaps some CAMAC modules, and MPS logic changes.

#### 4.6.3.4 Instrumentation

BPMs & Toroids. Sector 20 will have 31 new Beam Position Monitors, 11 each in the electron and positron chicanes, five in the final focus area, and four in the dump. The positron arm of the Sector 10 chicane will require a new BPM as well. Six new strip-line BPMs must be fabricated.

There are a few BPMs in Sector 20 which are needed both in the SLC system and EPICS system - SLC to support the SLC Model-based applications or SLC Fast Feedback needs, and EPICS to provide uniform pulse-ID tagged data for experimental support. Using a splitter, the signals from a physical strip-line BPM will be fed to both systems.

Experimenters are asking for EPICS BPM support from two BPMs in high-dispersion areas in the RTLs, (North and South Damping Ring To Linac sections) and from the two BPMs in the Sector 10 chicanes; these will all be shared between SLC and EPICS. EPICS BPM support in those areas will require new cabling, processors, IOCs, and crates.

The six toroids in Sector 20 will be processed as EPICS-only toroids, providing pulse-ID tagged data. These will require cabling, toroid signal processors, and IOCs with EVR modules.

Profile Monitors. Three new profile monitors will be installed in Sector 20. These will be controlled by EPICS.

Wire Scanners. The four new wire scanners in Sector 19 will be installed as EPICS devices.

Collimators. Each of the compressor arms (e- and e+) in Sector 20 will be outfitted with one 4-jaw, one 2-jaw, and one notch collimator. These will be instrumented for EPICS.

Vacuum. The seven new gauges and control for new vacuum valves will be implemented in EPICS.

Diagnostic Scopes. The need to replace old scopes or provide scopes in new locations is not yet well-defined. Any network-enabled scope will need a new network connection.

#### 4.6.3.5 Timing System

All FACET timing will derive from the SLC Master Pattern Generator (MPG), using a unique FACET beam-code. An EPICS timing system will be slaved to the MPG, as is now the case in LCLS, using EVG (Event Generator) and EVR (Event Receiver) modules, to provide the same timing signals to EPICS which are available in the SLC system. These timing signals are needed in EPICS for Pulse-ID-stamping BPM, Toroid, and experimental data.

These EVR and EVG units are the standard EPICS timing solution, and are available only from one source, in Finland. Since the timing subsystem is flexible, complex, and was costly to implement, it is crucial to use the same units so that the LCLS work can be leveraged.

#### 4.6.3.6 Magnets

All magnets in Sector 20 will be controlled by either network-based controllers or MCOR controllers, in both cases under EPICS control - as is done now in the LCLS. These will be EPICS-only magnets - no SLC-Awareness.

#### 4.6.3.7 Networking

The networks will be substantially upgraded in the Sector 20 area to support the EPICS IOCs, PLCs, and network-enabled power supply controllers. Some new support will be needed for the sector 19 wire scanners as well as BPMs in sectors 10 and 2.

#### 4.6.3.8 Hardware Support

There are an adequate number of CAMAC modules, Multibus crates, and CAMAC crates and power supplies on hand to support initial running. Some CAMAC test areas will be revived and staff added to provide technical support for this hardware.

#### 4.6.3.9 Software Support

Archiver instead of SLC History. We will be using the EPICS archive system to record and recall FACET data for both the SLC and EPICS systems, since we have support for the EPICS archive system and the SLC History system would need ongoing surveillance and maintenance.

Fast Feedback Changes. An energy feedback in sectors 19 and 20 now serves the positron extraction; an analog of this will be created to support energy feedback for FACET on the FACET beam-codes. This requires a few BPMs in the Sector 20 compressor as readout devices along with normal fast feedback implementation work (micro-micro communication links, model-based transport matrix generation, etc.).

Model Issues. The SLC Model is functional for sectors 0-19, so all existing model-based code can be run from the SCP.

By undertaking two well-understood tasks, the SLC Model and use of associated applications can be extended through Sector 20.

1) Generate the magnets, (non-shared) BPMs, and wire scanners into the SLC database for Sector 20 as dummy devices.

2) Implement the VMS software routines which convert magnetic field settings to and from an energy-independent model parameter such that these routines for this area access EPICS magnet data.

Servers and Licenses. FACET will either need its own application servers, Oracle servers and NFS servers, or negotiate with LCLS to share resources.

SLC Software (DBGEN, Micro, VMS). We plan to minimize any VMS software or SLC system DataBase GENeration procedures for FACET. If at all possible, we will not undertake any work at all on code which runs in the SLC Micros.

### 4.6.4 Related AIP Projects

#### 4.6.4.1 Linac Phase I Upgrade Project

Phase I of the Linac Upgrade Project is currently underway, aimed at completion in mid-2010. The goal is to replace the micros and multibus CAMAC controllers in the LCLS area

(sectors 20 through BSY), and move all remaining necessary high-level code off VMS and onto Unix. This then removes any role for the legacy SLC control system (and SCP) for LCLS.

In phase I the CAMAC crates and modules will not be replaced, but rather controlled via new CAMAC Branch controllers in VME crates. When all is ready and tested, the switch-over will consist of moving two CAMAC cables from the multibus controller to the VME controller, marking the old micro "offline" and booting the new IOC.

In sectors 0-20, there are types of modules which are not being addressed in this LCLS-based project; extra work will be required before this upgrade could be "rolled down" the Linac.

Phase II of this project will move us adiabatically off CAMAC. As devices are moved off CAMAC, the EPICS system need only redirect the hardware connections; higher-level applications will not be affected.

#### 4.6.4.2 RF Upgrade Project

This project is in the design stage. The goal is to replace the legacy SBI (SubBooster Interface) and PIOP (Parallel Input/Output Processor)/MKSU (Modulator Klystron Support Unit) low-level RF control with a modern package and much enhanced capability.

#### 4.6.4.3 CCR PPS Upgrade

There is one nexus of PPS in the old Central Control Room (CCR), in building 3. Moving this installation and re-implementing it in a modern fashion is a pre-cursor piece of work to having separate PPS for LCLS and FACET. There are discussions underway about how to expedite this PPS work.

#### 4.6.4.4 LINAC Network Upgrade

The current LINAC network infrastructure needs upgrading, both due to equipment obsolescence and to increased connectivity needs. If this AIP were to advance, it would obviate some piece-meal solutions for FACET.

### 4.6.5 Legacy System Support

Most CAMAC modules in use are SLAC-designed and have been maintained by a group within the Controls Department. There are just short of 2000 CAMAC modules in the FACET sectors. There is an inventory of over 500 modules, with more to be rescued from the SLC arcs and PEP-II. Nevertheless, repair capability for CAMAC modules and crates will need to be revived.

Many special purpose modules are far past end-of-life, as evinced by the non-availability of parts (chips) to repair them. It will need to be determined which modules have ample spares, which may need some short-term replacement, and which will need to be replaced as part of system upgrades in the 2- to 3-year time frame.

The bulk of in-house skill sets is now in Linux and EPICS support. It is therefore very important to minimize the software support needed in the legacy system. By implementing the experimental area purely in EPICS, changes to the SLC database are minimized. No software upgrades are planned for the SLC micros, since there is no technical requirement. Use of the EPICS Archiver instead of the SLC History Buffer system removes another high maintenance load from VMS.

It is also important to minimize the need for data bridges from SLC to EPICS, since the VMS processes responsible for these are already fairly heavily loaded. The above-described split between the Linac Sectors 0-19 in the SLC system and Sector 20 fully in EPICS will keep this load small.

The 56 cameras in the FACET region are analog (TV) cameras, interfaced to the SLCNET backbone. The subset needed for FACET has been identified. Operations is investigating reviving or updating the control room support of these analog cameras. Moving to LCLS-style digital cameras would be the preferred solution.

The replacement of failed diagnostic scopes with network-enabled scopes is also being investigated by Operations.

### 4.6.6 PPS and BCS

The PPS system for the linac tunnel as currently configured requires that the entire tunnel be vacated and locked as a condition for turning on power to the klystrons. This system will be modified to separate the linac tunnel into two functionally independent zones in such a way that persons will be able to enter the linac tunnel in Sector 20 or any sector upstream of this point while the LCLS is operating in Sector 21 and beyond. These new features will be implemented in the PPS system, with an electronically locked and monitored passage provided by the shielding wall between Sectors 20 and 21. The Sector 2-20 PPS zone will be divided to two PPS zones, FACET experimental zone and Sector 2-17 zone, to let experimenters entering experimental zone and keep RF in sector 2-17 on.

The klystron stations in Sectors 19 and 20, including four klystrons needed for LCLS operation, are powered by the same variable-voltage substation, which now must be interlocked off as a condition for any tunnel entries. To overcome this limitation, individual disconnect switches will be configured in each of the klystron modulators in this sector-pair, and the PPS logic will be modified to ensure that appropriate klystrons are off to allow access to the FACET area while the LCLS is operating. This change is relatively simple, but must be done with rigorous formality including full testing and certification.

## 4.7 Facilities

The scope of work for facilities includes providing necessary services, such as water and compressed air as well as power distribution. The cooling water and compressed air for the beamline elements will be provided, including the necessary sensors. The power distribution system will provide electrical power for the project power supplies. In addition, electrical lights, switches and wall plugs in the tunnel will be provided. For the Sector 20 systems, Ample 480 VAC power will be available from the new K-10 substation, which is scheduled to be upgraded in January –March 2010 as part of the LCLS project.

## 4.8 Cable Plant

The Cable Plant is an essential element of the FACET project and it will consist of several cable systems, cable trays, and rack installation. A reliable Cable Plant will be crucial to

the performance of the FACET facility. Cable system design encompasses every aspect of the project, including technical performance; materials, assembly, and installation costs, reliability and maintainability and adherence to electrical and building codes, resource conservation, and safety practices. The whole installation will be subject to the latest National Electric Code (NEC), SLAC National Accelerator guide lines, and Department of Energy safety standards. The planned installation will provide cables for the FACET electron beamline in Sector 20 and positron beamline in Sector 10. The cables for the positron phase of Sector 20 are left for a future upgrade.

### 4.8.1 Cables

Existing cables will be removed to make room for the new cables that meet the most up-to-date safety codes and performance requirements. The technical requirements of each system must be considered in the specification of cable hardware, and therefore, places cable selection on an equal level to any other accelerator component.

Each family of cables shall be documented by a layout drawing, indicating cable endpoints, cable numbers, routing, connectors, and dressing information. All cables will be documented in CAPTAR (Cable Plant Tracking and Reporting Database). A full set of installation specifications will be created. All this documentation will be used as a basis for estimating the work, for installation, as well as for future reference.

Cables shall be installed with strain relief when cables drop freely for more than six feet. Cables shall be dressed properly into the trays and electronic racks, providing the proper service loop to facilitate connector replacement. A typical cable installation is shown in Figure 4-31.

### 4.8.2 Cable Trays and Raceways

New cable trays will be installed in the Klystron Gallery as well as in the tunnel. Trays will be divided for cable segregation. The great majority of cable trays will be new; any existing trays used will need to meet the same codes and standards as the new trays. The trays should be heavy duty hot-dipped galvanized steel.

Continuously grounded trays installed as a complete system, integrated into the tunnel and gallery main ground grid, will ensure a safe reliable system and also serve as ground plane for low level instrumentation signals.

Engineering, Design, and Planning will consider the following:

1. Cable trays shall be continuously grounded, and engineered per NEC 392.

2. Cables shall be for use in trays and of Low Smoke Zero Halogen (LSZH).

3. Radiation resistant cables shall be specified, whenever possible.

4. Metallic conduits shall by grounded and terminated with insulated bushings for cable protection.

A typical cable tray is shown in Figure 4-32.


**Figure 4-31.** Typical linac gallery cable tray and rack installation (LCLS S20). A similar arrangement will be installed for FACET.

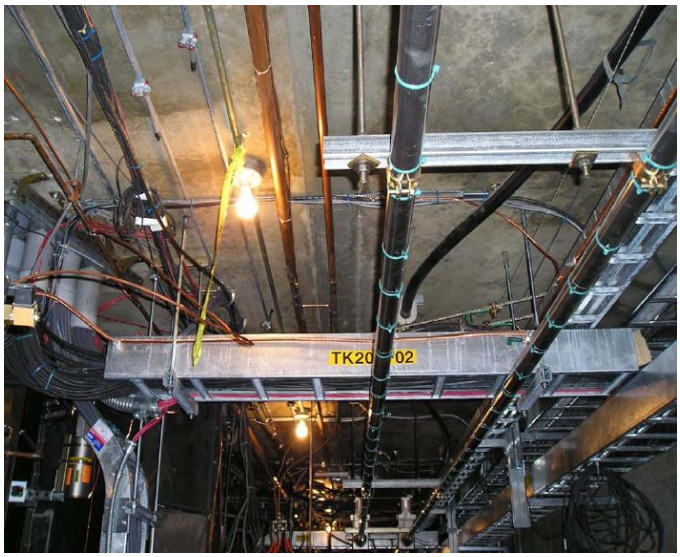

**Figure 4-32.** Typical linac tunnel cable tray installation (LCLS S20 &21). A similar arrangement will be installed for FACET.

## 4.9 Future Upgrades

The beam parameters achievable with the FACET facility will be adequate to support the science programs for experiments with either electron or positron bunches. FACET has been designed so that it can be upgraded to provide both electron and positron bunches delivered simultaneously to the Sector 20 Experimental area.

### 4.9.1 Sector 20 Beamline Upgrade

The FACET beam line chicane in Sector 20 could be upgraded to allow electron and positron bunches to enter half an RF wavelength apart (5 cm). They would then be injected into the plasma with a spacing of half a plasma period (100 μm). This would require a "sail-boat" arrangement of the chicanes to provide the needed path difference for electrons and positrons; see Figure 4-5.

# 5 Management of Scientific Program

FACET is both a user facility designed to support a national program in advanced accelerator science and a facility to advance the design of a plasma wakefield linear collider (PWFA-LC). It is expected that roughly 75% of the available beam time will be dedicated to the directed PWFA-LC research with the remaining 25% of the beam-time scheduled for other user experiments, some of which may be related to a broader exploration of plasma acceleration concepts. The success of the FACET program will be the responsibility of the SLAC Assistant Director for the Accelerator Research Division (ARD) who will report to the SLAC Director of Particle Physics and Astrophysics (PPA). The experimental program will be supported out of ARD while the beam operation will be the responsibility of the SLAC Accelerator Systems Division.

The SLAC PPA Director will establish an external Experimental Program Advisory Committee to meet annually to review the progress of the directed PWFA-LC research program and to recommend other proposed experimental programs for the remaining beam time. As for other beam-related user facilities at SLAC, there will likely be broad demand for beam time from the community and FACET will likely prove attractive for a broad scientific audience. Some of the possible topics are outlined in Section 3.

The directed PWFA-LC research will be performed as a collaborative effort devoted to the development of the PWFA-LC concepts through experiments at FACET, computer simulations, plasma physics theory and accelerator design efforts. This collaboration will have responsibility for establishing the research directions and managing the plasma wakefield R&D program. Progress in the PWFA-LC program will be reviewed by the external FACET review committee.

The PWFA-LC collaboration membership will be scientists and engineers dedicated to the PWFA-LC research program. At present the collaboration includes members from UCLA, USC, and SLAC, but additional university and national and international laboratories may join the collaboration as FACET is developed. The collaboration, in consultation with the SLAC PPA Director, will select a senior management team and a spokesperson. The spokesperson will represent the collaboration to DOE and SLAC management and will chair the senior management team. During the construction phase, the collaboration spokesperson will interact closely with the FACET Project Manager to ensure that the experimental needs of the PWFA-LC program are met by the FACET facility. The senior management team will be responsible to the SLAC Accelerator Research Director for the PWFA-LC experimental program, evaluating the readiness of the experiments, the status of the supporting simulations, and modifying the schedule as necessary to ensure that the goals of the FACET PWFA-LC program are achieved.

# 6 Environment, Safety, Health and Quality Assurance

It is SLAC's policy and objective to integrate safety and environmental protection into its management and work practices at all levels, so that its mission is accomplished while protecting the worker, the public, and the environment. To achieve this objective, SLAC has developed and implemented an Integrated Safety and Environmental Management System (ISEMS), required by DOE P450.4, Safety Management System Policy, which encourages and supports the use of: the Work Smart Standards process, development of measurable goals in the form of performance metrics, and uses existing programs and activities that have been deemed successful and which already incorporate the ISEMS elements. (ISEMS as a required element is implemented through the incorporation of a contract clause from the DOE Acquisition Regulations (DEAR), specifically DEAR 970.5204.-2, "Integration of Environment Safety and Health Into Planning and Execution". This clause was incorporated into the contract between DOE and Stanford University for operation of SLAC in February 1998.).

Fundamental to the ISEMS process is the application of Guiding Principals (GPs) and Core Functions (CFs). GPs are a series of best management practices or "basic philosophy" that ensure start-to-finish management of ES&H issues. CFs provide the necessary structure that describes the scope of work, identifies and analyzes the hazard, develops and implements hazard controls, allows work to be performed within the controls, and uses feedback from the work performed to improve the safety system. Responsibility for achieving and maintaining excellence in this system rests with line management, who implement the SLAC ES&H policy with the personnel under their supervision.

Existing and mature programs at SLAC will be used to ensure that all aspects of the design, installation, testing and operational phases of the project are properly managed. The FACET project has been presented to the SLAC Safety Overview Committee, which coordinates and assigns safety reviews for new projects or facility modifications to other citizen committees, which have knowledge or skills in a specific area. The hazards for FACET will require reviews from committees including but not limited to: Radiation Safety Committee, Electrical Safety Committee, Earthquake Safety Committee and the Fire Protection Safety Committee.

Operation of existing electron accelerators has provided familiarity with the principal hazards and risks associated with them. They are: Ionizing Radiation, Electrical Safety Issues, Non-Ionizing Radiation, Seismic Safety Issues, Fire Safety (including Emergency Preparedness), Construction Activities, Hazardous Material Issues and Environmental Protection; as they relate to the design, component manufacturing, system installation and operation of the FACET facility.

At SLAC, the FACET project will not generate any hazards that have not already been defined and addressed within the Work Smart Standards and will not present any significant challenges from the ES&H perspective. All aspects of the project will conform to the applicable Work Smart Standards SLAC has adopted and written into its contract with the DOE.

# 7 WBS Dictionary

## 7.1 Introduction

The Work Breakdown Structure (WBS) defines the work needed to be performed and will serve to track the cost and schedule of the project. On level two, the WBS is split into Systems or Areas. Each level two WBS element will be overseen and coordinated by a System Manager, who will typically act as Control Account Managers (CAM). On level three of the WBS, the work is broken down into sub-systems, each of which will have a manager, responsible for control of the cost, schedule, quality, safety and for meeting the performance expectations. The System Managers will set the performance requirements for each sub-system. The WBS will also serve to implement change control. The Preliminary Project Execution Plan will specify the levels of approval required for changes in cost and/or schedule at each level of the WBS. The WBS will also be used for cost reporting. The project will report costs and progress to the DOE monthly at level 2 of the WBS. The project management will review costs and progress monthly at level 3. The System Managers will review costs and progress monthly at the lowest levels of the WBS.

## 7.2 Level 3 Work Breakdown Structure

The WBS dictionary, presented below down to level three, describes the scope of work for each WBS element. Each element may typically include design, analysis, documentation, safety assessment, fabrication, testing, installation and validation and verification.

# 1 FACET Project (Total Estimated Cost, TEC)

The TEC captures all activities associated with the FACET project.

## *1.1 Project Management*

This WBS element captures the efforts on general management of the project, establishing and tracking the cost and schedule, preparation of financial and technical reports, organizing project reviews, and management of project-wide ES&H issues.

### 1.1.1 ES&H

This WBS element captures the efforts associated with management of safety issues in the design, fabrication and installation phases of the project.

### 1.1.2 Project Management

This WBS element captures the efforts associated with management and administrative activities of the project, including control of cost and schedule, generation of financial and technical reports, engineering coordination and management of Systems.

### 1.1.3 Technical Support

This WBS element captures the efforts associated with technical support and project review activities and collaboration activities related to the project.

## *1.2 Sector 20 Beamline System*

This WBS element includes activities and technical components required to perform final compression of the beam in Sector 20, its focusing into the experimental area and measurements of the beam properties.

### 1.2.1 Beamline Design Integration

This WBS element captures the efforts associated with design and integration of beamline components into the existing beamline and tunnel environment.

### 1.2.2 Magnets and Supports

This WBS element captures the efforts associated with design and fabrication or refurbishing of magnets and their supports. It also includes correctors and movers.

### 1.2.3 Vacuum System

This WBS element includes the efforts associated with design and production or refurbishing of beamline vacuum components and vacuum instrumentation.

### 1.2.4 Installation

This WBS element includes the efforts associated with installation and alignment of all hardware components in Sector 20 region. This element also includes efforts to remove existing components from Sector 20, prior to installation of new hardware, and also installation of instruments located between Sector 10 and 20.

## *1.3 Experimental Area*

This WBS element includes efforts required to define specifications and verify implementation of general purpose experimental area at the focal point of the Sector 20 beamline, suitable for plasma-wakefield acceleration experiments, solid state physics investigations, and for a variety of other studies. This WBS element also includes efforts to provide specific hardware as specified below.

### 1.3.1 Experimental Area Design Integration

This WBS element captures the efforts needed to integrate the design of the experimental area and to define specifications and verify implementation for subsystems that may be located in the experimental area, including the control system interfaces and channels, power, cooling water and compressed air for a generic set of instruments and devices.

### 1.3.2 Supports

This WBS element captures the efforts needed to define specifications and verify implementation for the supports of the components that form the experimental area.

### 1.3.3 Elevated Floor

This WBS element captures the efforts needed to define specifications and verify implementation for the elevated floor, in the experimental area, to allow convenient access to experimental equipment.

### 1.3.4 Optical Table

This WBS element includes the efforts needed to define specifications and verify implementation for the optical table in the experimental area.

### 1.3.5 Beam Dump

This WBS element includes the efforts associated with design and fabrication of the beam dump, including its shielding, water cooled absorber, water system and support.

### 1.3.6 Installation

This WBS element includes the efforts associated with installation of components in the Experimental Area.

## *1.4 Sector 10 Bunch Compressor System*

This WBS element includes efforts and technical components required to upgrade the Sector 10 bunch compressor, in order to allow compression and handling of both the electron and positron bunches.

### 1.4.1 Beamline Design Integration

This WBS element captures the efforts associated with design and integration of beamline components into the existing beamline and tunnel environment.

### 1.4.2 Magnets and Supports

This WBS element captures the efforts associated with design and fabrication or refurbishing of magnets and their supports. It also includes correctors and movers.

### 1.4.3 Vacuum System

This WBS element includes the efforts associated with design and production or refurbishing of beamline vacuum components and vacuum instrumentation.

### 1.4.4 Installation

This WBS element includes the efforts associated with installation and alignment of all hardware components in the Sector 10 bunch compressor.

## *1.5 Common Systems*

This WBS element includes efforts and technical components required to integrate and provide the common systems for the Sector 20 Beamline System, Sector 10 Bunch Compressor System, and the Experimental Area.

### 1.5.1 Accelerator Design Integration

This WBS element captures the efforts on accelerator integrated design including optics, tuning, tolerances and operational considerations to provide an optimal integrated design of the beamlines and the common systems.

### 1.5.2 Power Conversion

This WBS element captures the efforts and technical components required to power the beamline and other elements in both the Sector 10 bunch compressor and the Sector 20 beamline including system design, refurbishing or acquisition of power supplies and their installation.

### 1.5.3 Controls and Instrumentation

This WBS element captures the efforts and technical components required to design and implement the Control system, Personnel Protection System (PPS), Beam Containment System (BCS), and Machine Protection System (MPS), integration of the systems into SLAC control system, and providing required independent functionality of PPS, BCS and MPS for FACET. The items also include efforts to provide instrumentation hardware for the beamlines, such as beam position monitors and beam collimators. The WBS element captures the efforts for Sector 10 and Sector 20 as well as for locations in between, as necessary.

### 1.5.4 Facilities

This WBS element captures the efforts on providing the necessary services in the tunnel and supplying cooling water and compressed air for the beamline elements, including the necessary sensors. It also includes efforts on providing the power for the electrical lights, switches and wall plugs in the tunnel.

### 1.5.5 Cable Plant

This WBS element captures the efforts and technical components required to procure and install all the cables and cable trays for all the systems, as well as efforts associated with rack transportation and installation.

## 2 FACET (Other Project Costs, OPC)

This WBS element captures costs incurred prior to CD-1 approval and also the costs for validation and verification efforts to demonstrate CD-4 Key Performance Parameters.

## 2.1 Preparation of Conceptual Design Report

This WBS element includes efforts on preparation of CDR and other necessary documents, prior to CD-1 approval, as well as efforts associated with performing the necessary reviews.

## 2.2 Validation and Verification

This WBS element includes efforts on validation and verification of the FACET beamlines to demonstrated CD-4 Key Performance Parameters.

# 8 References


[1] R. Erickson, *et al*, SABER, The South Arc Beam Experimental Region Project at SLAC, http://www.slac.stanford.edu/grp/rd/epac/LOI/SABER.pdf, December 1, 2005.

[2] P. Emma, *et al*, Proposal for a Multi-Use Test Beam in the SLAC B-Line, SLAC-PUB-11244, PAC05, May 2005.

[3] P. Chen et al., Phys. Rev. Lett. 56, 1252 (1986); T. Katsouleas et al., Phys. Rev A 33, 2056 (1986); J. Rosenzweig et al., Phys. Rev. Lett. 61, 98 (1998); and R. Ruth et al., Particle Accelerators 17, 171 (1985).

[4] P. Muggli et al., IEEE Trans. Plasma Sci. 27, 791 (1999).

[5] C.L. O'Connell et al, Phys. Rev. STAB 9, 101301 (2006).

[6] C. Joshi and T. Katsouleas, Physics Today, 47 (June 2003).

[7] FACET Proposal to DoE.

[8] R. Hemker *et al.*, Phys. Rev. STA*B* **3**, 061301 (2000).

[9] Huang H., *et al*., "QUICKPIC: A highly efficient particle-in-cell code for modeling wakefield acceleration in plasmas, "Journal of Computational Physics. Vol. 217 no. 2 pp. 658-679 (2006).

[10] I. Blumenfeld et al., Nature 445, 741-744 (2007).

[11] P. Muggli, et al., Nature 411, 43-43 (03 May 2001).

[12] P. Muggli, et al., "Halo formation and emittance growth of positron beams in plasmas," accepted for publication Phys. Rev. Lett. (2008).

[13] M. J. Hogan *et al.,* Phys. Rev. Lett. **95**, 054802 (2005).

[14] M. Borland, Advanced Photon Source LS-287 (2000).

[15] W. R. Nelson *et al.*, SLAC-R-265 (1985).

[16] M. Borland, *et al.*, proceedings of the PAC 03 conference, p. 3461 (2003).

[17] P. Muggli, et al., proceedings of the PAC 07 conference, p. 3079 (2007).

[18] T. C. Chiou and T. Katsouleas, "High Beam Quality and Efficiency in Plasma Accelerators," Phys. Rev. Lett. 81 (16), 3411 (1998).

[19] J.B. Rosenzweig Phys. Rev. Lett. **58**, 555 (1987).

[20] C. E. Clayton, *et al,* Phys. Rev. Lett. **88**, 154801 (2002).

[21] P. Muggli et al, Phys. Rev. Lett. **93**, 014802 (2004).

[22] R. Gholizadeh *et al.*, proceedings of the PAC 07 conference, p. 3067 (2007), and AAC 07 Proceedings, AIP Conference Proceedings Volume 877, 504 (2006).

[23] G. Harapetian, *et al.*, Phys. Rev. Lett. **72**, 2403 (1994).

[24] J. S. T. Ng *et al.*, Phys. Rev. Lett. **87**, 244801 (2001).

[25] M. J. Hogan *et al*., Phys. Rev. Lett. **90**, 205002 (2003).

[26] P. Chen *et al.*, Phys. Rev. Lett. **64**, 1231 (1990).

[27] S. Lee, *et al.*, "Energy Doubler For A Linear Collider", Phys. Rev. ST Accel. Beams **5**, 011001 (2002).

[28] V. Yakimenko and R. Ischebeck, "Summary Report of Working Group 4: e-Beam Driven Accelerators", CP877 Advanced Accelerator Concepts: 12th Workshop, 158 (2006).

[29] B. Blue *et al*, Physical Review Letters **90**, 214801 (2003).

[30] X. Wang et al., AAC07 Proceedings, AIP Vol. 877, 568 (2007) and Proceedings of the PAC'07 Conference, 3082 (2007).

[31] C. Adolphsen *et al*., Proceedings of the PAC99 Conference, p. 3477 (1999).
[32] S. Lee *et al.* , Phys. Rev. E **64**, 045501 (2001).
[33] C.M. Fauser, Masters Thesis, University of Texas at Austin (1997).
[34] W. Kimura, Private Communication (2008).
[35] W. Gai *et al.,* Phys. Rev. Lett. **61**, 2756 (1988).
[36] M. E. Conde *et al*, Advanced Accelerator Concepts, AIP Conf. Proc. 472, 626 (1999).
[37] M. C. Thompson *et al*, Phys. Rev. Lett. **100**, 214801 (2008).
[38] "Wakefield Acceleration in Dielectric Structures", proposal by H. Badakov *et al.* (E-169 Collaboration).
[39] A. Kanareykin *et al*, Proc. AAC-2006, 320 (2006).
[40] ILC Reference Design Report: Detectors, Volume 4, SLAC-R-857 (2007).
[41] T. Shintake *et al.* Proceedings of the PAC95 Conference, p. 2444 (1995).
[42] W. Scandale, *et al*., Phys. Rev. ST Accel. Beams **11,** 63501 (2008):
[43] Yu.Chesnokov, *et a*l., "Radiation of photons in process of charge particle volume reflection in bent single crystal," IHEP Preprint 2007-16, Protvino (2005).
[44] J. Stöhr and H. C. Siegmann, "Magnetism: From Fundamentals to Nanoscale Dynamics", Springer Series in Solid-State Sciences **152**, (Springer, New York, 2006).
[45] D.J. Hilton et al., Optics Lett. **29,** 1805 2004: "Terahertz emission via ultrashort excitation of magnetic metal films".
[46] E. Baurepaire *et al.*, Appl. Phys. Lett. **84**, 3465, 2004: "Coherent terahertz emission from ferromagnetic films excited by femtosecond laser pulses".
[47] J.B. Héroux *et al.*, Phys.Stat.Sol.(c) **3**, 4271 (2006): "Magnetization induced terahertz radiation from GaMnAs".
[48] S. J. Gamble, Mark H. Burkhardt, W. Harrison, H. C. Siegmann, J. Stöhr, A. Kashuba, Rolf Allenspach, and Stuart S. P. Parkin, to be published.
[49] S.M. Cho, H.M. Jang, "Softening and mode crossing of the lowest-frequency A1 (transverse-optical) phonon in single-crystal PbTiO3", Appl. Phys. Lett., **76**, 3014 (2000).
[50] G. Shirane, J.D. Axe, J. Harada, J.P Remeika, "Soft ferroelectric modes in Lead Titanate", Phys. Rev. B **2**, 155 (1970).
[51] T.P. Dougherty, G.P. Wiederrecht, K.A. Nelson, M.H. Garrett, H.P. Jensen and C. Warde, "Femtosecond resolution of soft mode dynamics in structural phase transitions", Science **258**, 770 (1992).
[52] J. Li, B. Nagaraj, H. Liang, W. Cao, Chi. H. Lee, and R. Ramesh, "Ultrafast polarization switching in thin-film ferroelectrics", Appl. Phys. Lett., **84**, 1174, (2004).
[53] F.-J. Kao, D. G. Busch, D. Gomes da Costa and W. Ho, Phys. Rev. Lett. **70**, (1993) 4098.
[54] M. Bonn, S. Funk, Ch. Hess, D. N. Denzler, C. Stampfl, M. Scheffler, M. Wolf and G. Ertl Science, **285** (1999) 1042.
[55] K. Onda, B. Li, J. Zhao, K.D. Jordan, J. Yang, and H. Petek, Science, **308** (2005) 1154.
[56] J.A. Stroscio and D.M. Eigler, Science **254**, 1319 (1991).
[57] H. Ogasawara, D. Nordlund, A. Nilsson, SLAC-PUB-11503 (2005).
[58] J.O'M. Bockris and S.U.M. Khan, Quantum Electrochemistry, Plenum Press, New York (1979).
[59] SLAC Linear Collider (SLC) Design Handbook, R. Erickson Ed., SLAC-R-714, December 1984.

[60] Final Focus Test Beam: Project Design Report, M. Berndt, et al., SLAC-R-376, March 1991.
[61] Dimad code, http://www.slac.stanford.edu/accel/ilc/codes/bin.linux/dimad
[62] K.L.F. Bane, P. Emma (SLAC), "LiTrack: A fast longitudinal phase space tracking code with graphical user interface", SLAC-PUB-11035 (2005), Proceedings of PAC 2005, Knoxville, Tennessee, 16-20 May 2005, p. 4266.
[63] L. Bentson, P. Emma, P. Krejcik (SLAC), "A new bunch compressor chicane for the SLAC linac to produce 30 fsec, 30 kA, 30-GeV electron bunches", SLAC-PUB-9240 (2002), Proceedings of EPAC 2002, Paris, France, 3-7 June 2002.
[64] P. Bellomo, J.J. Lipari, A.C. de Lira, "PEP-II Large Power Supplies Rebuild Program at SLAC," Proceedings of 2005 Particle Accelerator Conference, Knoxville, Tennessee.
[65] P. Bellomo, A. Donaldson, D. MacNair, "B-Factory Intermediate Dc Magnet Power Systems Reliability Modeling and Results," Proceedings of the 2001 Particle Accelerator Conference, Chicago.
[66] P. Bellomo and A. de Lira, "SPEAR3 Intermediate Dc Magnet Power Supplies," EPAC'04, Lucerne, Switzerland, July 2004.
[67] A. de Lira, P. Bellomo, K. Luchini, and D. MacNair, "The Dc-Magnet Power Supplies for the LCLS Injector," Proceedings of PAC07, Albuquerque, New Mexico, USA.
[68] G. E. Leyh and A.R. Donaldson, "A Multi-Channel Corrector Magnet Controller," PAC'95, Dallas, May 1995.
[69] P. Bellomo, A. de Lira, "SPEAR3 Large Dc Magnet Power Supplies," Proceedings of EPAC 2004, Lucerne, Switzerland.
[70] D. MacNair, "Ethernet Power Supply Controller," SLAC Internal publication, March 2006.